

Russian Original Vol. 46, No. 3, March, 1979

September, 1979

SATEAZ 46(3) 161-258 (1979)

SOVIET ATOMIC ENERGY

АТОМНАЯ ЭНЕРГИЯ
(ATOMNAYA ÉNERGIYA)

TRANSLATED FROM RUSSIAN

CONSULTANTS BUREAU, NEW YORK

SOVIET ATOMIC ENERGY

Soviet Atomic Energy is a cover-to-cover translation of *Atomnaya Énergiya*, a publication of the Academy of Sciences of the USSR.

An agreement with the Copyright Agency of the USSR (VAAP) makes available both advance copies of the Russian journal and original glossy photographs and artwork. This serves to decrease the necessary time lag between publication of the original and publication of the translation and helps to improve the quality of the latter. The translation began with the first issue of the Russian journal.

Consultants Bureau journals appear about six months after the publication of the original Russian issue. For bibliographic accuracy, the English issue published by Consultants Bureau carries the same number and date as the original Russian from which it was translated. For example, a Russian issue published in December will appear in a Consultants Bureau English translation about the following June, but the translation issue will carry the December date. When ordering any volume or particular issue of a Consultants Bureau journal, please specify the date and, where applicable, the volume and issue numbers of the original Russian. The material you will receive will be a translation of that Russian volume or issue.

Subscription (2 volumes per year)
Vols. 44 & 45: $130 per volume (6 Issues)
Vols. 46 & 47: $147.50 per volume (6 Issues)

Single Issue: $50
Single Article: $7.50

Prices somewhat higher outside the United States.

CONSULTANTS BUREAU, NEW YORK AND LONDON

227 West 17th Street
New York, New York 10011

Published monthly. Second-class postage paid at Jamaica, New York 11431.

Soviet Atomic Energy is abstracted or indexed in *Applied Mechanics Reviews, Chemical Abstracts, Engineering Index, INSPEC—Physics Abstracts and Electrical and Electronics Abstracts, Current Contents,* and *Nuclear Science Abstracts.*

SOVIET ATOMIC ENERGY

A translation of *Atomnaya Énergiya*

September, 1979

Volume 46, Number 3 March, 1979

CONTENTS

	Engl.	Russ.
ARTICLES		
Increasing the Efficiency of Uranium Utilization in the RBMK-1000 Reactor – I. Ya. Emel'yanov, A. D. Zhirnov, V. I. Pushkarev, and A. P. Sirotkin	161	139
Theoretical and Experimental Research on the Temperature Effect of the Reactivity of Heterogeneous Critical Assemblies with Strongly Blocked Absorber – V. I. Bagretsov, V. I. Lependin, V. I. Matveenko, and V. N. Morozov	164	142
Optimization of Physical Characteristics of a Heterogeneous Reactor – B. P. Kochurov and V. M. Malofeev	168	146
Development of the Surface Pseudosource Method for Calculating Neutron Fields in Cells with a Bundle of Fuel-Element Rods – N. I. Laletin and N. V. Sultanov	172	148
Measurements of the Fission Cross Section of ^{239}Pu by Neutrons with Energy from 10 eV to 100 keV – Yu. V. Ryabov	178	154
Measurement of the Total Neutron Cross Sections of ^{153}Eu, ^{154}Eu, and ^{155}Eu – V. A. Anufriev, S. I. Babich, A. G. Kolesov, V. N. Nefelov, V. A. Poruchikov, V. A. Safonov, A. P. Chetverikov, V. S. Artamonov, R. N. Ivanov, and S. M. Kalebin	182	158
Blistering in Niobium under Implantation of Helium Ions at Energy Expected in Thermonuclear Reactor – S. Das, M. Kaminsky (USA), V. M. Gusev, M. I. Guseva, Yu. L. Krasulin, and Yu. V. Martynenko (USSR)	185	161
Helium Blistering under High Irradiation Doses – I. N. Afrikanov, V. M. Gusev, M. I. Guseva, A. N. Mansurova, Yu. V. Martynenko, V. N. Morozov, and O. I. Chelnokov	190	165
Microdosimetric Characteristics of Neutrons at Energies between 50 eV and 10 MeV – V. A. Pitkevich and V. G. Videnskii	197	170
Albedo of Concrete for Low-Energy Gamma Radiation – M. P. Panin and A. M. Panchenko	201	174
LETTERS		
Distribution of Scattered Gamma Radiation from a Pulsed Source – D. A. Kozhevnikov	206	178
Design of Tesla Transformers Used in Direct-Voltage Accelerators – D. Kh. Dinev	208	179
Radiation Alteration of the Properties of Graphite over a Wide Range of Irradiation Temperature and Neutron Flux – Yu. S. Virgil'ev, I. P. Kalyagina, and V. G. Makarchenko	210	180

CONTENTS

(continued)

	Engl./Russ.
The Formation of Transuranium Nuclides in Connection with the Combined Use of VVÉR and RBMK Power Reactors – T. S. Zaritskaya, A. K. Kruglov, and A. P. Rudik	213 183
Yields of ^{28}Mg upon the Irradiation of Magnesium and Aluminum by Alpha Particles – P. P. Dmitriev and G. A. Molin	216 185
Some Properties of Fluctuations of the Neutron Field in a Nuclear Reactor – E. A. Gomin and S. S. Gorodkov	219 187
Reciprocity Property of Systems for Suppression of Xenon Oscillations – B. Z. Torlin	222 189
Interpretation of Data on the Total Scattering Cross Section of Cold Neutrons in Condensed Hydrogen-Containing Media – V. E. Zhitarev and S. B. Stepanov	224 190
An Analytic Solution of the Kinetic Equations of a Point Model of a Reactor – A. A. Shepelenko	227 192
SPECIAL ANNIVERSARIES	
Academician Lev Andreevich Artsimovich – B. B. Kadomtsev	229 195
Nikolai Aleksandrovich Perfilov – K. A. Petrzhak	231 197
COMECON NEWS	
Thirty-Fifth Conference of the COMECON Permanent Commission Atoménergo – Yu. S. Troshkin	233 199
Diary of Collaboration	234 199
INFORMATION	
Soviet–French Collaboration in the Field of the Peaceful Utilization of Atomic Energy – B. A. Semenov	236 201
CONFERENCES, MEETINGS, AND SEMINARS	
International Exhibition and Conference on the Nuclear Industry, "Nuclex-78" – Yu. M. Cherkashov	239 203
Third American–Soviet Seminar on Steam Generators for Fast Reactors – V. F. Titov	241 205
Meeting of the International Working Group of IAEA on High-Temperature Reactors – V. N. Grebennik	243 206
International Conference on Neutron Physics and Nuclear Data for Reactors and Other Applied Purposes – G. B. Yan'kov	245 207
Symposium, "International Guarantees-78" – N. S. Babaev	247 209
Soviet–American Conference on "High-Frequency Plasma Heating in Toroidal Systems" – V. V. Alikaev	249 210
Nineteenth International Conference on High-Energy Physics – V. I. Zakharov	250 211
All-Union Seminar "Electronic (Automatic) Methods of Concentration of Minerals" – B. V. Nevskii, M. L. Skrinichenko, and A. P. Tatarnikov	252 212
Ninth Radiochemical Conference in Czechoslovakia – A. S. Solovkin	253 213
NEW BOOKS	
Atomic-Hydrogen Power Generation and Technology – Reviewed by Yu. I. Koryakin	256 215
V. V. Goncharov, N. S. Burdakov, Yu. S. Virgil'ev, V. I. Karpukhin, and P. A. Platonov. Action of Irradiation on the Graphite in Nuclear Reactors – Reviewed by A. P. Sirotkin	257 215
A. B. Mikhailovskii. Plasma Instabilities in Magnetic Traps – Reviewed by A. M. Fridman	258 216

The Russian press date (podpisano k pechati) of this issue was 2/26/1979. Publication therefore did not occur prior to this date, but must be assumed to have taken place reasonably soon thereafter.

Declassified and Approved For Release 2013/02/12 : CIA-RDP10-02196R000800010003-3

INCREASING THE EFFICIENCY OF URANIUM UTILIZATION IN THE RBMK-1000 REACTOR

I. Ya. Emel'yanov, A. D. Zhirnov,
V. I. Pushkarev, and A. P. Sirotkin

UDC 621.039.542.34

Increasing the unit power is one way of improving the economics of atomic power plants. As applied to RBMK (high-power water-cooled channel) reactors, this was reflected in the development of the RBMK-1500, RBMK-2000, and RBMK-2400. The possibility of increasing the channel power of the RBMK-1000 by a factor of 1.5 through heat-exchange intensification is realized in the RBMK-1500 and the power is thus increased to 1500 MW(E) without altering the reactor dimensions and design. In the RBMK-2000 design, the channel diameter, the number of fuel elements in the channel, and the lattice pitch have been increased, thus making it possible to develop a reactor with double the power, i.e., with 2000 MW(E), within the same overall dimensions as the RBMK-1000. The creation of a channel with increased power opens up new potentialities for improving the technical and economic characteristics: increasing the burn-up fraction and reducing the consumption of fuel assemblies and the specific consumption of natural uranium.

Operating experience with uranium–graphite reactors [1, 2] showed that fuel recharging can be carried out continuously in them during operation. This makes it possible to avoid considerable variations in reactivity during the reactor operation, to reduce the unproductive capture of neutrons in the control rods, and thus to intensity the energy production and the fuel burn-up fraction at a low uranium enrichment. As shown by the physical and technicoeconomic calculations of the RBMK-1000 [3, 4], with the present prices for fuel and fabrication of fuel elements, the reduced fuel component c_f of the electricity production costs is a minimum with an initial enrichment of 1.8-2%. At the same time, calculations established that with a higher enrichment and with the reactor operating in a continuous recharging mode the power of the freshly charged channels rises and the fuel residence time increases. On the basis of the available data and bearing in mind that, first, there was insufficient experience in operating fuel elements with a high burn-up fraction ($\sim$ 25-30 MW · day/kg U) with linear loads of 300-400 W/cm and a fuel residence time of five years and, second, the c_f minimum is not pronounced, a comparatively conservative solution was adopted in the RBMK-1000 for steady-state operating conditions of continuous recharging of fuel with a 1.8% enrichment (Table 1). The use of c_f as an optimization criterion is arbitrary to a certain extent.

Experience from the operation of the first RBMK-1000 reactors showed that in respect of both the linear loads in the fuel elements and maximum channel power (according to the conditions of heat-exchange crisis) the fuel element and fuel assembly design provides for certain reserves. Moreover, as the fuel is burned up and as the auxiliary absorbers, compensating the initial excess reactivity, are withdrawn, the stability of the energy distribution diminishes. As shown by calculations and confirmed by experiments, the deformation of the distribution of the energy release with a time constant ranging from several minutes to several tens of minutes for the first azimuthal harmonic is determined primarily by the positive steam void coefficient of reactivity α_φ. A decrease in this coefficient makes the energy distribution more stable. The most economic and optimal reduction of the steam void coefficient and increase in the stability of the energy distribution in the RBMK are attained by increasing the ratio of fuel nuclei to moderator nuclei. The fuel-to-moderator nucleus ratio is improved in operating reactors by raising the enrichment whereas in reactors in the design stage it is possible to reduce the number of moderator nuclei, e.g., by reducing the lattice pitch or the effective density of the moderator.

Increasing the fuel enrichment results in a higher burn-up fraction and a change in α_φ, improving the stability of the field, and in a lower consumption of fuel and fuel elements. An increase in the enrichment and the corresponding increase in the burn-up fraction in turn cause a rise in the power of the freshly charged channel, the fuel residence time, and the linear loads in the fuel elements. The possibility of increasing the channel power 1.5-fold is confirmed by the construction of the RBMK-1500 channel. The data given in Table 2 should be considered mainly as comparative and not absolute data inasmuch as the calculations were performed

Translated from Atomnaya Énergiya, Vol. 46, No. 3, pp. 139-141, March, 1979. Original article submitted July 17, 1978.

0038-531X/79/4603-0161 $07.50

TABLE 1. Characteristics of Reactor Using Fuel of Design and Increased Enrichment

Index	RBMK-1000					RBMK-1500	
Initial enrichment, %	1,8	2,0	2,4	3,0	3,6	1,8	2,0
Fuel burn-up fraction, MW·day/kg U	18,5	22,3	28,8	37,6	45,7	17,8	21,6
Comp. of discharged fuel, kg/ton:							
^{235}U	3,9	3,5	2,9	2,5	2,2	4,4	3,8
^{236}U	2,1	2,5	3,1	4,0	4,8	2,1	2,4
^{239}Pu	2,2	2,2	2,2	2,1	2,1	2,2	2,2
^{240}Pu	1,8	2,0	2,3	2,5	2,6	1,8	2,0
^{241}Pu	0,5	0,5	0,6	0,6	0,7	0,5	0,5
Poison	19,4	23,3	30,1	39,3	47,8	18,6	22,8
Change in α_φ rel. to design value, %	—	—1,3	—3,5	—6,4	—9,0	—1,5	—2,7
Uranium consump., ton/yr·GW(E) with							
$\varphi = 0.8$:	50,5	42	32,5	25	20,5	52,4	43,3
Enriched	169	158	151	148	148	174	165
Natural	16	13,3	10,2	7,9	6,5	16,5	13,6
Fuel component:							
electricity cost, kopek/kWh	0,252	0,232	0,216	0,208	0,208	0,260	0,240
reduced cost c_f, kopek/kWh	0,370	0,362	0,370	0,405	0,445	0,335	0,325

TABLE 2. Channel Power and Linear Load in Fuel Elements as Function of Enrichment of Charged Fuel

Characteristic	RBMK-1000					RBMK-1500	
Enrichment, %	1,8	2,0	2,4	3,0	3,6	1,8	2,0
Power of freshly charged channel with account for k_r, kW	2650	2800	3150	3500	3800	4050	4250
Limiting power of channel with account for $3\sigma_{ch}$, kW	3050	3250	3650	4050	4350	4680	4910
Linear load in fuel element in freshly charged channel q_l^{nom}, W/cm	295	315	350	390	420	455	485
Limiting value q_l with account for $3\sigma_t$, W/cm	360	385	430	480	520	560	595
Fuel assembly period, eff. days	1100	1350	1730	2260	2750	700	860

for a steady-state fuel-recharging mode. To determine the power of fresh channels we used the coefficients of nonuniformity k_r and k_z, obtained with allowance for the operating experience with the RBMK-1000, and the calculated overload factors. For reactors operating with 1.8% enriched fuel the coefficient of nonuniformity over the radius, k_r, was taken to be 1.4 and the coefficient of nonuniformity over the height, k_z, was taken to be 1.4. On the basis of operating experience with the RBMK-1000 the rms error σ_{ch} of the determination and maintenance of the channel power was assumed to be 5.2%, and that of the linear load in the fuel element, σ_t, was assumed to be 7.7%. In calculating the annual consumption of natural and enriched fuel, we assumed that the load factor φ was 0.8 and that the ^{235}U content in the spent material from the enrichment plants was 0.25%. The return of ^{235}U into the fuel cycle from the spent fuel was not taken into account. Thus, increasing the enrichment of the fuel in the RBMK-1000 is a realistic way of raising the efficiency of fuel utilization. In this case, from the point of view of the allowable channel powers and linear loads in the fuel element, enrichment to 3.6% is possible. It was decided to increase the channel power and linear loads in the fuel element by up to 1.5-fold in the RBMK-1500 [5, 6]. In the given case the fuel assemblies were provided with heat-exchange intensifiers. No changes were made in the channel construction and in the inlet and outlet equipment. With a more moderate increase in the enrichment and, therefore, in the channel power, fuel assemblies without intensifiers can be used. For example, a transition to a 2% enrichment of the fuel can be made without any structural changes in the fuel assemblies. The maximum values given in Table 2 for the power were obtained with the assumption that the algorithm for equalizing the power over the reactor core remains the same as in operating RBMK-1000 reactors. Along with this, we can propose measures (some of which have already been

tested in reactors) permitting an extension of the possibility for equalizing the energy distribution in the reactor core. Among these we can classify the use of absorption rods inserted in fresh fuel assemblies and withdrawn as the channel power decreases, the use of depleting absorbers, optimization of the recharging procedure, etc. A certain reserve in respect of equalization of the energy distribution is due to the possibility of increasing the operational reactivity margin resulting from the operating conditions of the atomic power plant in the energy system.

Increasing the enrichment leads to a reduction of the consumption of fuel elements and natural uranium. The annual consumption of fuel elements drops by 20-30% in the transition from variant to variant and is halved when 3% enrichment is employed. The consumption of natural uranium with this enrichment drops by 20 tons to 150 tons/yr. The ^{235}U content in the spent fuel is brought down to 0.25%, i.e., to the level in the spent material from enrichment plants, and is reduced to 0.2% when 3.6% enrichment is employed, thus removing the problem of the necessity of removing it from the spent fuel. Increasing the initial enrichment significantly changes the steam void coefficient of reactivity, reducing it in comparison with the 1.8% enrichment and shifting it in the negative direction. This improves the stability of the energy distribution but requires special consideration in the case of transient conditions.

If the change in the parameters under discussion (channel power, linear load in fuel element, change in steam void coefficient of reactivity) does not cast doubt on the possibility of raising the enrichment, then increasing the burn-up fraction to 40-45 MW · days/kg U and the calendar residence time of the fuel elements in the reactor core to 10-12 years with an enrichment of 3 and 3.6%, respectively, requires special investigation and verification, although the construction of fuel elements with an oxide fuel burn-up of 45-50 MW · days/kg U can be considered feasible [7, 8]. It is more difficult to ensure the life of fuel elements under reactor conditions over a long period of time.

Raising the channel power 1.5-fold opens up new prospects for the RBMK-1000 and markedly improves the economic factors of the fuel cycle through an increase in the fuel enrichment. The use of fuel with a 2.4-3% enrichment in the RBMK-1000 requires the construction and experimental testing of the efficiency, of fuel elements permitting a burn-up fraction of up to 40 MW · days/kg U and having a guaranteed viability for a residence of about 10 yr in the reactor core. This is one direction in which experimental and design work as well as research should be conducted in order to improve the RBMK-1000.

LITERATURE CITED

1. A. M. Petros'yants, Current Problems of Atomic Science and Engineering in the USSR [in Russian], Atomizdat, Moscow (1976).
2. Atoms in the Service of Socialism. An Album [in Russian], Atomizdat, Moscow (1977).
3. A. P. Aleksandrov et al., At. Energ., 37, No. 2, 95 (1974).
4. I. Ya. Emel'yanov, P. A. Gavrilov, and B. N. Seliverstov, Control and Safety of Nuclear Power Reactors [in Russian], Atomizdat, Moscow (1975).
5. N. A. Dollezhal' et al., At. Energ., 40, No. 2, 117 (1976).
6. A. P. Aleksandrov and N. A. Dollezhal', At. Energ., 43, No. 5, 337 (1977).
7. V. G. Aden et al., At. Energ., 43, No. 4, 235 (1977).
8. V. A. Tsykanov and E. F. Davydov, Radiation Resistance of Fuel Elements of Nuclear Reactors [in Russian], Atomizdat, Moscow (1977).

THEORETICAL AND EXPERIMENTAL RESEARCH ON THE TEMPERATURE EFFECT OF THE REACTIVITY OF HETEROGENEOUS CRITICAL ASSEMBLIES WITH STRONGLY BLOCKED ABSORBER

V. I. Bagretsov, V. I. Lependin,
V. I. Matveenko, and V. N. Morozov

UDC 621.039.519.4

Theoretical and experimental investigations on the temperature effects of reactivity in regular, heterogeneous critical assemblies with a simple shape permit a conclusion to be drawn about the most applicable methods of physical computation, which ordinarily cannot be done by studying actual systems. It is of particular interest in this connection to study cores containing a strongly blocked absorber since in this case the computations entail difficulties associated with the necessity of taking proper account of the pronounced anisotropy of the angular distribution of the neutron flux. The paper presents the results of investigations carried out over a wide range of temperatures (T = 2-240°C) in critical assemblies of the TÉS-ZM reactor [1], containing cadmium and gadolinium rods uniformly arranged in the lattice of fuel elements.

Characteristics of the Assemblies. High-temperature experiments were carried out on the MATR-2 stand in a thick-walled vessel allowing the critical assemblies to be heated to 300°C [2]. The maximum temperature in the measurements was limited by the technological capabilities of two-ring fuel elements of the K-17 type [3], designed for a pressure $P \sim 4$ MP/cm^2. Fuel elements with a length of 600 mm made of 17% enriched uranium dioxide and containing 3.48 g ^{235}U per cm of length were placed at the nodes of a hexagonal lattice with a pitch $a = 68$ mm. The dimensions of the fuel rings with a 0.3-mm stainless steel can were 41.8×2.9 and 29.2×2.9 mm. The design of the stand has provision for compensation of reversible changes in the reactivity with a three-blade shim rod of boron steel, placed in the space between the fuel elements. To ensure nuclear safety four rods of the control and safety system in 30×3-mm hermetically sealed steel tubes were placed between the fuel elements.

We studied three variants of critical assemblies, differing as to the number of fuel elements and absorbers, and absorber material. Instead of a central fuel channel each assembly was provided with a 50×3-mm cooled steel channel which held a neutron-sensing element for pulsed measurements of the reactivity. One of the assemblies studied consisted of fuel elements without absorbers (34 fuel elements); in two others the central water space of each fuel element held absorption rods of cadmium oxide (68 rods) or gadolinium oxide (74 rods) in a mixture with aluminum oxide. Diagrams of the active core are given in Figs. 1a, b, c.

The absorption rods of cadmium oxide with a density $\gamma = 0.5$ g/cm^3 and of gadolinium oxide ($\gamma = 0.65$ g/cm^3) had identical dimensions (diameter of absorber 10.4 mm, steel can 0.3 mm thick, length of absorber 480 mm) and occupied a central position over the height of the active core. In all the experiments the critical assemblies were surrounded with a water reflector 25 to 40 cm thick.

Experimental Procedure. In each variant the critical state of the assemblies completely flooded with water at a temperature of 15-20°C was attained by choosing the number of fuel elements in the assembly according to the adsorber used with the control and safety rods completely withdrawn from the active core. As the assemblies were heated up the shim rod was either moving or was in some fixed position, depending on the method of measuring the reactivity. For assemblies with a cadmium rod we experimentally assessed how the shim rod affects the temperature effect of the reactivity of the assembly depending on the position of the boron steel shim rod (at the top, in the middle, or at the bottom of the active core). The reactivity of the systems was determined in the experiments by two methods: by measuring $\partial\rho/\partial T = f(T)$ and then integrating this relation within the appropriate limits; and pulsed measurements with the shim rods in a fixed position.

In the first method the system must be put into the supercritical state and the supercriticality must be measured, with the temperature variation of the reactivity being compensated by moving the shim rods. The

Translated from Atomnaya Énergiya, Vol. 46, No. 3, pp. 142-145, March, 1979. Original article submitted January 30, 1978.

0038-531X/79/4603-0164$07.50

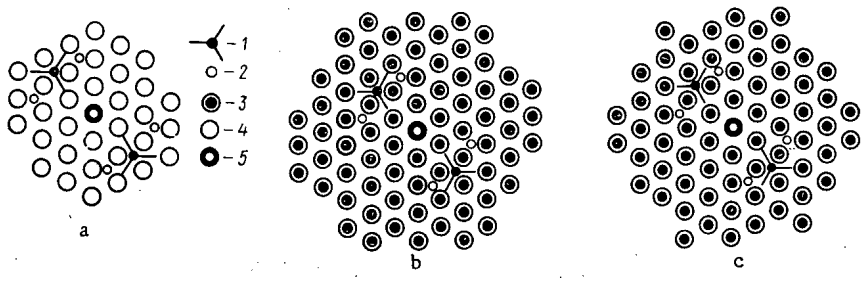

Fig. 1. Diagrams of critical assemblies: a) without absorber, b) with gadolinium rods, and c) with cadmium rods; 1) shim rod; 2) steel cans of rods of control and safety system; 3) absorption rod; 4) fuel element; 5) cooling channel with SNM-11 counter.

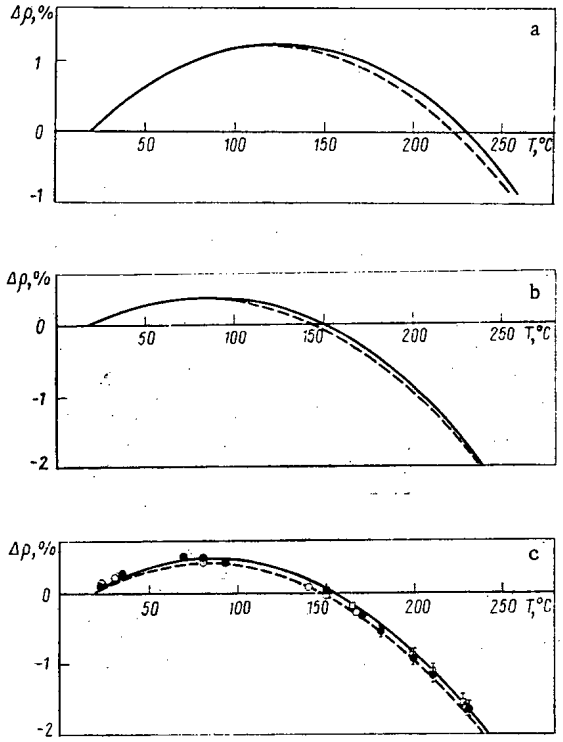

Fig. 2. Temperature dependence of reactivity of assemblies: a) without absorber, b) with gadolinium rods, and c) with cadmium rods. The experimental points (c) were obtained by a pulsed method with the shim rods at the top (□), in the middle (○), and at the bottom (●): ---) experiment with the relation $\partial\rho/\partial T = f(T)$; ——) calculation.

shim rod efficiency covered the positive temperature effect of the reactivity with a large excess in all assemblies studied and did not exceed $2.4\beta_{eff}$ for the pure assembly and $1.7\beta_{eff}$ for assemblies with absorbers.

In measurements by the second method a neutron generator was placed near the side of the high-pressure vessel and the reaction of the system to the pulse introduced was recorded by an SNM-11 corona counter installed in the center of the active core. The reactivity of the system (in units of β_{cr}) was found from the α-method formula [4]:

$$\rho/\beta_{cr} = \alpha\Lambda/\alpha_{cr}\Lambda_{cr} - \beta/\beta_{cr},$$

where α_{cr} is the damping decrement of the fundamental harmonic of instantaneous neutrons, Λ_{cr} is the generating time of instantaneous neutrons, β_{cr} is the effective fraction of delayed neutrons in the cold critical state at 20°C, and α, Λ, and β are the analogous values for the system at the temperature T.

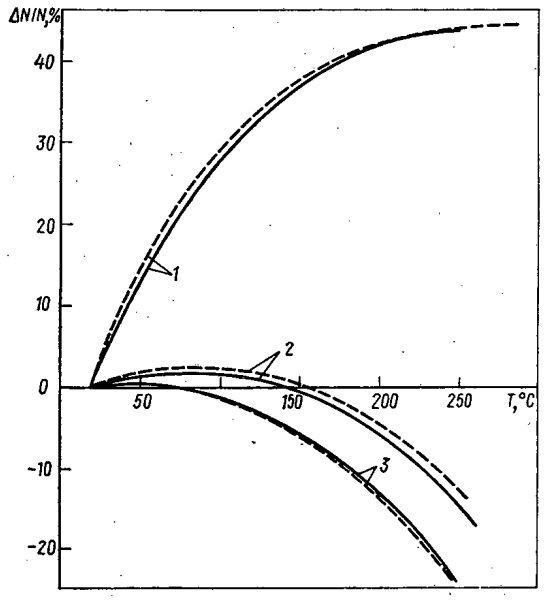

Fig. 3. Temperature dependence of relative change in number of fuel elements in critical state (N_{cr}) for assemblies with fuel-element spacing pitch of 3.15 cm (1), 2.36 cm (2), and 1.89 cm (3): $\frac{\Delta N}{N} = \frac{N_{cr}(20°) - N_{cr}(T)}{N_{cr}(20°)}$. ---) experiment [13]; ——) calculation.

The value of β is quite conservative and, as shown by calculations in a 21-group P_1 approximation by the 9M program [5], its variation with the temperature can be neglected.

A characteristic feature of the assemblies studied was that criticality was attained with the shim and control rods completely withdrawn for two substantially different assembly temperatures; this makes it possible to experimentally determine the change in Λ_{cr} at these temperatures, using the relation $\alpha_{cr} = \beta_{cr}/\Lambda_{cr}$ [4]. For the assemblies studied, with allowance for the calculated value of β in the cold and hot critical states, respectively, Λ_{cr} is equal to: $4.85 \cdot 10^{-5}$ and $4.67 \cdot 10^{-5}$ sec in the pure assembly, $4.41 \cdot 10^{-5}$ and $4.08 \cdot 10^{-5}$ sec in the assembly with gadolinium, and $4.44 \cdot 10^{-5}$ and $4.08 \cdot 10^{-5}$ sec in the assembly with cadmium. The results of the pulsed measurements were processed by taking Λ_{cr} into account with the assumption of a linear dependence of the neutron generation time on the temperature.

According to estimates, the error of determination of the reactivity of a system by both methods did not exceed 3-3.5%. This error doubles when the temperature effect is determined as the difference of reactivities.

Method of Calculation. Calculations of the physical characteristics of the assemblies were carried out according to the program of Polivanskii [6]. In doing this we used a low-group diffusion approximation and a multizone reactor model in a two-dimensional (r, z) geometry. The real geometry of the assemblies, consisting of three fundamental physical zones (active core, neutral measuring channel, reflector), was replaced in the calculations by a multizone model (7-12 zones) reflecting the real features of the composition. The presence of the steel cans of the control and safety rods in the active core was taken into account with the aid of perturbation theory.

In our calculations we employed a two-group approximation, with a group interface equal to 0.671 eV; the macroscopic group constants were determined by averaging over multigroup spectra obtained in various approximations. The constants of the epithermal groups of neutrons were averaged over a nine-group spectrum of the moderation of a homogeneous bare reactor with equivalent dimensions. In this case the constants of ^{235}U, Gc, and Cd were found by taking account of their heterogeneous distribution in the active core. The probability of avoiding resonance absorption in ^{238}U was found by taking account of the mutual screening of the fuel elements in accordance with [7]. In calculating the absorption of epithermal neutrons in gadolinium and cadmium, we used data on allowed and disallowed parameters from [8, 9]. The macroscopic constants of the thermal group of neutrons for the lattice of the active core and the central measuring channel were obtained by modeling these zones with Wigner–Seitz cells, by calculating the space–energy distributions of the density of the thermal neutron flux in these cells with account for the effects of thermalization and averaging the constants over the neutron spectra obtained.

The space–energy distributions of the density of the thermal neutron flux in the cells were calculated in a ten-group approximation by the formulas of a modification of the S_n method with a linear balance approximation [10]. The neutron scattering anisotropy was taken into account in the transport approximation only for those neutrons which, upon scattering, did not go beyond the limits of the energy group. In transitions to other energy groups the neutron scattering indicatrix was assumed to be isotropic. The ten-group macroscopic constants of the zones and the density of thermal-neutron sources in the zones were determined by using a procedure expounded in [11]. The function for neutron scattering on water molecules in the thermal region $0 \leq E \leq 0.671$ eV was calculated by the approximation formulas of [11]. In solving the ten-group system of kinetic equations we employed an algorithm which largely coincides with the algorithm of the S_n modulus of the Landysh system [12]. Preliminary methodological investigation made it possible to find the optimal parameters of the ten-group calculation of the density of the thermal neutron flux in the cell: the approximation of S_6 and the grid from the radial variable r contained 86 nodes with an uneven pitch in the five-zone cell. In the surface region of the zone of the absorption rod, corresponding to roughly 6-8 mean free paths of the thermal neutrons (in which flux depression largely occurs), the variable pitch of the grid was a minimum (0.001 cm).

Results. The results of theoretical and experimental investigations on the temperature effects of reactivity for three assemblies are given in Figs. 2a, b, c. The temperature effect is given in the form of the temperature dependence of the reactivity difference of the system:

$$\Delta\rho(T) = \rho(T) - \rho(20^\circ\text{C}),$$

where $\rho(T)$ and $\rho(20^\circ\text{C})$ are the values of the reactivity of the system at a given temperature and at 20°C, respectively. The dashed curves were obtained by integration of the measured relations $\partial\rho/\partial T = f(T)$ within appropriate limits. The results of pulsed measurements for three positions of the shim rods in the assembly with cadmium rods, given in Fig. 2c in the form of experimental points, show that:

1) the experimental relations obtained by two independent methods are in quite good agreement with each other, attesting to the reliability of the experimental results;

2) the shim-rod position has practically no influence on the temperature effect of the assembly reactivity since the experimental points at different shim-rod positions coincide within the limits of experimental errors.

The good agreement between the calculated and experimental relations of the temperature effect is shown in Figs. 2a, b, c. Theoretical investigation of the temperature effect of reactivity by using the two-group method with the application of the S_n approximation in determining the parameters of the thermal group was also tested for strictly regular and uniform critical assemblies, not containing absorbers, a description of which is given in [13]. The results of the investigations are described in detail in [14] and presented in Fig. 3, where good agreement is also observed between calculated and experimental data over a wide range of ^{235}U concentrations ($\rho_n/\rho_5 = 50$–600) and temperatures (T = 20–250°C).

The reliability of the experimental data obtained by different methods and systematic computational investigations, carried out during this study, permit the conclusion that the experimental and computational procedures presented in the paper can be used in studying regular assemblies with highly blocked absorber.

The authors are indebted to M. N. Lants, V. S. Bykovskii, R. K. Goncharov, V. M. Fedorov, A. F. Zolotov, A. N. Mezentsev, R. P. Borozdenko, and T. S. Pankratova for participating in the experiment and the calculations and to V. N. Gurin and G. A. Ilyasova for their useful comments in the discussion of the results.

LITERATURE CITED

1. V. V. Orlov et al., in: Problems of Nuclear Reactor Physics [in Russian], Otd. Nauchn.-Tekh. Inf., Fiz.-Énerg. Institut (ONTI FÉI), Obninsk, No. 1, Vol. 1 (1968), p. 349.
2. The Physics and Power Engineering Institute [in Russian], Atomizdat, Moscow (1974), p. 11.
3. E. I. Inyutin et al., Proc. Third Intern. Conf. on the Peaceful Uses of Atomic Energy, New York, Vol. 3 (1965), p. 23.
4. É. A. Stumbur et al., in: Theoretical and Experimental Problems of Transient Neutron Transport [in Russian], Atomizdat, Moscow (1972), p. 245.
5. A. I. Nevinitsa, in: Problems of Atomic Science and Engineering, Series "Reactor Construction. Methods and Algorithms for Nuclear Reactor Calculations" [in Russian], Fiz. Énerg. Inst. (FÉI), Obninsk, No. 6(20) (1977), p. 73.
6. Sh. S. Nikolaishvili et al., in: State of the Art and Prospects of Work on the Construction of Atomic Power Plants with Fast-Neutron Reactors [in Russian], Otd. Nauchn.-Tekh. Inf., Fiz.-Énerg. Inst. (ONTI FÉI), Obninsk, Vol. 2 (1967), p. 75.

7. V. V. Orlov, At. Energ., 4, 531 (1958).
8. S. M. Zakharova et al., Bulletin of the Nuclear Data Information Center [in Russian], Atomizdat, Moscow, No. 3 (1967), p. 194.
9. S. M. Zakharova, Bulletin of the Nuclear Data Information Center [in Russian], Atomizdat, Moscow, No. 5 (1968), p. 189.
10. V. N. Morozov, in: Theory and Methods of Nuclear Reactor Calculations [in Russian], Gosatomizdat, Moscow (1962), p. 91.
11. G. I. Marchuk et al., At. Energ., 13, No. 6, 534 (1962).
12. V. N. Morozov, in: Problems of Atomic Science and Engineering. Series "Reactor Construction. Methods and Algorithms for Nuclear Reactor Calculations" [in Russian], Fiz. Energ. Inst. (FÉI), Obninsk, No. 6(20), (1977), p. 83.
13. G. A. Bat' et al., At. Energ., 30, No. 4, 354 (1971).
14. V. I. Matveenko and V. N. Morozov, Preprint FÉI-694, Obninsk (1976).

OPTIMIZATION OF PHYSICAL CHARACTERISTICS OF A HETEROGENEOUS REACTOR

B. P. Kochurov and V. M. Malofeev

UDC 621.039.51

By using the method of solving the equations of a heterogeneous reactor proposed in [1] a difference analog of the initial equations can be obtained which eliminates the long-range interaction and which is formally similar to the equations for a homogeneous reactor. However, there is one distinctive feature which is important for the optimization problem. In the numerical realization the homogeneous finite difference equations represent an approximation of the differential equations, and the solution of optimization problems may involve so-called "slipping conditions" [2] which are characterized by extremely irregular behavior of the control function, which, as a rule, violates the initial assumption made in the homogeneous equations that the parameters can be averaged, and hampers the physical interpretation of the results. In a heterogeneous reactor the net is fixed with one node per channel, and therefore from the very beginning the difference equations appear as a system of algebraic equations of finite but rather high dimensionality. For a finite number of dimensions, slipping conditions do not occur, and therefore the results have a natural physical interpretation, although the nonlinear nature of the problems can, as before, lead to such difficulties as slow convergence of the solution or falling into local minima.

The physical statement of the problem and the notation are the same as in [1]. A heterogeneous reactor is considered with K cylindrical slugs placed at the nodes of a regular lattice. The vector of extrapolated values of the neutron fluxes obeys the system of equations:

$$\begin{gathered} HN=0; \quad H=H_2-\frac{1}{\lambda}H_1; \\ H_2=PV(U)+R\gamma_2(U); \\ H_1=(PI_0^{-1}K_0+R)\,\gamma_1(U), \end{gathered} \tag{1}$$

where P and R are local operators which depend on the properties of the moderator, λ is the eigenvalue (the effective multiplication factor), and I_0 and K_0 are matrices of the values of Bessel functions which are diagonal in **k**.

The channel characteristics $\gamma_{1,2}$ and V are related to the initial few-group ($G\times G$, where G is the number of groups) Λ matrices by the expressions

$$\begin{gathered} \Lambda=\Lambda_1-\Lambda_2;\ \gamma_1(U)=-I_0C^{-1}\Lambda_1(U); \\ \gamma_2(U)=-I_0C^{-1}\Lambda_2(U)+\partial I_0C^{-1};\ \partial=\rho_k(\partial/\partial\rho_k); \\ V(U)=I_0^{-1}[C^{-1}+K_0\gamma_2(U)], \end{gathered}$$

where C is a matrix which depends on the properties of the moderator.

Translated from Atomnaya Énergiya, Vol. 46, No. 3, pp. 146-148, March, 1979. Original article submitted March 13, 1978.

 0038-531X/79/4603-0168$07.50

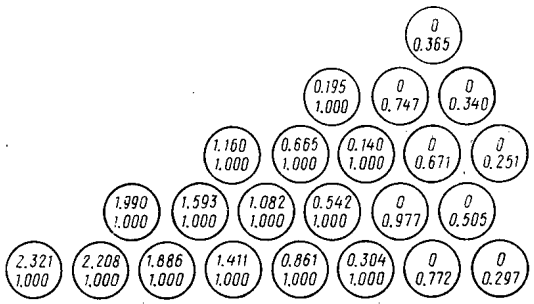

Fig. 1. Optimum values of control and thermal neutron fluxes.

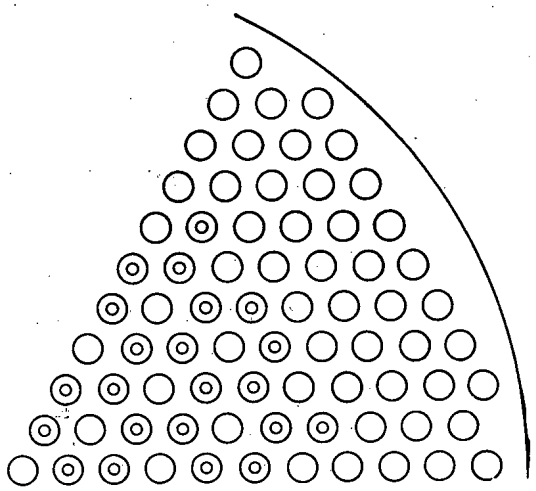

Fig. 2. Geometry of problem No. 2 (slugs with nonzero concentration of fuel are marked).

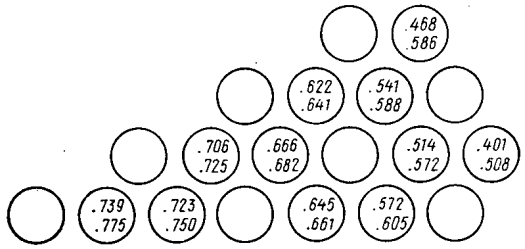

Fig. 3. Optimum values of control and thermal neutron fluxes for slugs with nonzero concentration of fuel.

It was assumed in [2] that the properties of the slugs can vary; i.e., the matrix of each slug $\Lambda(U)$ depends on the component of the "control" vector related to such characteristics as the geometry and composition of the channels.

The optimization problem is formulated as follows. It is required to find a vector U which satisfies Eqs. (1), restrictions on the control vector

$$U_{\min} \leqslant U \leqslant U_{\max}, \tag{2}$$

and restrictions on a certain set of functionals

$$b_j \leqslant F_j(N, U) \leqslant B_j; \quad (j = 0, 1, \ldots, J-1) \tag{3}$$

for which the functional $F_J(N, U)$ is maximum. Functionals of three types were admitted:

$$F^{(1)}(U) = \langle C(U),\ 1\rangle;$$
$$F^{(2)}(U) = \langle C^1(U)\, N/C^2(U)\, N\rangle;$$
$$F^{(3)}(U) = \max_k (C_k^1(U_k),\ N_k)/\langle C^2(U),\ N\rangle. \tag{4}$$

The symbol (,) denotes the scalar product of vectors which depend on the group index, and $\langle\ ,\ \rangle$ denotes the scalar product of vectors which depend on the group and spatial indices.

The optimization program was solved by the gradient method based on linear perturbation theory [3] and taking account of the specific properties of relations (1)-(4).

The variations of the functionals are related to the variations of the control by the equations

$$\delta F_0 = \delta(1/\lambda) = \langle W_0,\ \delta U\rangle;$$
$$\delta F_j = \langle W_j,\ \delta U\rangle; \tag{5}$$
$$W_{j,\,k} = (\partial F_j/\partial U)_k + [N_j^+,\ (\partial H/\partial U)\, N]_k,$$

where N_0^+ is the solution of the homogeneous equation, and the N_j^+ are the solutions of the inhomogeneous equations which are the adjoints k of Eqs. (1):

$$H^+ = H_2^+ - (1/\lambda)\, H_1^+;$$
$$H_1^+ = \gamma_1^+(U)\,(I_0^{-1}K_0P^+ + R^+);$$
$$H_2^+ = V^+(U)\, P^+ + \gamma_2^+(U)\, R^+;$$
$$H^+ + N_0^+ = 0;\ H^+N_j^+ = -\partial F_j/\partial N. \tag{6}$$

By taking account of the specific form of H and H^+ the vector function $W_{j,\,k}$ can be written in the form

$$W_{j,\,k} = (\partial F_j/\partial U)_k + [(I_0^{-1}K_0P^+ + R^+)\, N_j^+\ \times I_0C^{-1}(\partial\tilde{\Lambda}(U)/\partial U)]_k; \tag{7}$$
$$\tilde{\Lambda} = \Lambda_1/\lambda - \Lambda_2.$$

The maximum increment δF_J was calculated by using the solution of the linear programming problem with upper and lower restrictions described in [4] and the introduction of a penalty function for violating the restrictions on the functionals. At each step of the iteration process ($U \to U + \delta U$), every type 3 functional generates a certain number of type 2 functionals

$$F_{j,\,(l)} = (C_j^{-1}(U),\ N)_l/\langle C_j^2(U),\ N\rangle,$$

where l ranges over all the "dangerous" slugs. In maximizing a type 3 functional the maximum value of the form

$$v - \sum_j m^j v_j$$

is found in the linear programming problem under the condition

$$\sum_k W_{J,\,(l),\,k}\delta U_k \leqslant \max_k F_{J,\,(l)} - F_{J,\,(l)},$$

where m^j and v_j are coefficients and penalty variables.

The dimensionality of the problem can be reduced by collecting the slugs into certain fixed groups with identical values of the control. The iteration process is stopped when the linear programming problem has a zero solution (to a certain degree of accuracy).

The algorithm used to solve the homogeneous adjoint equation (6) is the same as that used to solve Eqs. (1) (cf. [1, 5]).

The inhomogeneous equations (6) were solved by the iteration method:

$$\varphi^{k+1} = (1/\lambda)\, T^+\varphi^k + Q;$$
$$T^+ = (H_2^+)^{-1}H_1^+;\quad Q = (H_2^+)^{-1}(\partial F_j/\partial N); \tag{8}$$
$$\varphi^0 = 0;\quad \varphi^k \to N_j^+.$$

The eigenvalue λ was fixed and the inversion of H_2^+ was reduced to the sequential solution of the equations

$$(\tilde{H}_2^+)_g\,\psi_g = q_g;\quad (\tilde{H}_2^+)_g = P_g^+ + \tilde{\gamma}_2^{gg}R_g^+;$$
$$q_g = \sum_{g'=1}^{g} [\tilde{\gamma}_1^{g'g}(I_0^{-1}K_0P^+ + R^+)_{g'}\,\varphi_{g'}^k] - \sum_{g'=g+1} \tilde{\gamma}_2^{g'g}R_{g'}\psi_{g'} + f_g; \tag{9}$$

$$\tilde{\gamma}_{1,2} = \gamma_{1,2} V^{-1};\ f = -(V^{+})^{-1}\,\partial F_j/\partial N,$$
$$(g = G,\ G-1,\ \ldots,\ 1).$$

Equations (9) were solved by the Tschebyscheff binomial method for accelerating the convergence described in [6].

By construction the source Q is orthogonal to the solution of the initial homogeneous equation

$$\langle H_1 N,\ Q\rangle = 0,$$

which ensures the existence of a solution of Eq. (8).

Calculations showed that the approximate method of determining N_j^+ does not lead to domination of the N_0^+ component, and it can be eliminated at the end of the iteration process by using the relation

$$\langle N_j^+,\ H_1 N\rangle = 0.$$

As an example we present the result of solving the problem of determining the minimum critical mass of a cylindrical reactor with a hexagonal lattice. The characteristics of the reactor are listed below. In the initial state the reactor was specified with values of the control U = 1 at all slugs and an eigenvalue λ = 1.

	1st variant	2nd variant
No. of groups	2	3
Radius of reactor, cm	220	220
Pitch, cm	28	20
Neutron age, cm^2	120	40; 80
Square of diffusion length, cm^2	5500	5500
No. of slugs	199	379
Radius of a slug, cm	6.4	6.4
Elements of matrix (by rows):	0; $-0.95711\,U$ 0; $0.9\,U$	0; 0; $-1.0426\,U$; 0; $0.05\sqrt{U}$; 0 0; 0; $0{,}9\,U$
Critical mass:		
Initial	199	379
Minimum	110.67	38.04

In the first case the absorption of epithermal neutrons was assumed zero. The result is characteristic for the solution of the Goertzel problem [7]: the optimum control is such that the extrapolated values of the thermal component of the neutron flux at the surfaces of the slugs is the same for all slugs with nonzero values of control (Fig. 1). The interpretation of this result, however, is somewhat different from the result of solving the homogeneous Goertzel problem.

In the second example the Λ_{22} term $\sim \sqrt{U}$ and simulated the blocking of resonance absorption of neutrons. In this case the solution of the optimization problem led not only to the formation of a reflector, but also to unloading of the lattice in the core (Figs. 2, 3), which is characteristic of problems with resonance absorption. The advantage in critical mass turned out to be significantly greater than in the first case.

The algorithm described was used to solve other problems also, for example, the flattening of the power distribution by varying the properties of the control rods.

LITERATURE CITED

1. B. P. Kochurov and V. M. Malofeev, At. Energ., 42, No. 2, 87 (1977).
2. A. M. Pavlovichev and A. P. Rudik, At. Energ., 40, No. 2, 173 (1976).
3. V. V. Khromov et al., in: Physics of Nuclear Reactors [in Russian], Atomizdat, Moscow (1968), p. 159.
4. S. N. Zukhovitskii and L. N. Avdeeva, Linear and Convex Programming [in Russian], Nauka, Moscow (1967).
5. B. P. Kochurov and V. M. Malofeev, Preprint ITÉF-74, Moscow (1977).
6. V. I. Lebedev and S. A. Finogenov, Zh. Vychisl. Mat. Mat. Fiz., 13, No. 1, 18 (1973).
7. G. Goertzel, J. Nucl. Energy, 2, 193 (1956).

DEVELOPMENT OF THE SURFACE PSEUDOSOURCE METHOD FOR CALCULATING NEUTRON FIELDS IN CELLS WITH A BUNDLE OF FUEL-ELEMENT RODS

N. I. Laletin and N. V. Sultanov

UDC 621.039.512.45

Surface Pseudosource Method for an Arbitrary Geometry. Reference [1], which suggested the surface pseudosource method (see also [2, 3]), also described its extension to complex geometries. However, since the detailed equations were written there only for one-dimensional geometries, we shall describe application of the method to an arbitrary geometry. First, we shall consider the single-velocity problem.

Let each zone in a multizone region be described by constant cross sections for neutron interaction with the medium (Σ_t is the total cross section and $\Sigma_s(\Omega' \to \Omega)$ is the differential scattering cross section). The zones also contain volume sources, described by the function $q(\mathbf{r}, \Omega)$. We require the determination of the neutron distribution function in this region, satisfying the one-velocity kinetic equation

$$\Omega\nabla\Psi(\mathbf{r}, \Omega) + \Sigma_t\Psi(\mathbf{r}, \Omega) = \int_{\Omega} \Sigma_s(\Omega' \to \Omega)\,\Psi(\mathbf{r}, \Omega')\,d\Omega' + q(\mathbf{r}, \Omega). \tag{1}$$

It is known that the neutron distribution within the zone is determined uniquely by the volume sources within it and by the angular distribution of neutrons arriving in the zone through the surface S. Therefore, we shall examine an auxiliary problem, in order to determine the neutron distribution function in each zone. We shall select a single zone. Let this zone contain the entire external space. We shall choose the volume neutron sources $q(\mathbf{r}, \Omega)$ in such a way that they coincide with the former sources in the zone considered, and, in all the remaining space, are described by functions which are an extrapolation of the source function $q(\mathbf{r}, \Omega)$ in some way. The extrapolation method may vary and is chosen in specific problems from considerations of convenience in obtaining the solution. At the boundary of the chosen zone we introduce surface pseudosources of strength $g_S(\mathbf{r}_S, \Omega)$ (these may be both sources and sinks), which will provide the same neutron distribution within the zone as in the original problem. As was noted above, the values $g_S(\mathbf{r}_S, \Omega)$ are important for $\Omega\mathbf{n} < 0$ ($\mathbf{n}$ is the normal to the zone boundary, directed outwards). In the rest of the half space of directions the function $g_S(\mathbf{r}, \Omega)$ may be extrapolated arbitrarily. For example, in solving problems with arbitrary geometry it is convenient to take $g_S(\mathbf{r}, \Omega)$ in the form

$$g_s(\mathbf{r}_s, \Omega) = -g_s(\mathbf{r}_s, -\Omega). \tag{2}$$

Then, from the linearity of Eq. (1), the solution in each zone i is written in the form

$$\Psi_i(x) = [G^i(x),\ q^i] + [G^i(x),\ \delta(\mathbf{r}-\mathbf{r}_s)\,g_s^i], \tag{3}$$

where $[G^i(x),\ q] \equiv \int_y G^i(y/x)\,q^i(y)\,dy$ is the scalar product; $G^i(y/x)$, Green's function of Eq. (1) for a homogeneous infinite medium with the sections of the chosen zone i; and y, (x), ensemble of all the variables $(\mathbf{r}, \Omega)$. A similar notation was used also in the second term on the right in Eq. (3).

From the continuity condition with respect to $\mathbf{r}$ and Ω for the neutron distribution function $\Psi(\mathbf{r}, \Omega)$ at the zone boundaries,* we arrive at the following system of integral equations for the surface pseudosources $g_S^i(\mathbf{r}, \Omega)$:

$$[G^i(x),\ q^i] + [G^i(x),\ \delta(\mathbf{r}-\mathbf{r}_{s,i})\,g_s^i] = [G^{i+1}(x),\ q^{i+1}] + [G^{i+1}(x),\ \delta(\mathbf{r}-r_{s,i+1})\,g_s^{i+1}]. \tag{4}$$

*In an approximate solution of the system of equations (4) it is better to consider the quantity $(\Omega\mathbf{n})\Psi(\mathbf{r}, \Omega)$ as continuous.

Translated from Atomnaya Énergiya, Vol. 46, No. 3, pp. 148-154, March, 1979. Original article submitted March 27, 1978.

0038-531X/79/4603-0172 $07.50

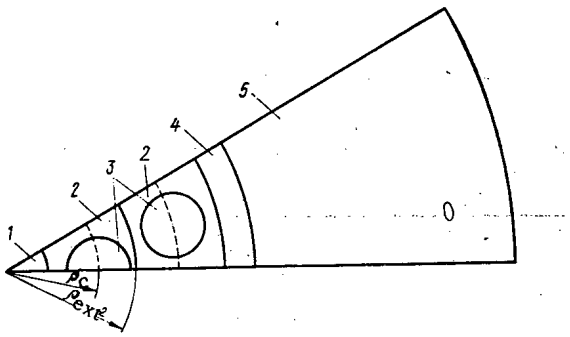

Fig. 1. A symmetry element (1/12) of a reactor channel: 1) zirconium rod; 2) water vapor mixture; 3) fuel element; 4) zirconium tube; 5) graphite.

TABLE 1. Deviation of Average Neutron Fluxes in a Reactor Channel with External Sources

Zone No. (n)	Zone composition	ρ_{ext}, n', ρ_c, cm	Σ_t, 1/cm	Σ_a, 1/cm	$(\bar{\Phi}-\bar{\Phi}_{M-C})/\bar{\Phi}_{M-C}\,100\%$						$\bar{\Phi}_{M-C}$
					G_1^0	$\tilde{G}_1^{0}$*	G_3^0	G_1'	$\tilde{G}_1'$*	G_3'	as calculated by the Monte Carlo method
1	Zr	0,75	0,3485	0,0085	—48	—52	—51	—22	—12	—3	1,34 (1±1,3·10⁻²)
2	H_2O	2,3	2,1318	0,0075	—35	—35	—35	—12	—5	—0,6	1,52 (1±0,6·10⁻²)
	UO_2	1,6	0,6114	0,2455	—36	—36	—36	—13	—6	—0,8	1,338 (1±0,7·10⁻²)
3	H_2O	4,0	2,1318	0,0075	14	14	14	6	2	0,3	3,08 (1±0,3·10⁻²)
	UO_2	3,09	0,6114	0,2455	8,5	8,5	8,4	3,1	1,2	0,2	2,364 (1±0,3·10⁻²)
4	Zr	4,4	0,3485	0,3485	20	19	20	6,2	2,1	0,2	4,64 (1±0,3·10⁻²)
5	C	5,4			20	17	19	7,8	2,0	1,2	5,10 (1±0,2·10⁻²)
6	C	6,4	0,3809	0,0002	18	15	16	8,2	1,2	1,2	5,60 (1±0,2·10⁻²)
7	C	7,7			18	13	15	8	0,5	0,3	6,091 (1±0,2·10⁻²)
8	C	9,0			18	13,5	15	9,3	1,2	1,1	6,473 (1±0,1·10⁻²)

*In this approximation the function $(\Omega n)\Psi(r, \Omega)$ is matched at the zone boundaries.

TABLE 2. Deviation of Average Neutron Flux in a Reactor Channel with External Sources

Zone No. (n)	Zone comp.	ρ_{ext}, n', ρ_c, cm	Σ_t, 1/cm	Σ_a, 1/cm	q, neutrons/cm³	$(\bar{\Phi}-\bar{\Phi}_{M-C})/\bar{\Phi}_{M-C}\,100\%$						$\bar{\Phi}_{M-C}$
						G_1^0	$\tilde{G}_1^{0}$*	G_3^0	G_1'	$\tilde{G}_1'$*	G_3'	as calc. by the Monte Carlo method
1	Zr	0,75	0,3475	0,0075	0,00755	—15	—16	—16	—6	—4	—1,9	0,105 (1±2,5·10⁻²)
2	H_2O	2,3	2,39	0,017	1,366	—15	—13	—14	—6	—1,7	—0,9	0,114 (1±0,9·10⁻²)
	UO_2	1,6	0,6708	0,3233	0	—13	—13	—13	—4	—1,5	—0,1	0,0895 (1±1,1·10⁻²)
3	H_2O	4,0	2,39	0,017	1,366	7	8	8	1,3	1,3	0	0,157 (1±0,6·10⁻²)
	UO_2	3,09	0,6708	0,3233	0	4,7	4,7	4,7	1,3	0,6	0,1	0,1175 (1±0,6·10⁻²)
4	Zr	4,4	0,3475	0,0075	0,00755	12,5	11	13	2,5	1	0,5	0,200 (1±0,9·10⁻²)
5	C	6,4	0,4	0,0636	0,0636	13	12	13	3,8	0,5	0	0,213 (1±1,3·10⁻²)
6	C	9,0	0,4	0,0636	0,0636	13	11	12	4	0,4	0	0,225 (1±0,9·10⁻²)

*In this approximation the function $(\Omega n)\Psi(r, \Omega)$ is matched at the joint boundaries.

Here the equality holds for all values $x=(r_S, \Omega)$, where r_S is any coordinate of the zone boundary.

Thus, using Green's theorem for a uniform infinite medium, we seek to determine a function which is not specified for the whole space, but only on the interzone surfaces.

In a numerical solution of the system of integral equations (4) the surface pseudosources $g_S(r_S, \Omega)$ are decomposed into an appropriate system of functions. Then we must choose the corresponding moments from equations (4). Thus, we transfer from the continuous variables r_S, Ω to discrete variables. For example, if we are dealing with a series of cylindrical surfaces, then it is convenient to expand the functions of the surface variables r_S in a trigonometric series with respect to the axial angle α. The dependence on the angular variable is represented in terms of the spherical functions $Y_n^m(\Omega)$:

$$\Omega \to n,\ m;\quad 0 \leqslant n < \infty,\quad m \leqslant n;$$
$$\mathbf{r}_{s,i} \to \rho_i^j,\ p;\quad 0 < \rho_i^j < \infty,\quad 1 \leqslant j \leqslant J,\quad 0 \leqslant p < \infty. \tag{5}$$

Here ρ_i^j is the radius j of the cylindrical boundary of zone i; p is the axial harmonic number.

We shall denote the entire set of discrete variables by k: $k \equiv (\rho_i^j,\ p,\ n,\ m)$. Then, equating moments at the zone boundary with the set k of the function $(\Omega n)\Psi(r, \Omega)$ we arrive at a matrix equation relative to moments with set k' of the surface pseudosources g_k^i:

$$Q_k^i + \hat{\tilde{G}}_{k',k}^{i} g_{k'}^{i} = Q_k^{i+1} + \hat{\tilde{G}}_{k',k}^{i+1} g_{k'}^{i+1}, \tag{6}$$

where Q_k^i is the moment with set k of the contribution to the distribution function from the volume sources; $\hat{\tilde{G}}_{k',k}^{i}$ is the matrix of moments of function $(\Omega n)\, G^i(y/x)$ with elements of the type $\int\int \varphi(y)\,(\Omega n)\, G(y/x)\, \varphi(x)\, dydx$. Here the functions are

$$\varphi(x) = \begin{Bmatrix} \cos p\alpha \\ \sin p\alpha \end{Bmatrix} Y_n^m(\Omega)\, \delta(\mathbf{r} - \mathbf{r}_{s,j}).$$

We shall restrict attention in the decomposition to the zero-order axial harmonic (P=0) of pseudosources and spherical functions with number $n \leq N$, and obtain the G_N approximation. If we retain harmonics with number $p \leq P$, in the expansion of pseudosources with respect to the axial angle α we have the G_N^p approximation.

Thus, the problem reduces to calculating the required moments of Green's function. Knowing these, from Eq. (6) we find the moments of the pseudosources. Substituting the latter into Eq. (3), we can determine the neutron distribution function at any point of the region. In the procedure for calculating the moments of Green's function, it is appropriate to perform part of the work analytically, writing this function in a convenient coordinate system.

Obtaining the G_N^p Approximation Equations. We apply a method for obtaining the equations of the G_N^p approximation, which allows us to make up an a priori representation of the accuracy of a specific approximation in the problem considered. This method is analogous to that used in [4] to construct other approximations. As was done in [4], we use the formulas of the perturbation theory of [5]. Let

$$L\Psi(x) = q(x); \tag{7}$$
$$L^+\Psi^+(x) = q^+(x), \tag{8}$$

where L is a linear operator; L^+ is the conjugate operator, i.e., it satisfies the relation

$$(u, Lv) = (v, L^+u). \tag{9}$$

Here u(x) and v(x) are any functions from the region of definition of the operators.

We also consider the perturbation operator

$$(L + \delta L)\, \Psi' = q(x). \tag{10}$$

Multiplying Eq. (10) by the conjugate function $\Psi^+(x)$, and Eq. (8) by the perturbed function $\Psi'(x)$, integrating over all the variables, subtracting the second equation from the first, and using Eq. (9), we obtain

$$(q^+, \Psi - \Psi') = (\Psi^+,\ \delta L \Psi'). \tag{11}$$

We use Eq. (11) to obtain the equations of the G_N^p approximation of the surface pseudosource method, treating the discrepancy $L\Psi' - q(x)$ as a perturbation of the original operator.

For the one-velocity case we write the original equation and its conjugate:

$$L\Psi = \Omega\nabla\Psi(x) + \Sigma_t\Psi(x) - \int_\Omega \Sigma_s(\Omega' \to \Omega)\, \Psi(\mathbf{r}, \Omega')\, d\Omega' = q(x); \tag{12}$$

$$L^+\Psi^+ \equiv -\Omega\nabla\Psi^+(x) + \Sigma_t\Psi^+(x) - \int_\Omega \Sigma_s(\Omega' \to \Omega)\, \Psi^+(\mathbf{r}, \Omega)\, d\Omega = q^+(x). \tag{13}$$

In solving Eq. (12) by the surface pseudosource method in the G_N^p approximation the distribution function $\Psi_N^p(x)$ satisfies the kinetic equation (12) within the zones, but is discontinuous at the zone boundary. Thus, the perturbation of the operator is associated with a discontinuity in the distribution function at the zone boundaries, and has the form

$$L\Psi_N^p - q = (\Omega n) \sum_{j=1}^{J} \delta(\rho - \rho_j) [\Psi_N^p(\rho_{j+0}, \alpha\, \Omega) - \Psi_N^p(\rho_{j-0}, \alpha, \Omega)], \tag{14}$$

where j = 1, 2 ...; J, number of the cylindrical boundary; and n, normal to the boundary.

We can write Eq. (11) as:

$$\Delta N = (q^+, \Psi - \Psi_N^p) = (\Psi^+, \delta L \Psi_N^p). \tag{15}$$

We can choose the function $q^+(x)$ in different ways, e.g.:

$$q^+(x) = \Psi(x); \qquad \Delta N \approx \langle \Psi_N^p \rangle^2 - \langle \Psi \rangle^2;$$
$$q^+(x) = \begin{cases} 1, r \in V_j \\ 0, r \bar{\in} V_j, \end{cases} \qquad \Delta N = \langle \Psi_N^p \rangle - \langle \Psi \rangle;$$
$$q^+(x) = \delta(\mathbf{r} - \mathbf{r}'); \qquad \Delta N = \Psi_N^p(\mathbf{r}') - \Psi(\mathbf{r}'),$$

where $\langle f \rangle \equiv \int_x f(x)\, dx$.

We shall expand the conjugate function $\Psi^+(r, \Omega)$ in a Fourier series with respect to the functions cos $p\alpha$, sin $p\alpha$, $Y_n^m(\Omega)$:

$$\Psi^+(\mathbf{r}, \Omega) = \sum_{\tilde{k}} \Psi_{\tilde{k}}^+(\rho) \begin{Bmatrix} \sin p\alpha \\ \cos p\alpha \end{Bmatrix} Y_n^m(\Omega), \tag{16}$$

where $\tilde{k}$ is the set of discrete variables (p, n, m). Substituting expansion (16) into the expression for the error ΔN, we obtain

$$\Delta N = \sum_k \Psi_k^+(\rho) \left(\begin{Bmatrix} \sin p\alpha \\ \cos p\alpha \end{Bmatrix} Y_n^m(\Omega),\ (\Omega n) \times [\Psi_N^p(\rho_{j+0}, \alpha, \Omega) - \Psi_N^p(\rho_{j-0}, \alpha, \Omega)] \right), \tag{17}$$

where $k \equiv (\rho_i^j, p, n, m)$.

Since the quantities $\Psi_k^+(\rho)$ diminish with increase of p and n, it is natural in a specific approximation to require the initial terms of the sum in Eq. (17) to go to zero, i.e., on the zone boundary one must match the moments of the functions $(\Omega n)\Psi(r, \Omega)$ with the smallest numbers. We note the analogy with the boundary conditions of the spherical harmonic method, where the matching of the moments of the function $(\Omega n)\Psi(r, \Omega)$ is also preferred to matching of the moments of the function $\Psi(r, \Omega)$ [6].

Neutron Distribution Function in the Reactor Channel. We now apply the above general procedure of the surface pseudosource method to calculate the neutron field in the engineering channel of a reactor. The channel geometry is illustrated in Fig. 1.

Under the assumption that the density of volume neutron sources is constant, the neutron distribution function takes the form

$$\Psi_i(x) = q_i/\Sigma_a^i + [G^i(x), \delta(\mathbf{r} - \mathbf{r}_s)\, g_s^i]. \tag{18}$$

To simplify the program we introduced an additional boundary between the first and second series of fuel elements, and located in the water. It can be seen from Fig. 1 that, because of symmetry, the surface pseudosources and the neutron distribution function, located on the cylindrical boundaries coaxial with the surface channel, and their expansion in trigonometric series with respect to the axial angle α will contain only terms with sin $p\alpha$ and cos $p\alpha$ (here p = 0, 6, 12 ...). The surface pseudosources and the neutron distribution function on the fuel element surface will evidently satisfy the following symmetry conditions:*

$$g(\rho, \alpha, \theta, \varphi) = g(\rho, 2\pi - \alpha, \theta, \pi - \varphi);$$
$$\Psi(\rho, \alpha, \theta, \varphi) = \Psi(\rho, 2\pi - \alpha, \theta, \pi - \varphi), \tag{19}$$

* This symmetry condition is exact for the functions $g(\rho, \alpha, \theta, \varphi)$ and $\Psi(\rho, \alpha, \theta, \varphi)$ for the first row of fuel elements and up to P = 5 of the second row of elements. Below we shall restrict the symmetry conditions (19).

where θ and φ are the polar and azimuthal angles of Ω. A convenient form for Green's function for all the zones, apart from the water zone, has the form [7]

$$G(\rho', \alpha', \Omega'/\rho, \alpha, \Omega) = \begin{cases} \sum_{p=0}^{\infty}\sum_{l=0}^{\infty}\int_{\nu}\frac{[\Psi^l_{\nu,p}(\rho', \alpha', \Omega')]^+ \times \Phi^l_{\nu,p}(\rho, \alpha, \Omega)}{\nu N(\nu, l, p)}\,d\nu, & \rho' > \rho; \\ \sum_{p=0}^{\infty}\sum_{l=0}^{\infty}\int_{\nu}\frac{[\Phi^l_{\nu,p}(\rho', \alpha', \Omega')]^+ \times \Psi^l_{\nu,p}(\rho, \alpha, \Omega)}{\nu N(\nu, l, p)}\,d\nu, & \rho' < \rho, \end{cases} \tag{20}$$

where the operation $\int_{\nu} f(\nu)\,d\nu = f(\nu_0) + \int_0' f(\nu)\,d\nu$; the regular $\Phi^l_{\nu,p}(\rho, \alpha, \Omega)$ and the singular $\Psi^l_{\nu,p}(\rho, \alpha, \Omega)$ cylindrical elementary solutions were given in [7]; $\nu N(\nu, l, p)$ is the norm of the cylindrical elementary solutions.

When examining the neutron distribution function in the water zone it is more convenient to write Green's function in different coordinates, i.e., to choose the centers of the primed and unprimed cylindrical coordinate systems at different places, e.g., one on the channel axis, the other on the fuel element axis. Transformation of Green's function from the form of Eq. (20) to the required form is very laborious [8]. But these lead to small changes in the initial form of Green's function, which reduce to multiplication in the integrand of the product of the cylindrical elementary solutions, each of which has been written in its own coordinate system, by a factor depending on the distance r between the centers of these coordinate systems. Thus, the values of the Green's functions on the surfaces of the channel of pseudosources, located on the fuel element surface, have the form [8]

$$G(\rho', \alpha', \Omega'/\rho, \alpha, \Omega) = \begin{cases} \sum_{p=0}^{\infty}\sum_{l=0}^{\infty}\int_{\nu}\frac{[\Phi^l_{\nu,p}(\rho', \alpha', \Omega')]^+ \times \Phi^l_{\nu,0}(\rho, \Omega)}{\nu N(\nu, l, p)}\,K_p\left(\frac{r}{\nu}\right)d\nu, & \\ & \rho' + \rho < r; \\ \sum_{p=0}^{\infty}\sum_{l=0}^{\infty}\int_{\nu}\frac{[\Phi^l_{\nu,p}(\rho', \alpha', \Omega')]^+ \times \Psi^l_{\nu,0}(\rho, \Omega)}{\nu N(\nu, l, p)}\,(-1)^p \times & \\ \times I_p\left(\frac{r}{\nu}\right)d\nu, \quad \rho - \rho' > r, & \end{cases} \tag{21}$$

where $I_p(r/\nu)$ and $K_p(r/\nu)$ are modified Bessel functions of first and third order, respectively.

Using the expressions obtained for Green's functions, we convert from continuous to discrete variables. Thus, our problem reduces to solving Eq. (6). Since the moment matrix of Green's function in this equation contains many zeros, we use the method of solution which takes this feature into account [8]. Knowing the moment of the surface pseudosources, we can determine the neutron fluxes at the zone boundaries, and then the average neutron fluxes along the zones of the channel.

Results of Calculations. To determine the accuracy of calculating the average neutron fluxes in the zones of the engineering channel investigated, in the various G^p_N approximations of the surface pseudosource method (the PRAKTINEK program) we compared the results with calculations for the same channels performed by the Monte Carlo method, carried out by A. S. Il'yashenko.

We first calculated for a channel in which the neutrons were flowing inward from outside. In the calculations with both programs the neutrons entering the cell through its outer boundary have a linear-anisotropic angular distribution (the anisotropic term is 7.25%). The initial data and the results of the channel computations are shown in Table 1. The fuel element radius is 0.68 cm. To compare the results of the computation the data were normalized, using the condition that the same number of neutrons should be adsorbed in unit time.

It can be seen from Table 1 that the axially symmetric approximation of the neutron distribution function (the G^0_N approximation) differs from the Monte Carlo calculation of average neutron flux in the zone by up to 50% (in the first row of fuel elements the difference is 35%, and in the graphite and zirconium tube it is 13-15%). Allowance for the first axial harmonic in expanding the neutron distribution function reduces this discrepancy

to 6% in the first row of elements and to 2% in the graphite and zirconium tube in the $\tilde{G}'_1$ approximation, and down to 1% in the G'_3 approximation. Thus, the G^p_N approximations converge rapidly.

We turn now to the matching conditions for the angular moments at the zone boundary: the matching of angular moments of the functions $(\Omega n)\Psi(r, \Omega)$ (in the $\tilde{G}^0_1$ and $\tilde{G}'_1$ approximations) led to better agreement with the higher approximations (G^0_3 and G'_3, respectively) than did matching of the angular moments of the functions $\Psi(r, \Omega)$ (in the G^0_1 and G'_1 approximations).

For the same engineering channel comparative calculations were also performed for the case with homogeneous uniform volume neutron sources throughout the zone (the source density was calculated as being proportional to the slowing-down capability of the zone). The neutron current at the external boundary was assumed to be zero. The mean neutron fluxes in the channel were normalized from the condition that a single neutron should be adsorbed per unit time. The initial data and results of the calculations are shown in Table 2. The results of the calculations repeat the conclusions of the previous computations, but with smaller deviations from the exact data, because of the better smoothness of the distribution function. The axisymmetric approximation (G^0_N) differs from the Monte Carlo method of computation by 5-15% (by 4% in the second row of fuel elements). The results of the calculations in the G'_3 approximation differed by only 1%. The results of the calculations in the $\tilde{G}'_1$ approximation agree better with the G'_3 approximation than with the G'_1 approximation.

Conclusion. This paper has suggested the surface pseudosource method (SPSM) to calculate neutron fields in complex two-dimensional heterogeneous cells in the one-velocity transport approximation. A system of equations has been obtained in the G^p_N approximations. The SPSM has been developed successfully for calculating zone average neutron flux in the engineering channel of a reactor. By comparing results as computed by the SPSM and the Monte Carlo method, one finds that the G^p_N approximations converge rapidly to the exact results, and even the G'_3 approximation gives an error in the average neutron flux of ~1% in all realistic geometry cases (~30 sec of computing time on the BÉSM-6 computer). The calculations show the importance of accounting for the first axial harmonic in the distribution function for neutrons in the channel.

In conclusion, we note that the SPSM is similar to the widely used first collision probability method (FCPM*) and to integral methods, i.e., the result of applying the SPSM in the average quantity over a certain region. The largest differences between the SPSM and the FCPM is that Green's function used in the FCPM for a pure adsorbing medium (the probability of first flight) leads to a requirement to divide the test region into zones with dimensions on the order of the neutron mean free path. There is no such restriction on the zone dimensions in the SPSM. In the FCPM all the zones are interconnected, while in the SPSM only zones having common boundaries are connected. Finally, the basic computing time, both in the FCPM and in the SPSM, arises from computing quantities describing the mutual relationship of zones. But in the SPSM these quantities are the appropriate moments of Green's function and have a form which allows analytical evaluation of a considerable part of the work. This fact is the main reason why the computing time of the programs used in the SPSM in the work examined is less by a factor of 5-10 than the computing time for programs based on the first collision probability method (FCPM), when the same level of accuracy is reached (within the framework of the one-velocity approximation).

LITERATURE CITED

1. N. I. Laletin, Preprint IAÉ-1374, Moscow (1967); in: Numerical Methods in Transport Theory [in Russian], Atomizdat, Moscow (1969), p. 228; in: Methods for Calculating Thermal Neutron Fields in Reactor Lattices [in Russian], Atomizdat, Moscow (1974), p. 187.
2. R. Benawens and J. Devooght, Nucl. Sci. Eng., 32, 249 (1968).
3. P. Benoist and A. Kavenoky, Nucl. Sci. Eng., 32, 270 (1968).
4. N. I. Laletin and A. V. El'shin, Preprint IAÉ-2721, Moscow (1976).
5. G. I. Marchuk and V. V. Orlov, in: Neutron Physics [in Russian], Gosatomizdat, Moscow (1961), p. 30.
6. V. S. Vladimirov, "Mathematical problems in one-velocity neutron transport theory," Tr. MIAN SSSR, Moscow (1961); G. Ya. Rumyantsev, At. Énerg., 10, No. 1, 26 (1961).
7. N. I. Laletin and N. V. Sultanov, Preprint IAÉ-2265, Moscow (1973).
8. N. V. Sultanov, Preprint IAÉ-3005, Moscow (1977).
9. D. Bell et al., Nuclear Reactor Theory [in Russian], Atomizdat, Moscow (1974).

*An account of the fundamentals of the FCPM is given, e.g., in [9].

MEASUREMENTS OF THE FISSION CROSS SECTION OF ^{239}Pu BY NEUTRONS WITH ENERGY FROM 10 eV TO 100 keV

Yu. V. Ryabov

UDC 539.173.4

The fission cross section of ^{239}Pu by neutrons plays an important role among the cross sections of materials applied in nuclear technology. In recent years special attention has been paid in measurements of $\sigma_f(E)$ to the determination of the sources of systematic errors and methods for taking them correctly into account in the final results.

TABLE 1. Basic Characteristics of the Procedure for the Measurements of $\sigma_f(E)^{239}$Pu

Characteristic of the mode	RP	R_2	R_1	SBP
Average power, kV	8—10	28—30	28—30	5—9
Moderator thickness, mm	40	40	40	40
Width at height of neutron pulse, μsec	65	70	70	1,5 3,0
Pulse tracking freq., Hz	0,26	4	4	50—100
Distance to neutron source, m	252,46	252,46	499,96	252,46
Channel width of time analyzer (4096 channels), μsec	16 64	16 64	8 16 64	0,5 1 4
Nominal resolution, μsec/m	0,265 0,361	0,284 0,376	0,141 0,144 0,190	0,0063 0,0120 0,0071 0,0125 0,0169 0,0198
Filter from recycled neutrons	Without filter	Cd	Cd	^{10}B

Remarks. 1. Water was used as the moderator in all measurement modes. 2. Co ($n = 1.1 \cdot 10^{21}$ nuclei/cm^2, $E_i = 0.132$ keV), Mn ($n = 5.4 \cdot 10^{21}$ nuclei/cm^2, $E_i = 0.334$ and 2.35 keV), and Na ($n = 1.9 \cdot 10^{22}$ nuclei/cm^2, $E_i = 2.85$ keV) background filters were used in all the measurement modes; in addition, Ti ($n = 4 \cdot 10^{22}$ nuclei/cm^2, $E_i = 17.5$ keV) was used in the R_i and SBP modes, and Al ($n = 5.8 \cdot 10^{22}$ nuclei/cm^2, $E_i = 35.2$ keV) was used in the SBP mode.

TABLE 2. Energies of the Resonances of ^{239}Pu [4] in the Different Measurement Modes

E_i, eV	RP	R_2	R_1	SBP
7,82	7,823	7,82	7,831	7,818
10,93	10,93	10,91	10,93	10,926
11,89	11,88	11,83	11,90	11,897
14,31	14,34	14,36	14,37	14,345
14,68	14,65	14,65	14,66	14,713
17,66	17,67	17,69	17,70	17,70
22,29	22,31	22,23	22,39	22,31

Translated from Atomnaya Énergiya, Vol. 46, No. 3, pp. 154-158, March, 1979. Original article submitted March 15, 1978.

0038-531X/79/4603-0178$07.50

TABLE 3. Fission Integrals of ^{239}Pu in the Energy Range 100-200 eV

Measurement	$\Sigma\sigma_f\Delta E$, b • eV	Ratio to normalized quantity
Los Alamos [6], 1966	1782	0,973
Harwell [7], 1970	1855	1,013
Dubna [8], 1970	1810	0,989
Oak Ridge [9], 1971	1820	0,994
Saclet [10], 1973	1890	1,032
Normalization value (this paper)	1831±41,8	1,000

TABLE 4. Estimate of Indeterminacy of the $\sigma_f(E)$ Measurements in Different Measurement Modes

Measurement errors	SBP	R_1	R_2	RP
Statistical indeterminacy $\delta\sigma_f/\sigma_f = c(E/\sigma_f\Delta E)^{1/2}$	$c=0,0054$	$c=0,0093$	$c=0,0093$	$c=0,0078$
Indeterminacy of normalization, %	4,56	3,41	3,09	2,98
Indeterminacy in taking background into account, %:				
Below the last high-energy point of the background filter	< 5,50	< 4,03	< 2,13	< 1,38
Above the last high-energy point of the background filter	< 6,1	< 5,42	< 3,81	< 3,95
Statistical indeterminacy and indeterminacy in taking background of the boron standard into account, %	< 4,8		< 4,2	
Indeterminacy of the relative behavior of the boron standard, %	0.3, 1, 2, and 3 for E_n = 10 eV, 1, 10, and 100 keV, respectively			

TABLE 5. Average Fission Cross Section of ^{239}Pu in the 10–3000 eV Energy Range

ΔE, eV	SBP		R_1		R_2		RP		Av. value
	$\langle\sigma_f\rangle \pm \Delta\langle\sigma_f\rangle$	$\langle\overline{\sigma_f}\rangle - \langle\sigma_f\rangle$, %	$\langle\sigma_f\rangle \pm \Delta\langle\sigma_f\rangle$	$\langle\overline{\sigma_f}\rangle - \langle\sigma_f\rangle$, %	$\langle\sigma_f\rangle \pm \Delta\langle\sigma_f\rangle$	$\langle\overline{\sigma_f}\rangle - \langle\sigma_f\rangle$, %	$\langle\sigma_f\rangle \pm \Delta\langle\sigma_f\rangle$	$\langle\overline{\sigma_f}\rangle - \langle\sigma_f\rangle$, %	$\langle\overline{\sigma_f}\rangle \pm \Delta\langle\overline{\sigma_f}\rangle$
10–20	99,83±4,32	+1,18	98,84±4,14	+0,19	98,24±3,22	–0,42	97,68±2,81	–0,99	98,648±0,920
20–30	30,78±1,38	–5,52	34,72±1,40	+6,46	31,02±1,01	–4,70	33,39±0,91	+2,73	32,478±1,903
30–40	3,37±0,43	–18,04	4,41±0,49	+9,80	4,08±0,27	+2,50	4,05±0,23	+1,78	3,978±0,521
40–50	26,07±1,37	+1,92	23,68±0,97	–7,98	26,80±0,89	+4,59	25,73±0,72	+0,62	25,570±1,337
50–60	73,47±3,67	+2,51	71,92±2,89	–0,41	71,77±2,36	–0,21	69,33±1,93	–3,31	71,623±1,711
60–70	56,96±2,93	–0,77	58,01±2,26	+1,05	57,69±1,92	+0,50	56,94±1,58	–0,81	57,400±0,536
70–80	63,93±3,06	+0,45	62,59±2,47	–1,68	64,18±2,19	+0,84	63,87±1,74	+0,36	63,643±0,714
80–90	67,13±3,18	+1,86	64,11±2,18	–2,76	66,27±2,08	+0,59	66,01±1,89	+0,20	65,880±1,273
90–100	32,02±1,83	+1,24	31,49±1,26	–4,22	30,85±1,08	–2,51	32,13±0,92	+1,58	31,623±0,586
100–200	18,31±0,78	—	18,31±0,62	—	18,31±0,57	—	18,31±0,55	—	18,310±0,418 *
200–300	17,57±0,99	–0,94	18,07±0,63	+1,85	17,94±0,57	+1,14	17,36±0,52	–2,16	17,735±0,328
300–400	8,67±0,50	+0,29	8,82±0,33	+1,98	8,89±0,31	+2,76	8,20±0,25	–5,43	8,645±0,310
400–500	9,34±0,57	–1,98	9,37±0,38	–1,64	9,08±0,32	–4,89	10,31±0,33	+7,62	9,524±0,539
500–600	16,34±0,92	–3,01	15,03±0,62	–5,44	15,69±0,54	–1,01	16,33±0,54	+2,95	15,848±0,624
600–700	4,83±0,29	–1,93	4,61±0,19	–6,79	5,03±0,17	+2,13	5,22±0,18	+7,61	4,923±0,303
700–800	6,39±0,35	+8,53	5,55±0,24	–5,32	5,80±0,21	–0,78	5,64±0,19	–3,64	5,845±0,378
800–900	5,33±0,39	+1,82	5,49±0,24	+4,68	5,09±0,19	–2,81	5,02±0,18	–4,24	5,233±0,217
900–1000	8,86±0,60	+1,61	8,97±0,39	+2,82	8,72±0,32	–0,03	8,32±0,28	–4,78	8,718±0,285
1000–2000	4,32±0,29	–4,05	4,87±0,22	+7,70	4,31±0,17	–4,29	4,48±0,15	–0,34	4,495±0,263
2000–3000	3,30±0,22	+2,58	3,20±0,15	–0,47	3,10±0,13	–3,71	3,26±0,12	+1,38	3,215±0,87

* Normalization value of the fission cross section.

With this goal a program of measurements of $\sigma_f(E)$ was carried out for ^{239}Pu in 1970-1972 whose results are presented in this paper. The measurements were carried out with the use of the same procedure for recording fissions as for determining and taking account of the energy dependence of the background in time-of-flight spectra under various operating modes of the neutron spectrometer, which determine the energy resolution and the relative amount of the constant background and the background which depends on the neutron energy.

Measurement Procedure and Data Reduction. Fission events were recorded by a fast-acting high-efficiency multilayer ionization chamber [1] containing 120 mg of ^{239}Pu (1.7% ^{240}Pu; the surface density of the ^{239}Pu

TABLE 6. Average Fission Cross Section of ^{239}Pu (SBP)

ΔE, keV	$\sigma_f(E) \pm \Delta\sigma_f(E)$	ΔE, keV	$\sigma_f(E) \pm \Delta\sigma_f(E)$	ΔE, keV	$\sigma_f(E) \pm \Delta\sigma_f(E)$
3,0—4,0	3,034±0,204	9,0—10,0	1,876±0,133	50,0—60,0	1,496±0,123
4,0—5,0	2,371±0,162	10,0—15,0	1,719±0,126	60,0—70,0	1,459±0,125
5,0—6,0	2,206±0,151	15,0—20,0	1,655±0,124	70,0—80,0	1,503±0,136
6,0—7,0	1,997±0,134	20,0—30,0	1,597±0,122	80,0—90,0	1,487±0,143
7,0—8,0	2,202±0,154	30,0—40,0	1,568±0,121	90,0—100,0	1,506±0,144
8,0—9,0	2,243±0,153	40,0—50,0	1,519±0,124		

TABLE 7. ^{239}Pu Fission Cross Section (R_1)

E, keV	$\sigma_f(E) \pm \Delta\sigma_f(E)$	E, keV	$\sigma_f(E) \pm \Delta\sigma_f(E)$	E, keV	$\sigma_f(E) \pm \Delta\sigma_f(E)$
3,11	3,32±0,17	6,29	1,83±0,11	16,70	1,78±0,11
3,27	3,29±0,17	6,76	2,01±0,13	18,80	1,69±0,11
3,45	3,24±0,17	7,28	2,16±0,13	21,30	1,69±0,11
3,63	3,05±0,16	7,86	2,18±0,13	24,27	1,62±0,11
3,83	2,84±0,15	8,52	2,19±0,13	28,13	1,63±0,11
4,05	2,67±0,15	9,26	1,97±0,12	32,83	1,56±0,12
4,29	2,65±0,15	10,10	1,82±0,12	38,82	1,53±0,12
4,55	2,29±0,13	11,05	1,61±0,10	46,62	1,51±0,12
4,84	2,33±0,14	12,17	1,74±0,11	57,03	1,50±0,12
5,15	2,25±0,14	13,45	1,66±0,10	71,39	1,53±0,12
5,49	2,01±0,12	14,95	1,67±0,10	91,97	1,48±0,13
5,87	2,17±0,13				

TABLE 8. ^{239}Pu Fission Cross Section (R_2)

E, keV	$\sigma_f(E) \pm \Delta\sigma_f(E)$	E, keV	$\sigma_f(E) \pm \Delta\sigma_f(E)$	E, keV	$\sigma_f(E) \pm \Delta\sigma_f(E)$
3,10	2,994±0,126	4,79	2,510±0,133	8,37	2,271±0,175
3,43	2,731±0,126	5,43	2,189±0,128	9,90	2,108±0,176
3,81	2,456±0,118	6,21	2,088±0,131	11,88	1,745±0,159
4,26	2,172±0,109	7,17	2,207±0,147		

TABLE 9. ^{239}Pu Fission Cross Section (RP)

E, keV	$\sigma_f(E) \pm \Delta\sigma_f(E)$	E, keV	$\sigma_f(E) \pm \Delta\sigma_f(E)$	E, keV	$\sigma_f(E) \pm \Delta\sigma_f(E)$
3,18	3,168±0,125	5,25	2,266±0,110	10,30	1,765±0,109
3,34	2,969±0,122	5,60	2,163±0,108	11,28	1,631±0,107
3,51	2,951±0,121	5,99	2,151±0,108	12,41	1,796±0,113
3,70	3,128±0,126	6,41	2,019±0,106	13,72	1,685±0,108
3,91	2,781±0,121	6,89	2,095±0,109	15,24	1,645±0,107
4,13	2,552±0,117	7,42	2,236±0,113	17,04	1,721±0,114
4,38	2,255±0,108	8,01	2,291±0,116	19,17	1,695±0,113
4,64	2,423±0,111	8,68	2,181±0,113	21,73	1,610±0,112
4,93	2,318±0,112	9,44	2,018±0,109	34,84	1,556±0,111

sample was $2.19 \cdot 10^{-5}$ atom/b). The chamber was placed at the center of a cavity made of borated paraffin and lead through whose center passed a well-collimated neutron beam.

The IBR-30 of the JINR was used as the pulse source of neutrons in the reactor mode (R), the rare-pulse mode (RP), and the subcritical booster pulse mode (SBP) with an LÉU-40 linear electron accelerator [2, 3]. The energy dependence of the fission counting rate was recorded by an Ai-4096 time analyzer with intermediate memory having a dead time of $\sim 1\,\mu$sec (Table 1).

The spectrum of the neutrons from the pulse source was measured by a bank of type NWI-62 proportional counters filled with BF_3 (82.3% ^{10}B). After taking the background into account, the analytic shape of the spectrum was calculated by the method of least squares (MLS).

The energy dependence of the background in the temporal spectra was determined experimentally with the help of absorbing resonance filters which extract neutrons of the appropriate energies from the beam. A series of measurements of the effect and the background were reduced to the same integral neutron flux with the help of several monitoring boron counters with independent recording mounted around the periphery of the neutron beam in front of the collimator and the background filters. This procedure of comparing two spectra was in good agreement with the ratio of the areas of the very same low-energy resonances of ^{239}Pu in the series of measurements of the effect and the background. The energy dependence of the smooth background

curve was analytically represented in the form of a quadratic polynomial whose coefficients were determined by MLS upon adjustment to background points under "black" filters.

The accuracy of the determination of the energy scale in the time-of-flight spectra was checked from the position of the low-energy resonance of ^{239}Pu. The energy position of the resonances determined in this paper and in [4], in which the measurements were made with a sample cooled to liquid-nitrogen temperature, is compared in Table 2. Good agreement is observed within the limits of the errors.

The relative behavior of $\sigma_f(E_i)$ was determined from the expression

$$\sigma_f(E_i) = \{k[N_f(E_i) - N_b(E_i)]E_i^q\}/\Delta E_i,$$

where E_i is the energy corresponding to the i-th time channel of the analyzer, $N_f(E_i)$ is the fission counting rate in the i-th channel, $N_b(E_i)$ is the energy width of a channel of the time analyzer, ΔE_i is the energy width of a channel of the time analyzer, E_1^q is the relative behavior of the neutron flux (q = 0.93 and 0.82 for the reactor and subcritical booster modes, respectively), and k is the normalization constant of the fission cross section. Above an energy of 1 keV a correction for the deviation of the cross section of the boron standard from the 1/v law [5] was introduced into the final result.

The normalization of the experimental curve of the fission counting rate was carried out in the 100-200 eV energy range, using the values of the fission integral (Table 3) obtained with the application of the same normalization, straight line or tangent, by $\sigma_f^{th} = 742.5 \pm 3.7$ b. The method of normalization in the 100-200 eV range was selected because it is identically applicable in all the operating modes of the neutron spectrometer, permits excluding possible systematic errors due to a difference in the energy resolution, and avoids the possible influence of the finite thickness of the sample being investigated, which arises in connection with normalizations in the region of low-energy resonances.

The indeterminacy in the $\sigma_f(E)$ measurements which is amenable to analysis is given in Table 4 on the assumption of constancy of the efficiency of the ionization chamber in the energy range being investigated.

Discussion of the Results. The average values $\langle\sigma_f(E)\rangle$ are given in Table 5 in standard energy ranges, which could be determined rather accurately in the different measurement modes up to 3 keV. The average value $\langle\overline{\sigma_f(E)}\rangle$ for each of the four measurement modes and the mean square deviation from the average are also given for each range. In order to estimate possible systematic errors in the total energy range, the results of each measurement mode are characterized also by the deviation from $\langle\overline{\sigma_f(E)}\rangle$ with the sign of this deviation taken into account. It is evident from Table 5 that there are no clear systematic deviations of a single sign in the results of any measurement mode in the total energy range. In addition, the distribution of the deviations from the average for all the measurement modes and in all the standard ranges within the limits of 10-3000 eV is well described by a Gaussian curve with $\sigma = \pm 5.4\%$. This value is close to the average error $\langle\overline{\sigma_f(E)}\rangle$ in the entire energy range. The values of $\sigma_f(E)$ from 3 keV to a maximum energy of ~100 keV are given in Tables 6–9. The calculation of $\sigma_f(E)$ in each measurement mode was restricted by the energy region in which the effect of fast neutrons of the pulse source did not yet appear directly and the background was extrapolated well by a quadratic polynomial. The increase in the error in the high-energy region is associated with the indeterminacy of the background extrapolation, an increase in the relative value of the background, and a decrease of statistical accuracy.

The fission cross sections obtained in the different measurement modes are in good agreement with each other within the limits of the errors. Accordingly, the discrepancies in the energy resolution of the neutron time-of-flight spectrometer have no appreciable effect on the results in connection with the experimental accuracy attained. However, one should note that above 30 keV the values of $\sigma_f(E)$ obtained in this paper are systematically lower by 2-4% on the average than the values recommended in the review [11]. A possible cause for this may be an overestimate of the background level in the last high-energy resonance of the appropriate filter without the introduction of a correction for the resolution of the time-of-flight spectrometer and the impossibility of using very thick background filters, which significantly alter the neutron flux in the entire energy region being investigated. But this systematic overestimate of $\sigma_f(E)$ does not excced the error limits of the measurements.

In conclusion, the author expresses his gratitude for much assistance in making the measurements to Tyan San Khak, Zen Chan Bom, and Yu. Kolgin, as well as to the operating staffs of the IBRa and the LNF measurement center for providing reliable operation of the recording instrumentation.

LITERATURE CITED

1. V. N. Kononov et al., Prib. Tekh Eksp., No. 6, 51 (1969).
2. G. E. Blokhin et al., At. Energ., 10, No. 5, 437 (1961).
3. V. L. Anan'ev et al., At. Energ., 20, No. 2, 106 (1966).
4. J. Blons et al., in: Proc. IAEA Symp. "Nuclear Data for Reactors – 1970," Vol. I, Helsinki (June 15-19, 1970), p. 469.
5. M. Sowerly et al., Report AERE-R6316 (1970).
6. E. Shunk et al., in: Proc. Symp. "Neutron Cross Sections Technology," Vol. II (1966), p. 979.
7. G. James, in: Proc. IAEA Symp. "Nuclear Data for Reactors – 1970," Vol. I, Helsinki (June 15-19, 1970), p. 267.
8. Yu. V. Ryabov et al., JINR Preprint RZ-5113, Dubna (1970).
9. R. Gwin et al., Report ORNL-4707 (1971).
10. J. Blons, Nucl. Sci. Eng., 51, 130 (1973).
11. T. Byer, At. Energy Rev., 10, No. 4, 529 (1972).

MEASUREMENT OF THE TOTAL NEUTRON CROSS SECTIONS OF ^{153}Eu, ^{154}Eu, AND ^{155}Eu

V. A. Anufriev, S. I. Babich,
A. G. Kolesov, V. N. Nefelov,
V. A. Poruchikov, V. A. Safonov,
A. P. Chetverikov, V. S. Artamonov,
R. N. Ivanov, and S. M. Kalebin

UDC 621.039.556

This article continues an investigation of the resonance parameters of radioactive nuclei and fission products with the neutron spectrometer of the SM-2 reactor and is devoted to the measurement of the total neutron cross sections of ^{153}Eu, ^{154}Eu, and ^{155}Eu. Such information is of interest in connection with calculations of the effect of fission products on reactor characteristics [1]. One should note that the laws of interaction of neutrons with the class of odd–odd nuclei have not yet been thoroughly studied; therefore, measurements of the neutron cross sections of ^{154}Eu are also of scientific interest. The total cross sections of $^{154, 155}$Eu averaged over the reactor spectrum which were obtained by the activation method are given in [2, 3]. The first results on the measurement of the total neutron cross sections of $^{154, 155}$Eu on a neutron time-of-flight spectrometer were obtained at the Institute of Nuclear Physics of the Academy of Sciences of the Ukrainian SSR [4, 5].

As an example of the method of obtaining radioactive ^{154}Eu and ^{155}Eu, irradiation of the original ^{153}Eu by the neutron flux of the SM-2 reactor was used. The measurements of the neutron cross sections of the europium samples were made with the spectrometer of the SM-2 reactor [6] with a best resolution of 50 nsec/m. SNM-17 helium counters and a 4096-channel time analyzer were used as the recording system. The measurements with the highly active nuclei of ^{154}Eu and ^{155}Eu were carried out on a special apparatus for the measurement of irradiated samples.

Europium-153. Information on the resonance parameters of ^{153}Eu obtained under the same conditions as in the case of the investigation of isotopes of europium is necessary for calculation and identification of the neutron levels of the samples. Samples in the form of Eu_2O_3 enriched in ^{153}Eu (98.9%) were used in the measurements of the transmission of ^{153}Eu (Table 1). The resonance parameters of ^{153}Eu in the 1.728–31.2 eV region are presented in Table 2. An appreciable discrepancy of the parameter $2g\Gamma^0_n$ from the value recommended in [7] is observed for the three energy levels 4.77, 15.25, and 22.56 eV: 0.037, 0.108, and 0.64 MeV, respectively.

Europium-154 and Europium-155. An accumulation of ^{154}Eu ($T_{1/2}$=8.6 years) and ^{155}Eu ($T_{1/2}$=4.7 years) was accomplished by means of the irradiation of the original europium isotopes (98.9% ^{153}Eu and 1.1% ^{151}Eu)

Translated from Atomnaya Énergiya, Vol. 46, No. 3, pp. 158-160, March, 1979. Original article submitted April 17, 1978.

0038-531X/79/4603-0182 $07.50

TABLE 1. Composition of Four Original Europium Samples, nuclei/cm^2

Isotope	Sample			
	1	2	3	4
^{151}Eu	$1{,}44\cdot10^{20}$	$7{,}93\cdot10^{19}$	$2{,}46\cdot10^{19}$	$1{,}35\cdot10^{19}$
^{153}Eu	$1{,}28\cdot10^{22}$	$7{,}04\cdot10^{21}$	$2{,}19\cdot10^{21}$	$1{,}21\cdot10^{21}$

TABLE 2. Parameters of Neutron Resonances of ^{153}Eu

E_0, eV	Γ, MeV	$2g\Gamma_n^0$, MeV	E_0, eV	Γ, MeV	$2g\Gamma_n^0$, MeV
1,728	87±5	0,037±0,002	16,68	110±10	0,33±0,002
2,450	88±5	0,73±0,03	17,52	90±17	0,11±0,01
3,302	101±5	0,47±0,07	17,95	90±7	0,99±0,02
3,905	90±3	0,51±0,05	18,68	147±18	0,65±0,02
4,77	91±4	0,014±0,003	19,95	124±17	2,17±0,23
6,16	101±6	0,25±0,02	22,56	91±14	0,44±0,05
8,85	88±8	1,23±0,10	23,68	91±17	0,59±0,08
11,61	94±5	1,16±0,04	26,2	90±10	0,03±0,02
12,42	76±10	0,034±0,011	28,65	67±13	0,31±0,01
13,22	90±5	0,088±0,003	29,9	90±10	0,04±0,02
15,25	110±9	0,069±0,008	31,2	116±10	0,35±0,07
16,33	90±10	0,004±0,002			

TABLE 3. Composition of the Europium Samples, nuclei/cm^2

Isotope	Sample 1 (cadmium-plated)		Sample 2 (bare)	
	prior to irradiation	after irradiation	prior to irradiation	after irradiation
^{151}Eu	$1{,}44\cdot10^{20}$	$1{,}20\cdot10^{20}$	$7{,}93\cdot10^{19}$	$7\cdot10^{17}$
^{152}Eu	—	$1{,}2\cdot10^{19}$	—	$7\cdot10^{18}$
^{153}Eu	$1{,}28\cdot10^{22}$	$1{,}18\cdot10^{22}$	$7{,}04\cdot10^{21}$	$5{,}4\cdot10^{21}$
^{154}Eu	—	$6{,}35\cdot10^{20}$	—	$1\cdot10^{21}$
^{155}Eu	—	$2{,}7\cdot10^{19}$	—	$2{,}8\cdot10^{20}$
^{152}Sm	$1{,}32\cdot10^{18}$	$2{,}54\cdot10^{18}$	$7{,}25\cdot10^{17}$	$4{,}62\cdot10^{18}$
^{156}Eu	—	—	—	—
(^{156}Cd)	—	$1\cdot10^{17}$	—	$2{,}1\cdot10^{20}$

TABLE 4. Parameters of Neutron Resonances of ^{154}Eu

E_0, eV	Γ, MeV	$2g\Gamma_n^0$, MeV	E_0, eV	Γ, MeV	$2g\Gamma_n^0$, MeV
0,188	160±15	0,157±0,032	9,48	113±9	0,57±0,06
0,842	126±12	0,035±0,003	10,70	108±15	0,12±0,02
1,372	108±5	0,26±0,02	10,95	115±10	0,17±0,02
3,51	115±15	0,10±0,02	12,54	175±22	0,28±0,04
4,14	130±20	0,27±0,02	13,68	117±20	0,170±0,013
5,22	140±6	0,18±0,01	15,97	100±21	0,095±0,012
5,63	127±10	0,110±0,005	21,07	135±18	0,91±0,04
6,65*	100	0,01	22,17	145±20	0,59±0,04
6,82	152±8	0,47±0,03	25,10	120±30	0,22±0,02
9,32	108±10	0,88±0,09	27,30	96±7	0,12±0,01

* Possibly a level of ^{155}Eu.

in the form of Eu_2O_3 in the SM-2 reactor. Two samples were investigated for identification of the neutron levels of ^{154}Eu and ^{155}Eu, the samples differing in the ratio of these isotopes.

The first sample (400 mg of Eu_2O_3), placed into a cadmium shield, was irradiated in the vertical channel of the SM-2 reactor at a flux density of the epicadmium neutrons of $\Phi_{epi} = 3.1 \cdot 10^{13}$ neutrons/(cm^2 · sec). The

TABLE 5. Parameters of Neutron Resonances of ^{155}Eu

E_0, eV	Γ, MeV	$2g\Gamma_n^0$, MeV	E_0, eV	Γ, MeV	$2g\Gamma_n^0$, MeV
0,602	90±6	4,30±1,03	20,70	110±18	3,08±0,15
2,04	100	0,032	26,2	100	0,64
7,19	100	0,078	33,10	100±20	13,9±2,4
15,48	100±9	1,49±0,11			

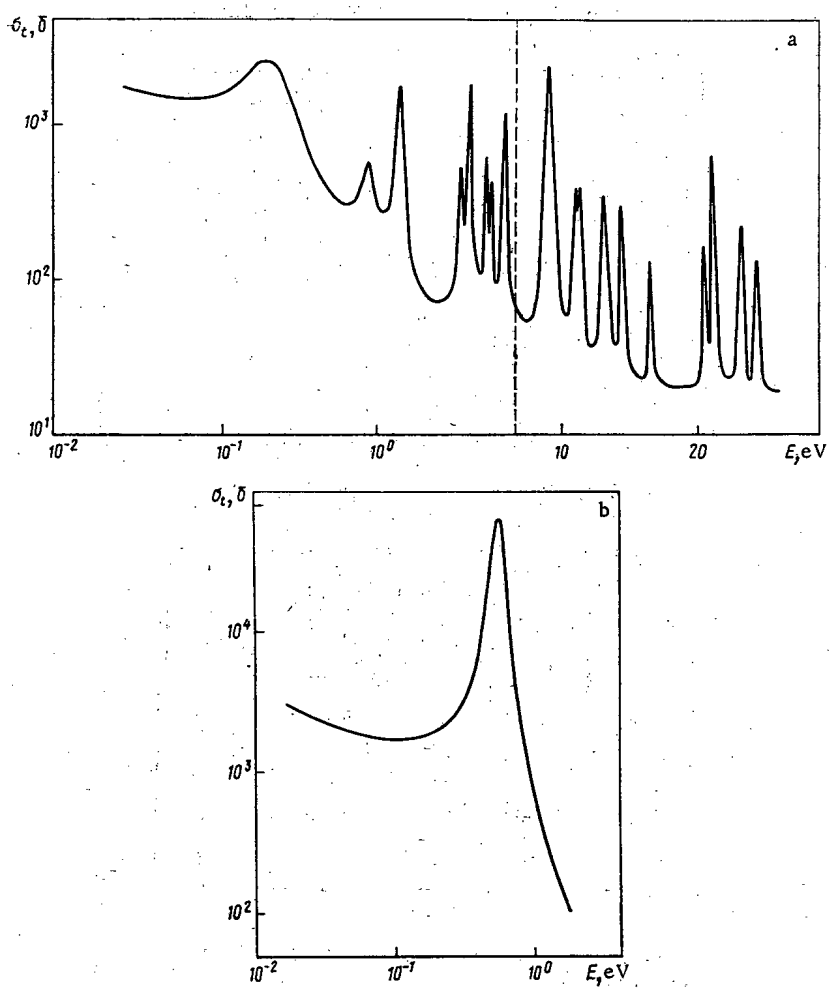

Fig. 1. Total neutron cross section of (a) ^{154}Eu (above 8 eV the the scale of the energy axis is changed) and (b) ^{155}Eu.

second sample with a mass of 200 mg was irradiated in the same channel of the reactor at a thermal neutron flux density of $9 \cdot 10^{14}$ neutrons/(cm^2 · sec).

The isotopic composition of the irradiated and non-irradiated europium samples was measured by the mass spectrometer method. The amount of nuclei in the samples (Table 3) was determined by tieing the isotopic composition to the amounts of ^{153}Eu and ^{151}Eu obtained from the known resonance parameters.

The measurements of the transmission of the samples were made relative to an "empty" false sample and a false sample made of the original europium. These measurements, as well as the inclusion of data on ^{153}Eu and the use of different samples, permitted identifying reliably the levels of ^{154}Eu and ^{155}Eu and calculating their resonance parameters.

In the 0.188–27.30 eV region 20 levels were identified for ^{154}Eu, and seven levels were found in the 0.602–33.10 eV region for ^{155}Eu. The resonance parameters calculated by the "shape" method are given in Tables 4 and 5. The dependences of the total cross sections on neutron energy are presented in Fig. 1 for ^{154}Eu and ^{155}Eu as calculated from the resonance parameters obtained on the basis of the expression

$$\sigma_t = \frac{1}{n} \ln \frac{1}{T},$$

where n is the number of nuclei of the isotope per 1 cm^2 and T is the transmission of the isotope calculated from the resonance parameters with the Doppler effect and spectrometer resolution taken into account.

A value $\bar{\Gamma}_\gamma = 130$ MeV is obtained for ^{154}Eu from the experimental results, which exceeds somewhat the average radiative width for stable ^{151}Eu and ^{153}Eu. The average distance between the levels of ^{154}Eu and ^{155}Eu amounts to 1.1 ± 0.1 and 4.8 ± 0.4 eV, respectively. The force functions are equal to $2.5 \cdot 10^{-4}$ and $2.35 \cdot 10^{-4}$, respectively, for the spin state, which is in agreement with the results of calculations according to static models in the mass-number region being studied [8]. The resonance capture integrals for ^{154}Eu and ^{155}Eu, which are equal to 1620 ± 240 and $17{,}600 \pm 4000$ b, respectively, were also calculated from the parameters obtained.

LITERATURE CITED

1. J. Tyror, Panel Meeting on Fission Nuclear Data, IAEA, Bologna (Aug. 26-30, 1973).
2. R. Hayden, Phys. Rev., 75, 1500 (1949).
3. R. Mowatt, Can. J. Phys., 48, 1933 (1970).
4. V. F. Razbudei et al., in: Trans. of Conf. on Neutron Physics, TsNIIatominform, Moscow (1976), Part 3, p. 161.
5. V. P. Vertebnyi et al., ibid., (1977), Part 2, p. 267.
6. T. S. Belanova et al., Preprint NIIAR P-6 (272), Dimitrovgrad (1976).
7. BNL-325, 3rd edition (1973).
8. G. Lautenbach, RNC-191 (1973).

BLISTERING IN NIOBIUM UNDER IMPLANTATION OF HELIUM IONS AT ENERGY EXPECTED IN THERMONUCLEAR REACTOR

S. Das, M. Kaminsky (U.S.A.),
V. M. Gusev,* M. I. Guseva,
Yu. L. Krasulin, and Yu. V. Martynenko (USSR)

UDC 539.12.04:621.039.616

In accordance with present ideas, the first wall of thermonuclear reactors will be subjected to bombardment with helium ions with a broad spectrum, which will result in erosion of the wall because of the effects of sputtering and blistering. Until recently radiation-induced blistering was studied by irradiating metals with monoenergetic helium ions. Erosion due to blistering depends appreciably on the distribution of implanted ions and defects over the depth. Earlier [1], a beam with a broad energy spectrum was simulated by successive bombardment of a target with monoenergetic beams of helium ions of energy 3-500 keV. In the first approximation, uniform distribution of the helium atoms over the depth of the target was attained. The metal chosen for the target was niobium, in which helium has a low penetrability, and, therefore, the distribution of implanted helium ions could not noticeably vary in the time between successive bombardments. In niobium it was shown that with the same dose of irradiation with monoenergetic and polyenergetic He^+ ions, a substantial difference is observed in the laws governing the formation of blisters.

In the present paper we simulate how a niobium target is affected by He^+ ions with an energy spectrum which can be expected in thermonuclear reactors and with an ion temperature of 20 keV inside a plasma filament and 1 keV in the outer layer.

In thermonuclear reactors the energy spectrum of deuterium and tritium particles impinging on the first wall can be approximated [2] by

*Deceased.

Translated from Atomnaya Énergiya, Vol. 46, No. 3, pp. 161-165, March, 1979. Original article submitted December 5, 1977.

0038-531X/79/4603-0185 $07.50

$$f=\frac{2\sqrt{E}}{\sqrt{\pi}\,(T_1^{3/2}+\alpha T_2^{3/2})}\left[\exp\left(-\frac{E}{T_1}\right)+\alpha\exp\left(-\frac{E}{T_2}\right)\right], \quad (1)$$

where T_1 is the mean temperature of the coldest surface layer of the plasma, T_2 is the mean temperature of the internal hot layers of plasma, and α is the fraction of hot particles striking the wall. In accordance with [2], $\alpha \approx 10^{-3}$.

The energy of α particles produced in the D–T reaction is 3.5 MeV. It may be assumed [5], however, that part of these particles are "thermalized" and will have the spectrum (1), another part will have an energy close to E_α, and the remainder will have a uniform energy distribution. Accordingly, as a rough approximation we may assume (Fig. 1) that

$$f_\alpha = A\delta(E-E_\alpha)+B\sqrt{E}\left[\exp\left(-\frac{E}{T_1}\right)+\alpha\exp\left(-\frac{E}{T_2}\right)\right]+C. \quad (2)$$

The relative values of constants A, B, and C can be chosen from the following conditions. On the basis of the results of [3] it may be assumed that the number of α particles with an energy E_α is ~10% and if it is assumed that the fraction of "thermalized" particles will be the same as in [3], then

$$C \approx \frac{10^{-1}B}{E_\alpha}(T_1^{3/2}+\alpha T_2^{3/2}). \quad (3)$$

In a real thermonuclear reactor the He^+ ion spectrum may be somewhat different. Evidently, account must also be taken of the ion distribution over the angles of incidence. No data are as yet available on these distributions and it is thus desirable to simulate the effect of spectrum (2) on a niobium target (see Fig. 1).

Experiment. The energy ranges were chosen so that the distribution of implanted ions from two successive irradiations overlapped quite well and the minimum energy was $E_1 < T_1$. In accordance with these requirements niobium targets were successively irradiated with He^+ ions possessing an energy of 0.5, 1, 2, 3.5, 5, 8, 13, 20, 45, 65, 90, 150, 200, 250, 300, 500, 1000, 1500, 2500, 3000, and 3500 keV. Irradiation with an energy of $E_k \leq 90$ keV was carried out at the I. V. Kurchatov Institute of Atomic Energy and with $E_k \geq 150$ keV, at the Argonne National Laboratory (U.S.A.). Two series of experiments were carried out. In the first, the irradiation was started from 0.5 keV and the energy was then gradually increased to 3.5 MeV, whereas in the second, the irradiation was carried out in the reverse order, starting from 3.5 MeV. The density of the ion current was 20-30 $\mu A/cm^2$. Segments with a diameter of 3 mm irradiated with integrated doses of $7.7 \cdot 10^{17}$ and $7 \cdot 10^{18}$ ions/cm^2 were obtained on the target. Of the integrated dose, 87.7% came in the energy range 0.5-90 keV with 74% in the range 0.5-3.5 keV.

Comparison of the microstructures (Figs. 2a and b) reveals that there are no blisters on the irradiated surface. It should be also noted that the dose of irradiation with helium ions having an energy of 1 and 2 keV exceeded the critical values.

The change in the topography of the surface for an integrated dose of $7 \cdot 10^{18}$ ions/cm^2 is illustrated by Fig. 3. Figure 3a shows blistering damage to niobium surface after irradiation with He^+ ions possessing an energy of 0.5 to 90 keV with a total dose of $6.25 \cdot 10^{18}$ ions/cm^2. Blisters of various sizes are visible, some of which have had their skin peel off. The size distribution of the blisters is given in Fig. 4. In accordance with the energy spectrum (see Fig. 1), most of the blisters are produced by He^+ ions with an energy of 0.5-3.5 keV and have a diameter < 1 μm. The maximum blister diameter (~5 μm) corresponds to He^+ ions with an energy of 90 keV [4]. Although such blisters are few in number, most of them have had their skin peel off. The thickness of the skin of these blisters is 0.36 μm, as can be seen well under high magnification. The erosion rate calculated from the photomicrograph (see Fig. 3a) is $2.6 \cdot 10^{-2}$ atoms/ion. For comparison, we shall show that according to the data of Kaminsky and Das [5] the rate at which the deposited niobium is eroded under the action of monoenergetic He^+ ions with an energy of 100 keV and an irradiation dose of $3.12 \cdot 10^{16}$ ions/cm^2 is 1 atom/ion, i.e., approximately 40 times that for He^+ ions with an energy of 0.5 to 90 keV with twice the dose.

Figure 3b presents the microstructure of the surface of the same target after further irradiation with He^+ ions with an energy of 150-3500 keV at a dose of $7.7 \cdot 10^{17}$ ions/cm^2. As is seen from comparison with Fig. 3a, the implantation of energetic He^+ ions does not appreciably affect the blistering from the implantation of ions of lower energy.

If the irradiation was started from a maximum energy of 3.5 MeV and the irradiation energy was then gradually decreased, then after irradiation in the energy range 3.5 MeV-150 keV with a dose of $7.7 \cdot 10^{17}$ ions/cm^2 blisters were not detected on the surface of the niobium. The micrograph in Fig. 5 shows the surface after irradiation with an integrated dose of $7 \cdot 10^{18}$ ions/cm^2 in the range from 3.5 MeV to 0.5 keV. Most of the

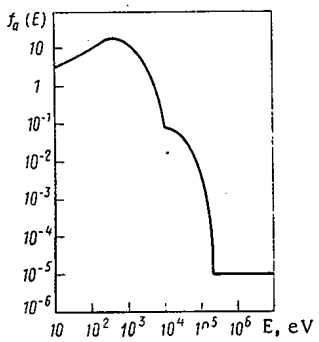

Fig. 1. Energy spectrum of α particles.

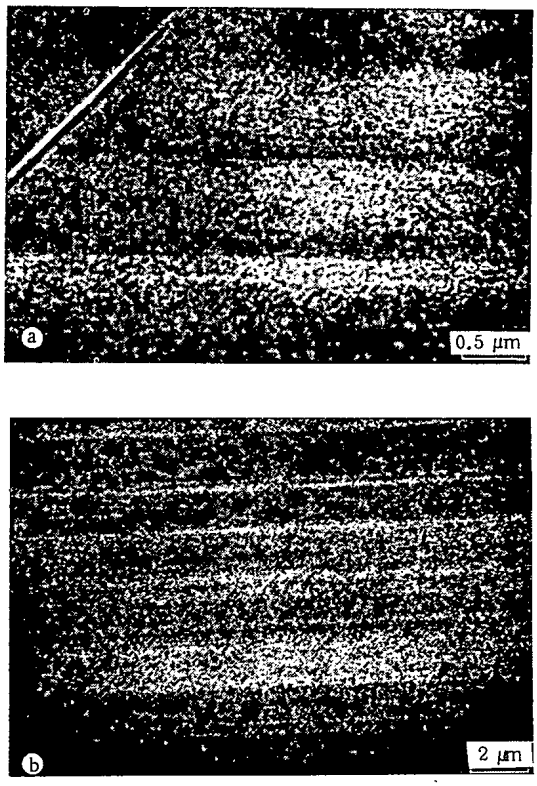

Fig. 2. Microstructure of surface of niobium target before (a) and after (b) irradiation with He^+ ions with an integrated dose of $7.7 \cdot 10^{17}$ ions/cm^2.

blisters have an undamaged skin. The blisters are smaller than in the case of irradiation in the order from 0.5 keV to 3.5 MeV with the same dose (see Fig. 4). The maximum blister diameter does not exceed 0.9 μm. According to [6], blisters of this size are formed by 20-KeV ions. When the skins of these, largest-sized blisters are peeled off small blisters with a diameter of 0.05-0.2 μm, produced by He^+ ions with an energy of 1-5 keV (see arrow in Fig. 5), can be seen on the bottom of the craters. As follows from Fig. 1, maximum radiation doses with the energy spectrum studied correspond to this energy range. The area occupied by such craters does not exceed 2%. Bearing in mind also that the thickness of the skins of blisters formed by 20-keV He^+ ions is approximately one-third [7] that in the case of implantation of 90-keV ions, we may conclude that the erosion rate when the energy of bombarding He^+ ions is decreased gradually from 3.5 MeV to 0.5 keV is approximately one order of magnitude smaller than under irradiation in the reverse order.

Discussion of Results. It has thus been demonstrated experimentally that when a target is successively irradiated with He^+ ions of different energies, the blistering is considerably smaller than under monoenergetic irradiation [1]. Similar results were also obtained in studies with uniform distribution of implanted helium atom over the depth of the target [6, 7]. In [6] the explanation given for the expression of blistering under preliminary irradiation with less energetic ions was that such "prebombardment" causes damage near the surface from which helium atoms can emerge on the surface. This explanation does not, however, make it

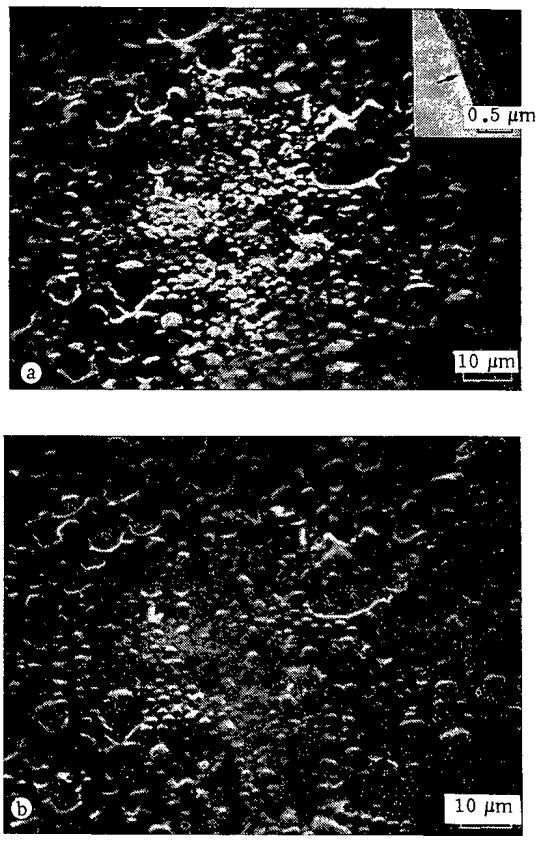

Fig. 3. Microstructure of surface of niobium target after irradiation with He^+ ions at integrated doses of $6.25 \cdot 10^{18}$ over the range 0.5-90 keV (a) and $7 \cdot 10^{18}$ ions/cm^2 in interval 0.5-3500 keV (b).

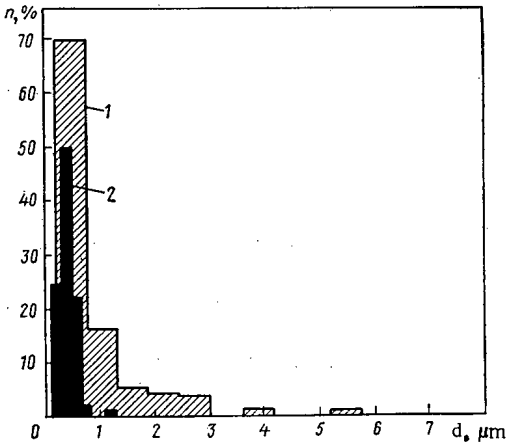

Fig. 4. Distribution of blisters according to diameter under irradiation with dose of $7 \cdot 10^{18}$ ions/cm^2 over range from 0.5 to 3500 keV (1) and in reverse order (2).

possible to understand why an even greater reduction of blistering is observed when the ion energy is gradually decreased from 3.5 MeV to 0.5 keV (see Fig. 3b and Fig. 5).

It was suggested in [8] that in the layer containing helium atoms and vacancies, combined into small bubbles, there exists an elevated pressure

$$P = H\,[C_{He} - C_V\,(\Omega_V/\Omega_{He}], \qquad (4)$$

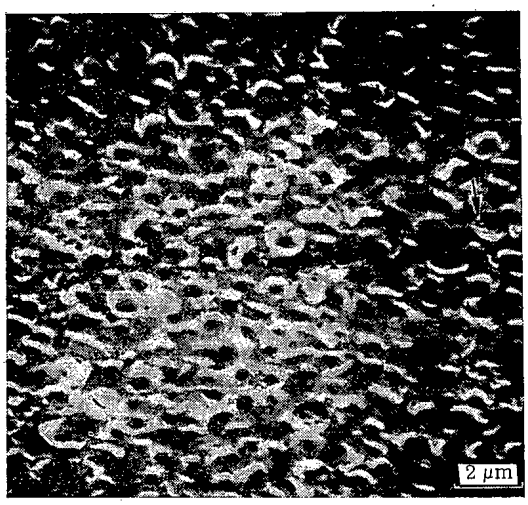

Fig. 5. Microstructure of surface of niobium target after irradiation with He^+ ions in the order from 3.5 MeV to 0.5 keV.

where H is the energy of dissolution of helium in the metal, C_{He} is the helium concentration, C_V is the concentration of vacancies associated with helium atoms, and Ω_V and Ω_{He} are the atomic volumes of the vacancies and helium, respectively. If we assume that the concentrations $C_{He}(x)$ and $C_V(x)$ have a Gaussian distribution over the depth [the deviation from the Gaussian distribution is more pronounced to the left of the $C_V(x)$ and $C_{He}(x)$ maxima whereas it is the shape of the distribution to the right of the maxima that is of interest to us], then

$$C_{He}(x)=\frac{D}{\overline{\Delta R}\sqrt{2\pi}}\exp\left[\frac{-(x-\overline{R})^2}{\overline{\Delta R^2}}\right];$$
$$C_V(x)=\frac{D_V}{\overline{\Delta R_d}\sqrt{2\pi}}\exp\left[\frac{-(x-\overline{R_d})^2}{\overline{\Delta R_d^2}}\right]. \quad (5)$$

Here D is the irradiation dose, V is the number of vacancies per helium atom, R and R_d are the projective paths of the ions and defects, and $\overline{\Delta R}$ and $\overline{\Delta R_d}$ are the spreads of the projective paths of the ions and defects. The maximum of the pressure (4) is at a depth x_{max}:

$$x_{max}=\frac{\overline{R}_d\,\overline{\Delta R^2}-\overline{R}\,\overline{\Delta R_d^2}}{\overline{\Delta R^2}-\overline{\Delta R_d^2}}+\sqrt{\left(\frac{\overline{R}_d\,\overline{\Delta R^2}-\overline{R}\,\overline{\Delta R_d^2}}{\overline{\Delta R^2}-\overline{\Delta R_d^2}}\right)-\frac{L\,\overline{\Delta R^2}\,\overline{\Delta R_d^2}+\overline{R}^2\,\overline{\Delta R_d^2}-R_d^2\,\overline{\Delta R^2}}{\overline{\Delta R^2}-\overline{\Delta R_d^2}}}, \quad (6)$$

where $L=\ln\left(\frac{\Omega_V}{\Omega_{He}}\frac{x-\overline{R}_d}{x-\overline{R}}\frac{\overline{\Delta R_d^2}}{\overline{\Delta R^2}}\right)$. Usually, $\overline{R}>\overline{R}_d$ and $\overline{\Delta R^2}>\overline{\Delta R_d^2}$. As a result the pressure maximum lies at a depth greater than R. For example, if $\overline{\Delta R^2}=\overline{\Delta R_d^2}$ and $\overline{R}>\overline{R}_d$, then

$$x_{max}=\frac{\overline{R}+\overline{R}_d}{2}+\frac{\overline{\Delta R^2}}{\overline{R}-\overline{R}_d}L. \quad (7)$$

If $\overline{R}=\overline{R}_d$ and $\overline{\Delta R^2}>\overline{\Delta R_d^2}$, then

$$x_{max}=\overline{R}+\sqrt{\frac{\overline{\Delta R^2}\,\overline{\Delta R_d^2}}{\overline{\Delta R^2}-\overline{\Delta R_d^2}}}\sqrt{L}. \quad (8)$$

It is natural to assume that the combination of small helium bubbles into large ones occurs primarily at a depth x_{max}. Then the thickness d of the blister caps will be x_{max}. Equations (6)-(8) qualitatively explain the experimentally observed dependence of d on the ion energy E. At low values of $E\sqrt{\overline{\Delta R^2}}\gtrsim\overline{R}$ and x_{max} is considerably greater than $\overline{R}$ and at high energies, when $\sqrt{\overline{\Delta R^2}}\ll\overline{R}$, the thickness $d\to\overline{R}$. The distribution $C_{He}(x)$ and $C_V(x)$ must be known in order to make a qualitative comparison. It is qualitatively obvious, however, that when $x<x_{max}$ bubbles with a relatively low helium content (and low pressure) are formed along with a large number of vacancies which are pinned in the metal by helium atoms. With a sufficiently large dose, such bubbles may join up to form channels [6] through which the helium will emerge onto the surface. As a

result of this [6], in the case of prebombardment with less energetic He^+ ions (the order of irradiation from 0.5 keV to 3.5 MeV) the blistering is observed to diminish in comparison with irradiation with monoenergetic ions. In the case of initial implantation of high-energy ions (order of irradiation from 3.5 MeV to 0.5 keV) the mechanism of suppression of blistering is different. With subsequent irradiation of niobium with less energetic helium ions the atoms penetrate into a region with a large number of vacancies which reduce the pressure in the bubbles and hinder the formation of blisters.

The results obtained here indicate that with an He^+ ion energy spectrum close to that expected in thermonuclear reactors and an integrated dose $\leq 7 \cdot 10^{18}$ ions/cm^2 blisters with a diameter characteristic of low-energy ions form on the surface and the efficiency of blister formation is determined by low-energy ions. In the case of irradiation with polyenergetic ions the surface erosion depends essentially on the order of irradiation. On the whole, the blistering with such a spectrum of He^+ ions is considerably less pronounced than with monoenergetic irradiation.

LITERATURE CITED

1. M. Guseva et al., J. Nucl. Mater., 63, 245 (1976).
2. L. A. Artsimovich, Nucl. Fusion, 12, 215 (1972).
3. L. Berry et al., in: Proc. Intern. Atomic Energy Conf. on Plasma Physics and Controlled Nuclear Fusion Research, Tokyo, Nov. 11-15 (1974), CN-38.
4. S. Das and M. Kaminsky, Radiation Effects on Solid Surfaces, Am. Chem. Soc., Washington (1976).
5. S. Das and M. Kaminsky, J. Appl. Phys., 44, 25 (1973).
6. K. Wilson, L. Haggmark, and R. Langley, Sand 76-8688, Sandia Lab. (1976).
7. J. Roth, R. Behrisch, and B. Scherzer, J. Nucl. Mater., 57, 365 (1975).
8. Yu. V. Martynenko, Fiz. Plazmy, 3, 6976 (1977).

HELIUM BLISTERING UNDER HIGH IRRADIATION DOSES

I. N. Afrikanov, V. M. Gusev,*
M. I. Guseva, A. N. Mansurova,
Yu. V. Martynenko, V. N. Morozov,
and O. I. Chelnokov

UDC 539.12.04:621.039.616

Much attention has been recently devoted to investigations on volume and surface radiation-induced effects in stainless steels and chromium–nickel alloys in view of their possible use as structural materials for fabricating the wall of the vacuum chamber of a thermonuclear reactor [1-4]. One of the principal processes responsible for surface erosion of steel is radiation-induced blistering. It is well known that with a fixed energy of bombarding He^+ ions the blistering depends essentially on the irradiation dose [5-8] and the target temperature [2, 6]. The rate of erosion of grade 304 steel at 450°C has been studied as a function of the dose of irradiation with 500- and 100-keV He^+ ions [6-8]. It was found that the surface erosion of the steel increases with the irradiation dose and that 15 layers peel off at a dose of $1.2 \cdot 10^{20}$ ions/cm^2 (E = 100 keV). In the case of H^+ and He^+ ions with an energy of 20 keV [3, 4] (when one generation of blisters is formed on the surface of the steel or alloy) it was established (as earlier in the case of niobium [9]) that there is suppression of blistering at doses necessary for the skin of the blisters to be evaporated by the bombarding ions.

In the present paper we study the development of blistering in the stainless steel 0Kh16N15M3B and in the chromium–nickel alloy 01Kh18N40M5 at a temperature of no more than 100°C and under irradiation with 40-keV He^+ ions.

* Deceased.

Translated from Atomnaya Énergiya, Vol. 46, No. 3, pp. 165-170, March, 1979. Original article submitted April 4, 1978.

0038-531X/79/4603-0190$07.50

Fig. 1. Microstructure of alloy 01Kh18N40M5 surface after irradiation at doses of: a) $3 \cdot 10^{18}$, b) $6 \cdot 10^{18}$, and c) $6 \cdot 10^{19}$ ions/cm^2 with 40-keV He^+ ions (j = 30 A/cm^2).

Experiment. Electrochemically polished specimens of the austenitic stainless steel 0Kh16N15M3B and the chromium–nickel alloy 01Kh18N40M5 were irradiated simultaneously in the ILU accelerator [10] with 40-keV He^+ ions. The current density j on the target was 30 μA/cm^2. The temperature of the specimens during irradiation did not exceed 100°C. In order to study the effect of the ion-beam intensity on the blistering we performed a number of experiments at j = 100 μA/cm^2. The irradiation dose varied from $3 \cdot 10^{18}$ to 10^{20} ions/cm^2. There were two series of experiments. In the first, seven 1-cm^2 targets of each material were irradiated simultaneously by a horizontally scanning He^+ ion beam and as the necessary dose was accumulated ($3 \cdot 10^{18}$, $6 \cdot 10^{18}$, $1.2 \cdot 10^{19}$, $3 \cdot 10^{19}$, $6 \cdot 10^{19}$, and 10^{20} ions/cm^2) the specimens were removed from the holder. In the second series of experiments the same irradiation doses were built up successively in the same specimen with intervals for electron-microscopical examination of the surface of the irradiated targets in a Stereoskan-180 scanning electron microscope.

Fig. 2. Microstructure of surface of the alloy 01Kh18N40M5 after irradiation with a beam of 40-keV He^+ ions at high intensity ($j = 100\ \mu A/cm^2$, $D = 6 \cdot 10^{18}$ ions/cm^2).

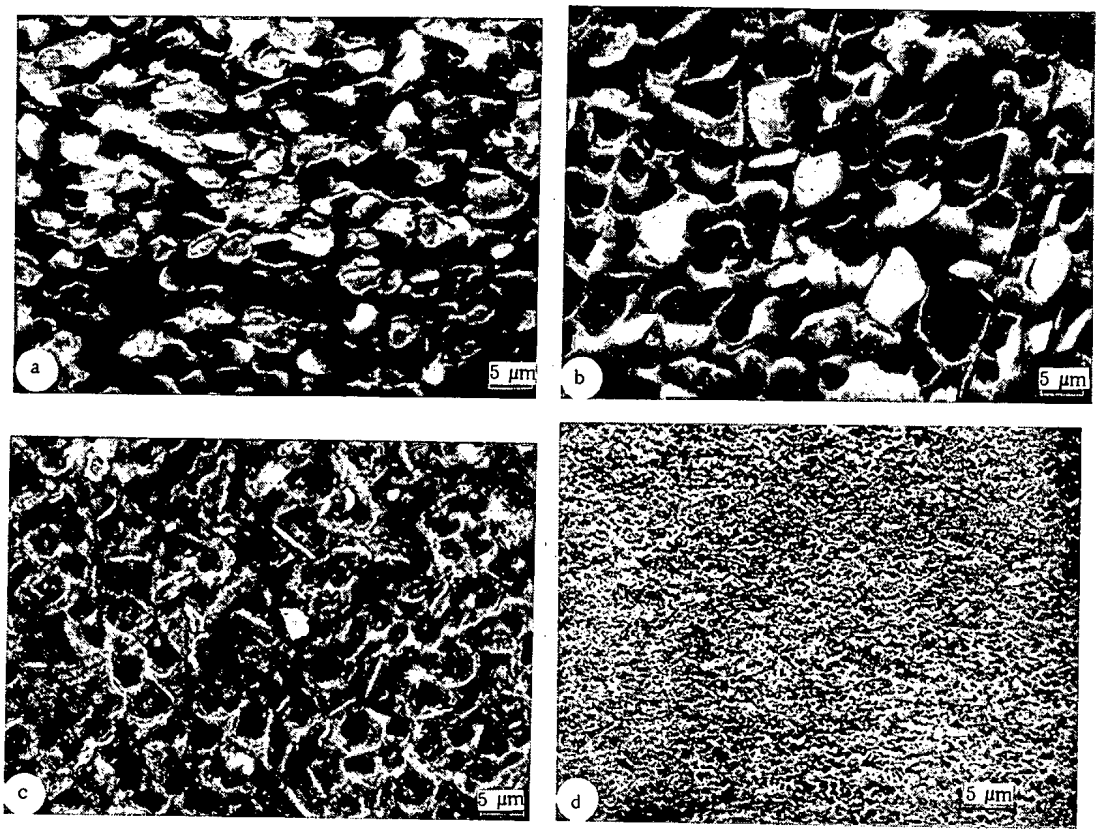

Fig. 3. Microstructure of surface of the steel 0Kh16N15M3B after irradiation at doses of: a) $3 \cdot 10^{18}$, b) $6 \cdot 10^{18}$, c) $6 \cdot 10^{19}$, and d) 10^{20} ions/cm^2 with 40-keV He^+ ions ($j = 30\ \mu A/cm^2$).

Experimental Results. Figure 1 shows how the doses of irradiation with He^+ ions affect the structure of the surface of chromium–nickel alloy. At a dose of $3 \cdot 10^{18}$ ions/cm^2 (see Fig. 1a) principally blisters of one generation with a maximum diameter of 5 μm are formed on the surface of the alloy. The skins of most of the blisters cracked along the contour but there was practically no peeling. Doubling the dose results in a sharp increase in surface erosion (see Fig. 1b). The upper layer almost completely peels off and the uncovered surface displays a large number of craters formed as the result of the cupolas breaking away from blisters of the second and third generations. There is a characteristic decrease in the diameter of the craters with the depth. The density of the craters is $1.25 \cdot 10^7$ ions/cm^2. When the dose is increased by an order of magnitude (see Fig. 1c) the portions of the target between the blister craters sputter and the surface acquires a porous, spongelike structure. The characteristic pore size on the surface is 1000–2000 Å and the pore

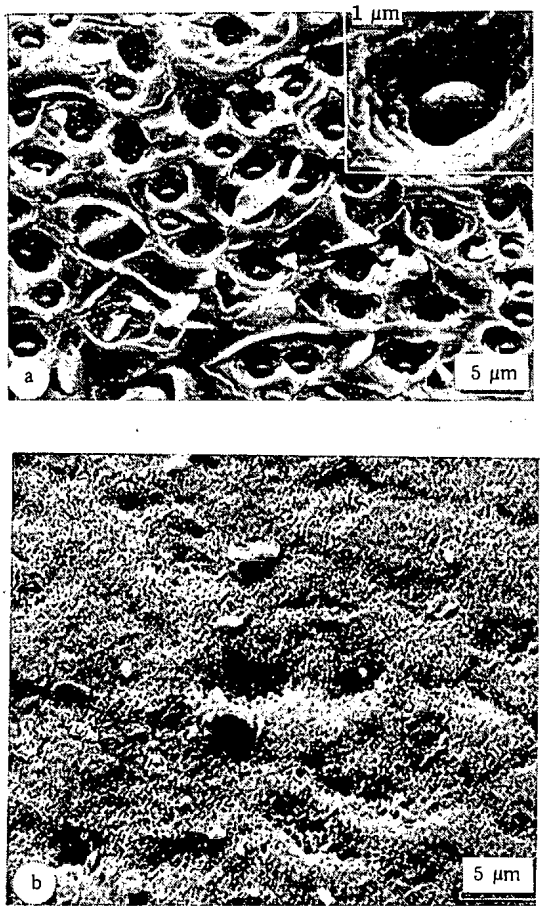

Fig. 4. Microstructure of alloy 01Kh18N40M5 surface irradiated with: a) 100-MeV He^+ ions at a dose of $6 \cdot 10^{18}$ ions/cm^2 and b) successively with 40-keV He^+ ions at a dose of 10^{20} ions/cm^2 and 100-MeV He^+ ions at a dose of $6 \cdot 10^{18}$ ions/cm^2.

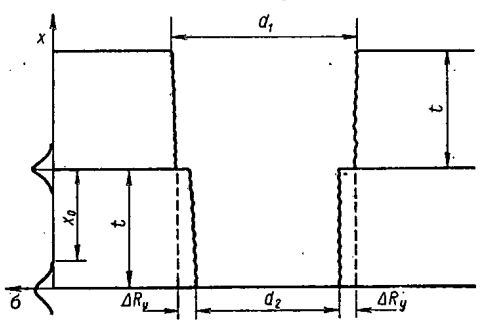

Fig. 5. Formation of blisters of second generation.

density is $1.6 \cdot 10^9$ ions/cm^2. Further bombardment of the target does not result in the formation of new blisters. It can thus be concluded that when 40-keV He^+ ions are implanted in the alloy 01Kh18N40M5 (at a temperature close to room temperature) at a dose of $6 \cdot 10^{19}$ ions/cm^2 there is suppression of blistering.

A surface microstructure similar to that shown in Fig. 1c was obtained earlier by Behrisch et al. [7] after irradiating niobium with He^+ ions possessing an energy of 50 and 100 keV at a dose of $(1.2\text{-}4) \cdot 10^{20}$ ions/cm^2 and $j = 1$ mA/cm^2.

It should be noted that increasing the current density 2-3 times at doses lower than that at which blistering ceases leads to increased erosion of the surface (Fig. 2). The number of layers peeled off grows from one at $j = 30$ μA/cm^2 (see Fig. 1b) to three and blisters of two generations also form under the third layer. The

thickness of the blister skin is 1400 Å, which practically coincides with the depth to which 40-keV He^+ ions penetrate into nickel. The results are in agreement with the data of [11].

Similar changes in the topography of the surface with the growth of the irradiation dose were detected in the steel 0Kh16N15M3B (Fig. 3). As in the case of Fe–Cr–Ni alloy, we recorded two characteristic doses at which there is a pronounced change in the structure of the surface. The dose at which the intensity of the blistering rises sharply is $6 \cdot 10^{18}$ ions/cm^2 (see Fig. 3b). In this case we also observed peeling of one layer and the formation of craters beneath it from one or two generations of blisters. At the same time, the dose at which the irradiated surface acquires a spongy structure and suppression of blistering is observed (see Fig. 3d) rises to 10^{20} ions/cm^2. Evidently, this effect is due to the lower (by a factor of 1.5) value of the sputtering ratio ($S_{St} = 3 \cdot 10^{-2}$ atom/ion) for sputtering of the steel by 40-keV He^+ ions in comparison with the value of S for the alloy under study ($S_{al} = 4.5 \cdot 10^{-2}$ atom/ion).

After implantation of He^+ ions at the dose required to attain an equilibrium spongy structure (10^{20} ions/cm^2), the specimen of chromium–nickel alloy was subjected to irradiation with 100-keV He^+ at a dose of $6 \cdot 10^{18}$ ions/cm^2 and $j = 30\ \mu A/cm^2$. Photomicrographs of the spongy surface of the alloy and of a portion of the same target, not prebombarded with He^+ ions, after irradiation under these are shown in Fig. 4. Under ordinary conditions of irradiation with 100-keV He^+ ions one layer is observed to peel off the surface of the alloy and six generations of blisters form under the layer (see Fig. 4a). At the same time, after reirradiation of the porous surface with high-energy He^+ ions there is no blistering (see Fig. 4b). The result obtained is of fundamental importance since under the real conditions of a thermonuclear reactor, in addition to energetic particles (3.5 MeV), streams of D^+, T^+, and He^+ ions which have an energy of 1-20 keV impinge on the wall of the vacuum chamber, the intensity of these streams being one to two orders of magnitude greater than that of the α particles; these ion streams will sputter the blister skins and stimulate the formation of a porous surface, which hinders the development of blisters from high-energy ions.

Theory. It was suggested in [11] that blistering arises as the result of fracture of the material and the formation of a crack at a depth $x = t$, where maximum stress σ is attained in the material. The stress in the implanted layer is found from the relation

$$\sigma = H\left[C_{He}(x) - C_V(x)\,(\Omega_V/\Omega_{He})\right], \tag{1}$$

where H is the energy of dissolution of helium in the metal, $C_{He}(x)$ and $C_V(x)$ are the helium and vacancy concentrations at the depth x, and Ω_{He} and Ω_V are the volumes of the helium atom and the vacancies, respectively. With the assumption that $C_{He}(x)$ and $C_V(x)$ have a Gaussian distribution and that $\bar{R}_{He} > \bar{R}_V$ and $\overline{\Delta R}^2_{He} > \overline{\Delta R}^2_V$, where $\bar{R}_{He}$ and $\bar{R}_V$ are the mean depths of helium penetration and defect formation, and $\overline{\Delta R}^2_{He}$ and $\overline{\Delta R}^2_V$ are the rms spreads of the distributions of implanted ions and of the defects they generate, it was shown [10] that the thickness t at which σ is a maximum is always greater than R_{He} but that $t \to R$ at higher energies. Cracking occurs when the maximum stress reaches the value of the ultimate strength (or yield point). Apparently, such a cracking mechanism was described by Evans [12]. Blistering, however, occurs most probably by a mechanism described in [10, 11, 13], i.e., is controlled not only by the gas pressure but also by the stress in the blister skin. After a certain dose of irradiation either part of the first layer of thickness t peels off when the main role is played by the gas pressure or the skins of blisters break away as the result of stresses in them. As a result, a part of the surface is exposed for blisters of subsequent generations. In that part of the surface where the first layer was not removed, at a depth $x = t$ there still is a crack, but evidently it is not continuous. This crack facilitates the escape of the helium introduced during the next irradiation. For that reason blisters of later generations are not formed on a surface covered by the remains of the first layer (see Figs. 1b and 3b).

Blisters of later generations are formed on the same part of the surface from which the layer of blister skins of the first generations has been removed. The process of second-generation blistering has the following distinctive features. First, near the edge of the region open to blisters of the second generation the concentration of the implanted helium is lower than at the center of that region, owing to an edge effect (Fig. 5). The characteristic dimension of the region in which the helium concentration is lower is equal to the lateral spread of the ion paths $\sqrt{\overline{\Delta R_y^2}}$. Therefore, if the diameter of first-generation blisters is d_1, then the diameter of the second-generation blister is

$$d_2 = d_1 - 2\sqrt{\overline{\Delta R_y^2}}. \tag{2}$$

Second, even during the formation of first-generation blisters a certain quantity of helium was introduced into the layer of second-generation blisters, setting up stresses at a depth greater than t (from the original surface). As a result, in addition to a maximum at a depth $x = t$ (from the surface of the second layer of

blisters), the stresses σ for second-generation blisters have a maximum near the surface (see Fig. 5). The integrated stress S, which is equal to [13]

$$S = \int_0^t \sigma(x)\, dx, \tag{3}$$

is higher for second-generation blisters. Blisters of the second generation can, therefore, form at a lower dose (reckoned from the moment when the first-generation blisters open). Indeed, at a dose of $3 \cdot 10^{18}$ ions/cm^2 only first-generation blisters formed on the surface of the chromium–nickel alloy specimen (see Fig. 1a), whereas the addition of such a dose resulted in the formation of another two generations of blisters (see Fig. 1b).

Moreover, increasing S for blisters of the second and subsequent generations leads to, according to [13], a transition from peeling of a large part of the first layer to the formation of blisters of a particular size. This also promotes a lowering of the temperature of the blister skins as a result of a decrease in the blister diameter and an improvement in the heat transfer.

The blister diameter diminishes from generation to generation and for the n-th generation is*

$$d_n = d_1 - (n-1)\, 2\,\overline{\Delta R_y}. \tag{4}$$

At the same time, in accordance with [12], the blister diameter d, the skin thickness t, and the integrated stress S are related by

$$d = 3.8\,(E/3S)^{1/2}\, t^{3/2}, \tag{5}$$

where E is Young's modulus. Since t remains constant for all generations of blisters and d diminishes, S should grow if blistering is to occur. It follows from Eqs. (1) and (3), however, that there is a maximum possible integrated stress S_{max}. Let us evaluate S_{max}. It follows from Eq. (1) that $\sigma \neq 0$ only when $x > x_0$, which is found from

$$C_{He}(x_0) = C_V(x_0)\,(\Omega_V/\Omega_{He}). \tag{6}$$

Moreover, in the case of yield without hardening $\sigma \leq \sigma_y$, where σ_y is the yield point. Therefore,

$$S_{max} \approx S_s + \sigma_y\,(t - x_0), \tag{7}$$

where S_s is the contribution from the surface peak $\sigma(x)$.

Assuming that first-generation blisters are formed when $S = S_1$, which is characteristic of the moment when $\sigma_{max}(x) = \sigma_y$, from Eqs. (1) and (3) we get

$$S_1 \approx \left(\tfrac{1}{2} \text{ to } \tfrac{1}{3}\right) \sigma_y\,(t - x_0). \tag{8}$$

Also assuming that $S_s \approx S_1$ for our estimates, we have

$$S_{max} = (3 \text{ to } 4)\, S_1. \tag{9}$$

It follows from this and from Eq. (5) that blisters do not form when $d < d_{min}$:

$$d_{min} = 3.8 \left(\frac{E}{3S_{max}}\right)^{1/2} t \approx (0.5 \text{ to } 0.6)\, d_1, \tag{10}$$

where d_1 is the diameter of the first-generation blisters. Indeed, our experiments show that the diameter of blisters of the last, third, generation is $\sim 0.7\, d_1$. Such agreement should be considered extremely good, bearing in mind the accuracy of the estimates and the spread of the experimental values of d.

The maximum number of generations of blisters is

$$n_{max} = \frac{d_1 - d_{min}}{2\sqrt{\overline{\Delta R_y^2}}} \approx (0.2 \text{ to } 0.25)\, \frac{d_1}{\sqrt{\overline{\Delta R_y^2}}}. \tag{11}$$

Assuming for our estimates that for $M_1 \approx 0.01\, M_2$ we have $\Delta R^2_y \approx 3R^2_p$ [14] and $R_p\,(40\text{ keV}) \approx t$, we get $n_{max} \approx 3$, which is also in good agreement with experiment.

*We speak here of blisters with a particular diameter; the case of peeling of the surface will be discussed further on.

Let us note that if blisters formed under the effect of the gas pressure and not the internal stress in the metal, then it would be possible for blisters to also form when $d < d_{min}$. In the case when initially blisters of a particular size do not form and a large part of the surface peels off, the number of generations of blisters may be greater than that given by Eq. (11) but in all cases the size of the surface peeled off decreases from generation to generation and, starting from a certain generation, blisters of a particular diameter form. Thus, in all cases only a finite number of generations of blisters is possible.

The formation of an equilibrium porous surface, which is observed at large doses ($\geqslant 10^{20}$ ions/cm^2), occurs only when a layer of thickness $\geqslant t$ is sputtered. In this case pores of the pinhole type may form on the site of blisters, gradually decreasing from generation to generation, and also as the result of the formation of vacancy pores. The latter form with particular intensity at a high helium concentration, which exerts a stabilizing effect for vacancy pores. But at the same time, if $C_V > (\Omega_{He}/\Omega_V) C_{He}$ (and this should indeed be satisfied for equilibrium distributions of C_V and C_{He} at high doses), then the pressure in the vacancy pores is low and does not cause either appreciable stresses to be set up in the layer or cracking to occur. Linking up of vacancy pores results in channels through which helium can escape from the irradiated specimen [15]. Consequently, we observed suppression of blistering caused by 100-keV He^+ ions on a porous surface formed previously.

Thus, blistering at a temperature $\leq 100°C$ is of a transient nature even under irradiation with a monoenergetic beam of He^+ ions.

LITERATURE CITED

1. S. Das and M. Kaminsky, J. Appl. Phys., 44, 2520 (1973).
2. W. Bauer and G. Tomas, J. Nucl. Mater. 53, 134 (1974).
3. J. Roth, R. Behrisch, and B. Scherzer, J. Nucl. Mater., 57, 365 (1975).
4. N. P. Busharov et al., At. Energ., 42, No. 6, 486 (1977).
5. S. Das and M. Kaminsky, Radiation Effects on Solid Surfaces, Am. Chem. Soc., Washington (1976).
6. S. Das and M. Kaminsky, J. Nucl. Mater., 53, 115 (1974).
7. R. Behrisch et al., in: Proc. Ninth Symp. on Fusion Technology, Garmisch-Partenkirchen (1976).
8. S. Das et al., J. Nucl. Mater., 76, 256 (1978).
9. J. Martel et al., J. Nucl. Mater., 53, 142 (1974).
10. V. M. Gusev et al., Prib. Tekh. Eksp., 4, 19 (1968).
11. S. Das et al., in: Proc. Seventh Conf. on Atomic Collisions in Solids, Moscow (1977).
12. J. Evans, J. Nucl. Mater., 68, 129 (1977).
13. R. Behrisch et al., Appl. Phys. Lett., 27, 199 (1975).
14. K. Winterborn, P. Sigmund, and I. Sanders, Kgl-danske vid. selscab. Mat.-fys. medd, 37, 14 (1970).
15. K. Winsol, L. Haggmark, and R. Langley, Sand 76-8688, Sandia Lab. (1976).

MICRODOSIMETRIC CHARACTERISTICS OF NEUTRONS AT ENERGIES BETWEEN 50 eV AND 10 MeV

V. A. Pitkevich and V. G. Videnskii

UDC 539.125.5

In recent years, there has been a considerable increase in the number of papers devoted to the possibility of using neutron beams in experimental and clinical medicine and to the investigation of the mechanisms by which they act on the cellular and subcellular structure. This requires thorough investigation of the processes of neutron-energy absorption in functionally active elements of a cell with a characteristic size of the order of 1 μm. In accordance with the recommendations of the International Commission on Radiological Protection, the conditions of irradiation are characterized by the distribution function F(Z, D). The initial information used to obtain this distribution function is the absorbed-energy spectrum $f_1(\varepsilon)$.

A program for the Monte Carlo calculation of the absorbed-energy spectrum for monoenergetic neutrons of energy up to $E_n = 6$ MeV is described in [1]. The following assumptions are made in the program: the interaction cross section of the neutrons and the angular distribution in elastic scattering are used in accordance with the 91-group system of constants; the retardation of charged particles in the material is considered in the continuous-deceleration approximation, while the effect of energy-loss scatter for the protons is approximately taken into account using the data of [2]; for protons, the effect of δ electrons is taken approximately into account using the results of [3].

The aim of the present work is to develop a program for the calculation of the spectra $f_1(\varepsilon)$ for an arbitrary neutron spectrum with a maximum energy of 10 MeV without using the group approximation for the neutron interaction cross section. This is because no system of group constants has yet been developed for use in microdosimetry problems. For the same reason, the problem of calculating $f_1(\varepsilon)$ for the neutron spectrum is formulated, since in the past it has not been clear for how many E_n it is necessary to calculate $f_1(\varepsilon; E_n)$ in order to obtain the function $f_1(\varepsilon)$ for an arbitrary neutron spectrum.

Initial Data and Approximation

In the given range of E_n, elastic scattering on C, N, O, and H nuclei are the most important reactions. For inelastic scattering, the excited states of the nuclei after collision are neglected; this is acceptable if the cross sections of these reactions are small (~ 10 mb) or if the reaction threshold is high (6-10 MeV) [4]. Also, no account is taken of capture reactions with the emission of γ quanta in the calculation, since the thickness of the converter is small (~ 1 mm) and the probability of such reactions is small at $E_n > 50$ eV. When $E_n > 1$ MeV, inelastic scattering on O and C and the capture reactions (n, p), (n, d), and (n, t) on N and (n, α) on C, N, O are taken into account.

In order to take account of the resonance structure of the interaction cross section for neutrons and tissue-equivalent material, the whole energy interval is divided into several subintervals within which the cross section is calculated from the data of [5, 6] by means of linear interpolation on an equally spaced energy grid. Integral information on the cross sections used in the calculation is given in Fig. 1 in the form of curves of the free path length λ_n of neutrons in a tissue-equivalent plastic and a tissue-equivalent gas. The composition of the plastic (10^{22} nuclei/g) is: $n_C = 4.07$; $n_N = 0.254$; $n_H = 5.99$; the composition of the gas (density 1 g/cm^3) is: $n_C = 2.3$; $n_H = 6.12$; $n_O = 1.54$; $n_N = 0.152$. It is evident from Fig. 1 that the tissue-equivalent plastic and gas differ by no more than 20% over the free path length of the neutrons. Over the interaction cross section this difference is more considerable. The angular distribution of neutrons in inelastic and elastic scattering on hydrogen is assumed to be isotropic in the center-of-mass system. The anisotropy of elastic scattering on heavier nuclei is taken into account by two methods. In the first, the angular distribution is taken into account by a 26-group system of constants [7]. The scattering anisotropy is more accurately taken into account by the method proposed in [8]. Capture reactions and inelastic scattering are calculated by the form-

Translated from Atomnaya Énergiya, Vol. 46, No. 3, pp. 170-174, March, 1979. Original article submitted March 6, 1978.

0038-531X/79/4603-0197$07.50

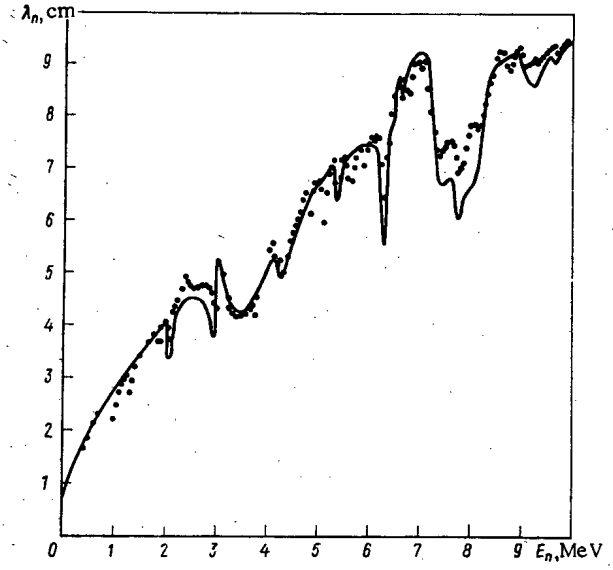

Fig. 1. Mean neutron free path length λ_n in tissue-equivalent plastic (continuous curve) and tissue-equivalent gas (density 1 g/cm^3; filled circles) as a function of the neutron energy E_n.

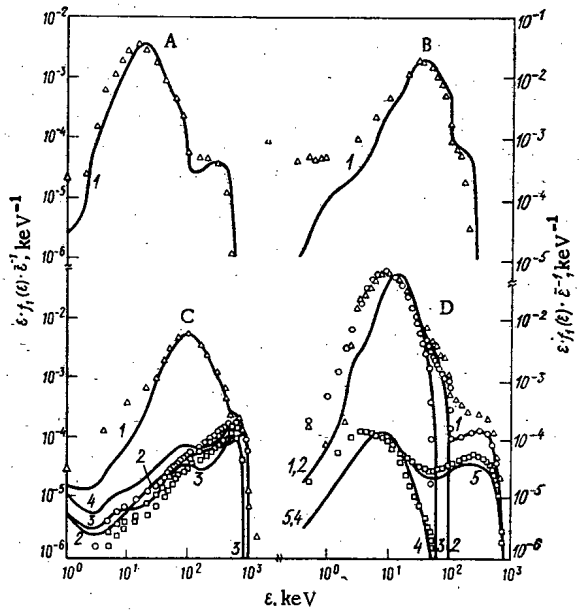

Fig. 2. Absorbed-energy spectra of monoenergetic neutrons in spherical volumes of material of diameter 1 μ (A, B, D) and 6.5 μ (C); E_n = 3.45 MeV (A, C), 1.02 MeV (B), and 5.85 MeV (D); Δ) data of [1]; C: curve 1 gives the total spectrum; curve 2 and the open squares correspond to the carbon nucleus, taking account of point group anisotropy; curve 3 and the unfilled squares and curve 4 and the unfilled circles correspond to the oxygen nucleus and tracks of insider type, again taking point group anisotropy into account. D: curve 1 and the unfilled circles correspond to the total spectrum when the straggling effect is and is not taken into account; curve 2 is protons, the straggling effect accounted for; curve 3 and the unfilled circles correspond to protons with E > 400 keV, completely crossing the cavity; curve 4 and the unfilled squares correspond to protons with E >400 keV forming in the cavity; curve 5 and the unfilled squares correspond to protons of any energy forming in the cavity.

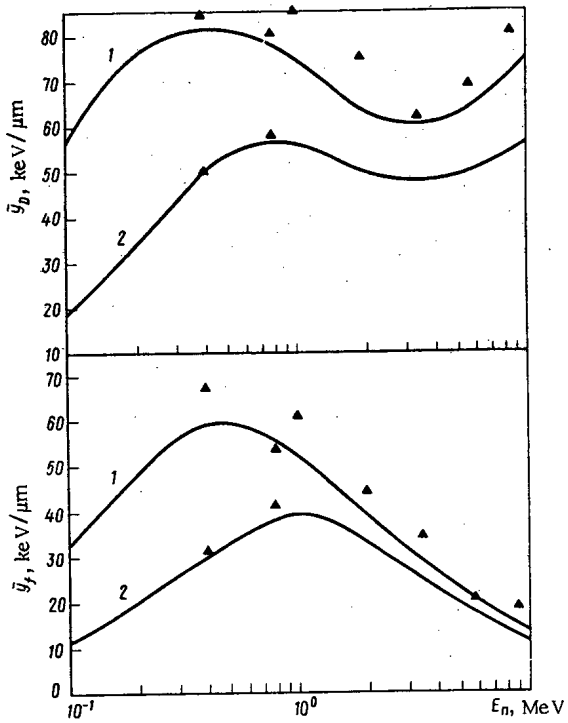

Fig. 3. Mean-frequency $\bar{y}_f$ and mean-dose $\bar{y}_D$ events as a function of the neutron energy E_n: the continuous curves give the data of [15], while the symbols corresponds to calculation; 1) spherical-volume diameter 1 μm; 2) 5 μm.

ulas proposed in [9, 10]. The values of the reaction energy are taken from [4]. Data on the retarding properties of the tissue-equivalent materials for all the charged particles formed by neutrons are taken from [11]. The scatter of the charged-particle energy loss over a section of the track is taken into account as in [2], except that no account is taken of indirect energy-absorption events in the microvolume (the δ-electron effect). Such events may make a contribution to the given spectrum in the region of small (~ 1 keV) energy liberation, where the approximation adopted leads to an error exceeding the δ-electron contribution.

Geometry and Calculation Algorithm

The model adopted in experimental microdosimetry is used to calculate the absorbed-energy spectra [12]. The charged-particle tracks present within the microvolume may be divided into four types: crossers, stoppers, starters, and insiders [13]. Fluctuations of the energy loss are taken into account only for tracks of the first three types. The coordinates of the neutrons and charged particles in phase space, and also their paths and energy losses in the converter and the cavity, are random quantities. Their values are chosen from the general set using tables, in order to achieve the maximum speed of calculation of the neutron histories. Rather than give a detailed description of the whole algorithm, attention will be directed mainly to the methods used to reduce the dispersion of the statistical estimates.

A statistical weight is assigned to each point of the neutron trajectory

$$W = W_s W_k W_p (\Sigma_{i,c}/\Sigma_c). \quad (1)$$

The first factor is necessary to improve the statistics of choosing the neutrons from the beam. For a plane-parallel beam, for example, it is equal to the probability that a neutron from the source will fall within an annular band of width ΔR within which the neutron distance to the beam axis is distributed according to the corresponding distribution law. The second factor is introduced to improve the statistics of choice from the neutron energy spectra and is equal to the probability that a neutron from the source will fall within the energy group numbered k. The boundaries of the energy groups are chosen in accordance with the 26-group system of constants adopted in the Soviet Union. The neutron energy is chosen successively within each group in accordance with the shape of the energy spectrum. The reason for the third factor may be explained as follows: the trajectory of a neutron from the source may cross the converter alone or the converter and the cavity. Let S_1, S_2, and S_3 be, respectively, the neutron path length in the near (in the direction of motion) wall of the converter, in the cavity, and in the far wall. The method outlined in [14] may be used to model the coordinates of the points of interaction of the neutrons in the three regions, to give

$$W_{p,j}=1-\exp\{-\Sigma_j S_j\},\quad j=1,\ 2,\ 3, \tag{2}$$

where Σ_j is the total macroscopic cross section for the interaction of a neutron with the converter material or the internal cavity. In the general case, these first interaction points serve as the initial points of the tree of neutron trajectories. Successive points of the tree are obtained analogously: each new interaction point serves as the starting point for no more than three (in the present case) branches of the tree until the statistical weight becomes less than some value W_0 (10^{-6}-10^{-9}). The neutrons of subsequent generations are calculated without branching. Capture reactions are taken into account simultaneously using the last factor.

The calculation algorithm for the absorbed-energy spectra may be written in general terms as follows.

1. For each of the 10 sections of the converter radius in turn the point of intersection of the neutron trajectory with a spherical layer is modeled.

2. For this point, the neutron energy in the spectrum is chosen at random from each energy group in turn.

3. For each neutron of the given energy and entry point, a tree of trajectories is constructed and analyzed.

After completing the third stage, the second is again carried out. This continues until the trees of all the energy groups have been analyzed, after which the first stage is again carried out. After considering all the sections of the layer radius, the neutron history is concluded, and the analysis of the next neutron history begins.

Results of the Calculations and Discussion

Using the method developed, the functions $f_1(\varepsilon)$ and their errors may be estimated for all types of particles and tracks making a contribution to the total energy-liberation spectrum. So as to be able subsequently to take more accurately into account the fluctuations of the energy transfer on a section of the track from rebound protons with a path in the cavity much longer than the diameter, which produce tracks of the first and third types, information is obtained on the energy spectra of such protons and the track-length distribution in the gas cavity. The characteristic statistical error of the calculated spectra is no more than 5-10% in the main region (the number of particle histories is $\sim 10^3$). At the edges of the distribution, the error is ~15-40%.

Results are obtained for a series of monoenergetic neutrons, and also for neutron spectra corresponding to the fission of the isotope ^{252}Cf and channels P-2 and B-3 of the BR-10 reactor. These data are compared with the results of [1] in Fig. 2, which shows values of $\varepsilon f_1(\varepsilon)$ for four values of E_n of monoenergetic neutrons and spherical-volume diameters of 1 and 6.5 μm. In [1], data were obtained without taking into account the fluctuations of energy transfer by protons. Thus, it may be agreed that the present results in the main part of the spectrum are in satisfactory agreement with the data of [1]. The explanation for the discrepancy at an energy liberation of less than 5-10 keV is that in [1] no account was taken of the straggling effect for protons (which shifts the spectrum to the left in the region of the maximum; for E_n = 5.85 MeV and a sphere of diameter 1 μm this shift is 25%), and in the present work no account is taken of the effect of δ electrons. In Fig. 2C, the continuous curves 2, 3, and 4 and the filled symbols show the results of calculations for neutrons with E_n = 3.45 MeV and a sphere diameter of 6.5 μm which were made to elucidate the effect of data on the elastic-scattering anisotropy of the neutrons. The use of group anisotropy constants increases the mean absorbed energy from the heavy recoil nuclei (for the given result, by 40-50%) but this has a slight effect on the total spectrum. The mean-frequency $\bar{y}_f$ and mean-dose y_D event magnitudes are shown as a function of the neutron energy. The discrepancy with the data of [15] is due to disregarding straggling and neutron resonances (for example, at a neutron energy of 1 MeV) and the approximations in the formula obtained. For a diameter of 1 μm, the accuracy of these approximations may be estimated at 10-20% for $\bar{y}_f$ and 5-15% for $\bar{y}_D$. For a diameter of 5 μm, the error is lower, of course.

The program here developed may be used in research on the interpretation of radiobiological effects due to neutrons of different energies. The calculation of absorbed-energy spectra in spherical volumes of diameter >0.5 μm for different neutron energies and spectra will form the subject of a future work.

LITERATURE CITED

1. U. Oldenburg and J. Booz, Rad. Res., 51, 551 (1972).
2. M. Coppola and J. Booz, Biophysik, 9, 225 (1973).

3. H. Paretzke and G. Burger, in: Microdosimetry, EUR-4452, EURATOM, Brussels (1970), pp. 615-630.
4. W. Snyder, in: Radiation Dosimetry, Vol. 1, Proc. of Intern. Summer School on Radiation Protection, Cavtat, Yugoslavia, September 21-30, 1970, Institute of Nuclear Sciences, Beograd (1971), pp. 160-184.
5. Evaluated Nuclear Data File (ENDF/B), Version IV, National Neutron Cross Section Center, BNL, Upton, New York (1974).
6. Lawrence Livermore Laboratory Evaluated Neutron Data Library (ENDL), University of California, Livermore, California (1973).
7. N. O. Bazazyants, M. N. Zabrodskaya, and M. N. Nikolaev, in: Nuclear Parameters, No. 8, Part 2, Provision of Fast-Reactor Calculations [in Russian], TsNIIatominform, Moscow (1972).
8. P. Nagaragan et al., A Random Sampling Procedure for Anisotropic Distributions, B.A.R.C.-789, Bombay (1975).
9. I. Caswell and I. Coyne, Rad. Res., 52, No. 3, 448 (1972).
10. A. M. Baldin, V. I. Gol'danskii, and I. L. Rozental', Nuclear-Reaction Kinetics [in Russian], GIFML, Moscow (1959).
11. T. Armstrong and K. Chandler, SPAR, A FORTRAN Program for Computing Stopping Powers and Ranges for Muons, Charged Pions, Protons, and Heavy Ions, USAEC Report, ORNL-4869 (CCC-228), Oak Ridge, Tennessee (1973).
12. H. Rossi and W. Rosenzweig, Radiology, 64, 404 (1955).
13. R. Caswell, Rad. Res., 27, 92 (1966).
14. N. P. Buslenko, I. M. Golenko, and V. G. Sobol', Method of Statistical Testing [in Russian], GIFML, Moscow (1962), p. 106.
15. R. Caswell and J. Coyne, "Microdosimetry," in: Proceedings of Fifth Symposium on Microdosimetry, Verbania–Pallanza, Italy, Sept. 22-26, 1975, EURATOM, Brussels (1976), p. 97.

ALBEDO OF CONCRETE FOR LOW-ENERGY GAMMA RADIATION

M. P. Panin and A. M. Panchenko

UDC 539.122:539:121.72

Many papers have appeared on the backscattering of gamma radiation. The most complete results with a detailed analysis of various regularities of the albedo are presented in [1]. The energy range below 100 keV is considered in only a few papers. Among these the most detailed is [2], but even in it only integral functionals of the field are presented. Recently considerable interest has been shown in low-energy gamma radiation as a result of the spread of low-energy x-ray facilities.

We have used the Monte Carlo method to calculate various current characteristics of the number albedo a_N and the energy albedo a_E for incident gamma photon energies from 20 to 100 keV. In addition to integral functionals we obtained differential angle $(da_N/d\Omega)$ (E_0, θ_0, θ), energy (da_N/dE) (E_0, θ_0, E), and spectral-angle $(d^2a_N/d\Omega \cdot dE)$ $(E_0, \theta_0, \theta, E)$ distributions of the number albedo. The component due to single scattering of the radiation was recorded separately. Angles of incidence θ_0 were varied from 0 to 89°, and angles of reflection θ from −89° to +89°. Negative values of θ correspond to scattering in the half plane $\varphi = 180°$, and positive values to $\varphi = 0°$. Values of the differential-angle albedo in directions not lying in the plane of incidence were found by using the method of reducing the number of calculations as in [3]. Its applicability for low energies was checked by random tests. The error did not exceed 6-7%.

Integral values of the albedo were calculated by using the estimate

$$a_N = M\sum_{i=1}^{k} W_i \exp(-\tau_i)\,\chi(n\Omega_i), \qquad \chi(t) = \begin{cases} 1, & t > 0; \\ 0, & t \leqslant 0, \end{cases} \tag{1}$$

Translated from Atomnaya Énergiya, Vol. 46, No. 3, pp. 174-177, March, 1979. Original article submitted March 6, 1978.

0038-531X/79/4603-0201 $07.50

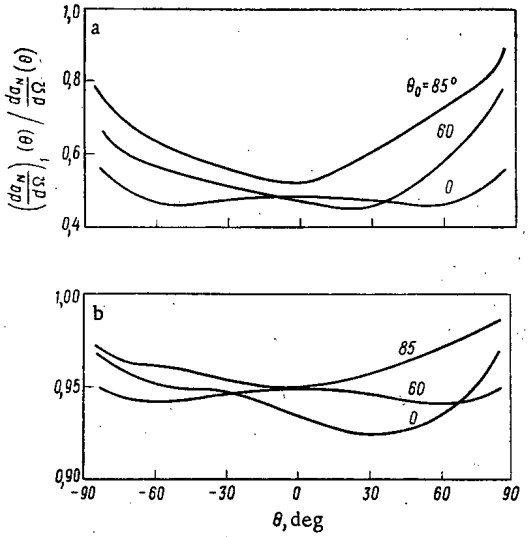

Fig. 1. Contribution of single scattering to the differential angle number albedo as a function of the angle of reflection θ for initial energies of a) 100 and b) 20 keV.

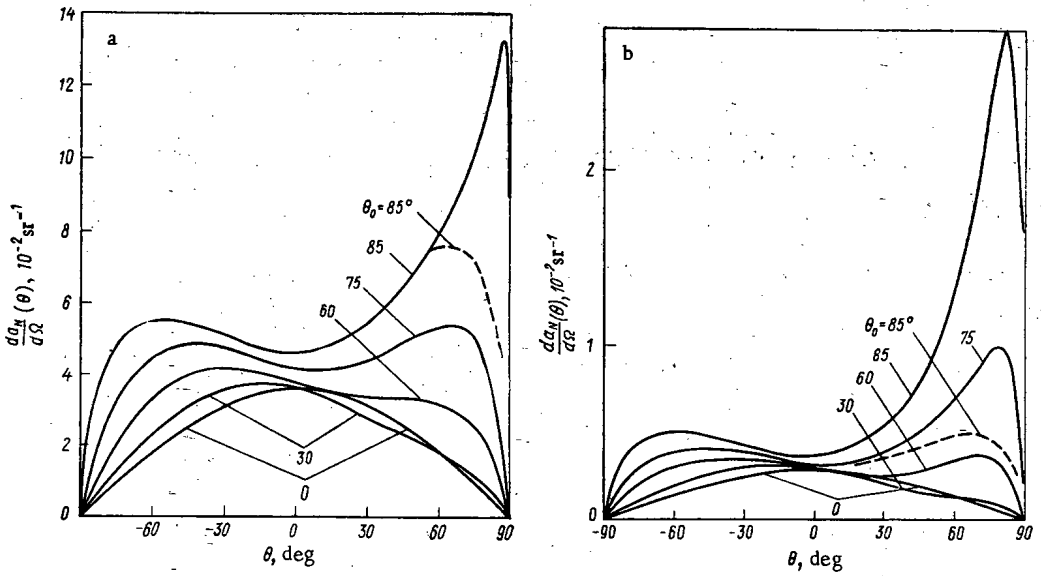

Fig. 2. Angle number albedo as a function of the angle of reflection for initial energies of a) 60 and b) 20 keV (dashed line denotes data obtained without taking account of electron binding in atom).

where M is the mathematical expectation; i, number of the scatter; Ω_i, direction of the gamma photon after scattering; τ_i, optical thickness in the material along the direction Ω_i; n, normal to the surface; and W_i, statistical weight of the photon after the i-th scatter.

We are interested in the scattering of low-energy gamma radiation and therefore took account of the binding of the electrons in an atom; i.e., we considered both incoherent scattering from bound electrons and coherent scattering from an atom. At each i-th scatter the estimate for a detector of direction ω in the calculation of the angle albedo was found from

$$\Phi_i = \frac{W_{i-1}}{\Sigma(E_{i-1})}\left\{n_e\left(\frac{d\sigma}{d\Omega}\right)_C (E_{i-1}, \Omega_{i-1}\omega) S(q) e^{-\tau(E)} + n_a\left(\frac{d\sigma}{d\Omega}\right)_T (\Omega_{i-1}\omega) F^2(q) e^{-\tau(E_{i-1})}\right\}. \quad (2)$$

Here $(d\sigma/d\Omega)_C$ and $(d\sigma/d\Omega)_T$ are the differential microscopic cross sections for Compton and Thomson scattering, respectively; n_e and n_a, electron and atom densities in the scattering material; S, incoherent scattering function; F, atomic form factor; q, momentum transfer in scattering from the direction Ω_{i-1} to ω for an incident

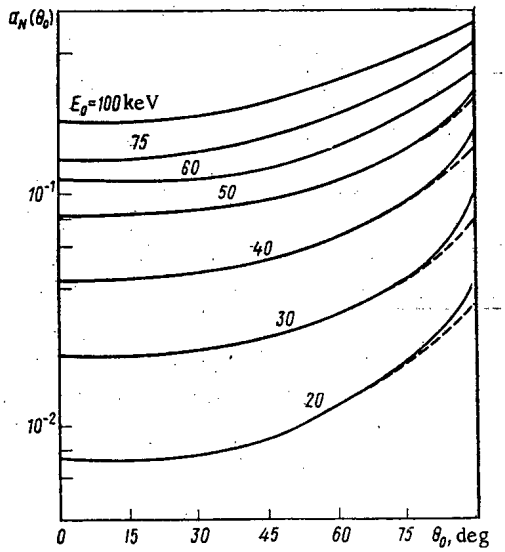

Fig. 3. Integral values of number albedo as a function of angle of incidence (dashed line denotes data obtained without taking account of electron binding in atom).

TABLE 1. Coefficients of Semiempirical Representation Found by the Method of Least Squares

E_0, keV	A_1	A_2	E_0, keV	A_1	A_2
20	1,5—4 *	8,1—5	60	1,4—2	2,2—3
30	3,3—4	8,3—4	75	2,1—2	5,8—3
40	2,2—3	1,8—3	100	3,4—2	8,2—3
50	7,6—3	1,9—3			

*Read $1.5 \cdot 10^{-4}$.

gamma photon of energy E_{i-1}; $\tau(E)$ and $\tau(E_{i-1})$, respectively, the optical thicknesses in the material for the energy of a gamma photon after incoherent and coherent scattering; and Σ, total microscopic interaction cross section. Calculations were performed in parallel for 13 detectors corresponding to 13 angles θ. The statistical errors of the differential functionals for the statistics of 10^3 histories did not exceed 5%.

The results of the calculations, part of which are shown in Figs. 1-3, exhibit a number of special features which are characteristic of the laws of backscattering of low-energy gamma radiation. One of the most important of these features is the controlling role of single scattering in the formation of the field of backscattered radiation. Figure 1 shows that the singly scattered fraction is a complicated function of the angles θ_0 and θ, but increases monotonically with decreasing initial energy. This is related to the increase in the photoelectric absorption cross section. The derivative $d\Sigma_\tau/d\cos\theta_s$ is a measure of the change of probability of absorption in a single scatter. The cross section for the photoelectric effect $\Sigma_\tau \sim E^{-n}$, where $n \approx 3$ [4], and therefore in scattering through an angle θ_s

$$\frac{d\Sigma_\tau}{d\cos\theta_s} = \frac{d\Sigma_\tau}{dE}\frac{dE}{d\cos\theta_s} \sim -\frac{1}{E^2}. \quad (3)$$

At higher energies when the photoabsorption cross section and the derivative (3) are small, the components of the field corresponding to various multiplicities of scattering are little different. The somewhat unusual dependence of the differential angle albedo on the angle of reflection θ (Fig. 2) is also a result of the low initial energy. The curves in Fig. 2 show maxima at negative values of θ for $\theta_0 > 0°$. This is a result of the increase in the probability of scattering with a change in the scattering angle θ_s from 90° to 180°. The lower the energy the larger its increase, and in the limit it corresponds to the law $1 + \cos^2\theta_s$. It is obvious that as $E_0 \to 0$ both branches of the curves in Fig. 2 would become nearly symmetric for $\theta_0 \approx 90°$. However, the effect of electron binding in the atom distorts this picture considerably. The sharp peak at $\theta \approx 80°$ at glancing angles of incidence

is formed by coherent scattering at small angles, and is obtained solely as a result of taking account of electron binding. For comparison Fig. 2 shows results obtained without taking account of binding. The results for 60 keV are from [1] for aluminum, and those for 20 keV were obtained by special calculations. The data presented indicate the range of energies where it is necessary to take account of this effect in calculating the angular characteristics: for $E_0 \leqslant 60$ keV where $\theta_0 \geqslant 80°$ and $\theta \geqslant 60°$; for $E \leqslant 30$ keV for $\theta_0 \geqslant 60°$ and $\theta \geqslant 15°$.

This effect undoubtedly has a somewhat smaller influence on the integral characteristics of the albedo shown in Fig. 3. Only for large angles of incidence $\theta_0 \geqslant 85°$ and $E_0 \leqslant 50$ keV is there a sharp increase in the dependence of a on θ_0. This is a result of coherent scattering becoming important for small-angle scattering. In order to compare the results obtained by taking account and not taking account of binding the curves for $a_N(\theta_0)$ were extrapolated from $\theta_0 \approx 75°$-$85°$ to 90° by using the extrapolation function

$$a'(\theta_0) = K\{2.67 - 0.5\cos\theta_0 - \cos^2\theta_0 + 1.5\cos^3\theta_0 + \\ + 3\cos^4\theta_0 + (2\cos^3\theta_0 - 3\cos\theta_0 - 3\cos^5\theta_0)\ \ln[(1+\cos\theta_0)/\cos\theta_0]\}. \quad (4)$$

The coefficient K was chosen to make the functions $a'(\theta_0)$ and $a_N(\theta_0)$ agree in the $\theta_0 \approx 75°$-$80°$ range and has the approximate value

$$K \approx n_e \pi r_0^2 / 2\Sigma(E_0),$$

where r_0 is the classical radius of the electron.

The extrapolation Eq. (4) was obtained from an estimate of the single scattering integral albedo based on the assumption of Thomson scattering with no change in energy. The extrapolated values are in good agreement with data in [2] for the number albedo. The monotonic dependence of the albedo on the initial energy shown in Fig. 3 is characteristic of the low-energy region and results from the decrease of the probability of photoabsorption with increasing energy.

The results for the energy albedo are similar to those for the number albedo. The ratio a_E/a_N is practically independent of the angle of incidence θ_0. This results from the fact that the spectrum of reflected radiation lies within narrow energy limits. For given θ_0 and θ it consists of a single line from single scattering

$$E_1 = E_0/[1 + (E_0/m_0c^2)(1 - \cos\theta_s)] \quad (5)$$

and is close to the uniform distribution formed by multiple scattering. The boundaries of the distribution are nearly the same as those of the spectrum of doubly scattered photons:

$$\left(\frac{E_0}{1+[2+\sqrt{2(1+\cos\theta_s)}](E_0/m_0c^2)},\ \frac{E_0}{1+[2-\sqrt{2(1+\cos\theta_s)}](E_0/m_0c^2)}\right). \quad (6)$$

With a decrease in E_0 the singly scattered fraction increases and the single line E_1 and the limits of the spectrum (6) are shifted toward E_0, which means that the spectrum is narrowed.

For $E_0 = 100$ keV a very broad spectrum is observed from the range considered. The spectrum is hardened as θ_0 is increased, since the average scattering angle is decreased. As a result of all this the ratio a_E/a_N at 100 keV does not remain constant but increases somewhat with increasing θ_0. The angular distributions of the number albedo can be described by a semiempirical formula which includes an exact analytical calculation of the singly scattered component

$$\left(\frac{da_N}{d\Omega}\right)_1(E_0, \theta_0, \theta) = n_e\left(\frac{d\sigma}{d\Omega}\right)_{KN}\frac{S(q)}{\Sigma + \Sigma'\cos\theta_0/\cos\theta} + n_a\left(\frac{d\sigma}{d\Omega}\right)_T\frac{F^2(q)}{\Sigma(1+\cos\theta_n/\cos\theta)} \quad (7)$$

and an empirically selected representation for the multiply scattered component (the values of the coefficients A_1 and A_2 are given in Table 1):

$$(da_N/d\Omega)_M = [A_1 + \theta_0 A_2]\cos\theta; \quad (8)$$

$$(da_N/d\Omega)(E_0, \theta_0, \theta) = (da_N/d\Omega)_1(E_0, \theta_0, \theta) + (da_N/d\Omega)_M(E_0, \theta_0, \theta). \quad (9)$$

The errors in % given by Eq. (9) are listed below:

E, keV	$\theta_0 \geqslant 75°$	$\theta_0 \leqslant 45°$
20—30	$\leqslant 6$	$\leqslant 3$
50—60	$\leqslant 13$	$\leqslant 6$
75—100	$\leqslant 16$	$\leqslant 9$

A similar representation can be used for the energy albedo also.

LITERATURE CITED

1. B. P. Bulatov et al., The Albedo of Gamma Radiation [in Russian], Atomizdat, Moscow (1968).
2. M. Berger and D. Raso, Rad. Res., 12, 20 (1960).
3. N. Shoemaker and C. Huddleston, Nucl. Sci. Eng., 18, 113 (1964).
4. V. I. Ivanov, A Course in Dosimetry [in Russian], Atomizdat, Moscow (1970).

LETTERS

DISTRIBUTION OF SCATTERED GAMMA RADIATION FROM A PULSED SOURCE

D. A. Kozhevnikov

UDC 539.122:539.12.172

The theory of the unsteady transport of gamma radiation in matter is becoming increasingly important as a result of the development of nanosecond measuring techniques, and has important applications (e.g., [1]). In using total absorption detectors the study of the distribution of multiply scattered radiation in the energy range of single scattering is of fundamental practical interest. The solution of the spatially homogeneous problem can reveal important regularities of the unsteady transport of gamma radiation.

The spectral-time distribution of scattered radiation from a pulsed monoenergetic source satisfies the transport equation [2]

$$[\hat{L}(\lambda)-\hat{K}]\,\Psi(t,\ \lambda\,|\,\lambda_0)=\delta(t)\,\delta(\lambda-\lambda_0), \tag{1}$$

where Ψ is the collision density of gamma photons, $\hat{L}$ and $\hat{K}$ are the transport and collision operators

$$[\hat{L}\Psi](\lambda)=\left[\tau(\lambda)\frac{\partial}{\partial t}+1\right]\Psi;\ [\hat{K}\Psi](\lambda)=\int_{\lambda}^{\lambda_0} h(\lambda')\,W(\lambda'\,|\,\lambda)\,\Psi\,d\lambda';$$

$\tau(\lambda)=[c\mu(\lambda)]^{-1}$ is the mean free time; $\mu(\lambda)$, total absorption coefficient; c, velocity of light; $h(\lambda)$, total scattering probability; and $W(\lambda_0/\lambda)$, Klein–Nishina–Tamm Compton scattering indicatrix. This indicatrix can be approximated as follows (Fig. 1):

$$\widetilde{W}(\lambda_0\,|\,\lambda)=W(\lambda_0)\,(\lambda/\lambda_0)^{\varkappa},\ \lambda_0\leqslant\lambda\leqslant\lambda_0+2;$$
$$W(\lambda)=\frac{1}{\sigma_K(\lambda)}\int\widetilde{W}(\lambda\,|\,\lambda')\,d\lambda'. \tag{2}$$

Here $\varkappa\equiv\varkappa(\lambda_0)$, but in the energy range of the bremsstrahlung spectrum it is possible to neglect the dependence of $\varkappa$ on λ_0 and take $\varkappa=\text{const}=1.82$.

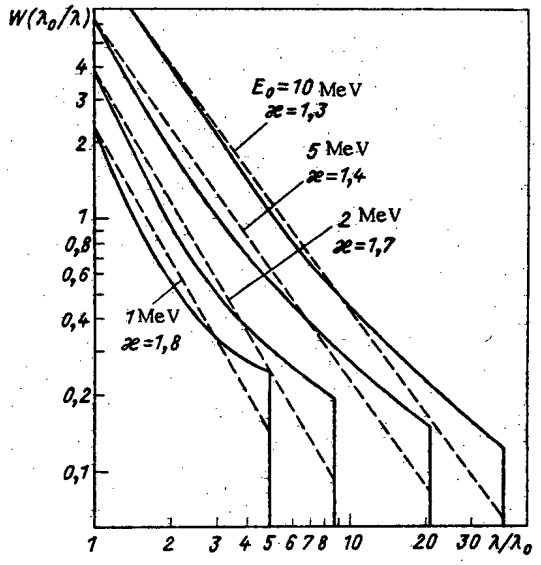

Fig. 1. Exact Compton scattering indicatrix (solid curve) and its approximation (dashed curve) for gamma photons of various energies.

Translated from Atomnaya Énergiya, Vol. 46, No. 3, pp. 178-179, March, 1979. Original article submitted November 22, 1976.

0038-531X/79/4603-0206$07.50

We separate out the singular part of the solution (the unscattered radiation) and introduce the notation

$$\Phi(s,\ \lambda\,|\,\lambda_0)=\int_0^\infty \Phi(t,\ \lambda\,|\,\lambda_0)\exp(-st)\,dt.$$

where $\Phi=\mu^{-1}\Psi$ is the flux density of scattered radiation.

Then

$$\Phi(s,\ \lambda\,|\,\lambda_0)=\frac{\Phi(\lambda\,|\,\lambda_0)\exp[I(s,\ \lambda)]}{[1+s\tau(\lambda_0)]\,[1+s\tau(\lambda)]}; \tag{3}$$

here $\Phi(\lambda\,|\,\lambda_0)$ is the spectrum of the scattered radiation:

$$\Phi(\lambda\,|\,\lambda_0)=\frac{h(\lambda_0)\,\widetilde{W}(\lambda_0\,|\,\lambda)}{\mu(\lambda)}\exp\left[\int_{\lambda_0}^{\lambda} h(\lambda')\,W(\lambda')\,d\lambda'\right]; \tag{4}$$

$$I(s,\ \lambda)=-\frac{sr_0^2n}{2c}\int_{\lambda_0}^{\lambda}\frac{d\lambda'}{[\mu(\lambda')+s/c]\,\mu(\lambda')}, \tag{5}$$

where n is the electron density of the medium and r_0 is the classical radius of the electron. Setting $\mu(\lambda)=\mu(\lambda_0)+(\lambda-\lambda_0)\dot{\mu}$, we obtain

$$\Phi(s,\ \lambda\,|\,\lambda_0)=c^2\Phi(\lambda\,|\,\lambda_0)\frac{[\mu(\lambda_0)]^{\beta+1}}{[\mu(\lambda)]^{\beta-1}}\frac{[c\mu(\lambda_0)+s]^{\beta-1}}{[c\mu(\lambda)+s]^{\beta+1}}, \tag{6}$$

where $\beta=r_0^2n/2\dot{\mu}$. The inverse Laplace transform of (6) is

$$\Phi(t,\lambda\,|\,\lambda_0)=\frac{\Phi(\lambda\,|\,\lambda_0)}{\tau(\lambda_0)\,\tau(\lambda)}\left[\frac{\mu(\lambda_0)}{\mu(\lambda)}\right]^{\beta}\frac{ct[\mu(\lambda)-\mu(\lambda_0)]}{c[\mu(\lambda)-\mu(\lambda_0)]}\times F\{(\beta+1);\ 2;\ ct[\mu(\lambda)-\mu(\lambda_0)]\}\exp[-t/\tau(\lambda_0)]. \tag{7}$$

For times

$$t\gg(\beta+1)/c[\mu(\lambda)-\mu(\lambda_0)], \tag{8}$$

the asymptotic representation of $F(\alpha,\ \gamma,\ x)$ can be used to simplify the result:

$$\Phi(t,\ \lambda\,|\,\lambda_0)=\frac{\Phi(\lambda\,|\,\lambda_0)}{\tau(\lambda_0)\,\tau(\lambda)}\left[\frac{\mu(\lambda_0)}{\mu(\lambda)}\right]^{\beta}\frac{\{ct[\mu(\lambda)-\mu(\lambda_0)]\}^{\beta}}{\mu(\lambda)-\mu(\lambda_0)}\frac{\exp[-ct\mu(\lambda_0)]}{\Gamma(\beta+1)}. \tag{9}$$

Calculations [3] by the Monte Carlo method led to a similar expression for the approximation of the time decay of gamma radiation from a pulsed source. It is interesting that the same distribution describes the kinetics of neutron slowing down [4].

LITERATURE CITED

1. N. V. Belkin et al., Dokl. Akad. Nauk SSSR, 224, No. 3, 569 (1975).
2. U. Fano, L. Spencer, and M. Berger, The Transport of Gamma Radiation [Russian translation], Gosatomizdat, Moscow (1963).
3. I. G. Dyad'kin, B. N. Krasil'nikov, and V. N. Starikov, At. Energ., 35, No. 4, 272 (1973).
4. D. A. Kozhevnikov, At. Energ., 40, No. 4, 338 (1976).

DESIGN OF TESLA TRANSFORMERS USED IN DIRECT-VOLTAGE ACCELERATORS

D. Kh. Dinev

UDC 621.384.6

Direct-voltage charged-particle accelerators, employing the Tesla transformer as a high-voltage generator, have come into wide use in recent years [1, 2]. In such accelerators the load to the secondary transformer circuit is the accelerating tube which accelerates beams with pulse currents ranging from tens to several thousand amperes. The present paper considers theoretically the effect of this load on the processes in the Tesla transformer and on its parameters.

Suppose that the current I_0 passes through the accelerating tube in a time $t_2 - t_1$ near the maximum accelerating voltage. The system of Kirchhoff equations for the primary and secondary circuits of the Tesla transformer with allowance for the load due to the beam is of the form

$$\left.\begin{aligned} L_1\frac{di_1}{dt}+R_1i_1+\frac{1}{C_1}\int_0^t i_1\,dt-U_0+M\frac{di_2}{dt}=0;\\ i_2=i_{C_2}+I_0H(t-t_1),\ t\leqslant t_2,\\ L_2\frac{di_2}{dt}+\frac{1}{C_2}\int_0^t i_{C_2}\,dt+M\frac{di_1}{dt}=0; \end{aligned}\right\} \quad (1)$$

where H(t) is a unit function; R_1, L_1, and C_1, primary-circuit parameters; L_2 and C_2, secondary-circuit parameters; M, mutual inductance; U_0, initial voltage across C_1; i_1, primary-circuit current; i_2, current in L_2; and i_{C_2}, current in C_2.

Here only damping in the primary circuit is taken into account since the logarithmic damping decrement in the primary circuit ($\Delta_1 = R_1/2L_1f_0$) is usually much greater than that of the secondary circuit ($\Delta_2 = R_2/2L_2f_0$). The solution of this system was found by operational methods.

Let us introduce the coefficient of coupling the two circuits of the transformer,

$$K^2 = M/L_1L_2; \quad (2)$$

the natural frequency

$$\omega_0^2 = 1/L_1C_1 = 1/L_2C_2; \quad (3)$$

the frequencies

$$\Omega_0^2 = \omega_0^2/(1+K),\quad \Omega_2^2 = \omega_0^2/(1-K); \quad (4)$$

parameters taking account of the damping

$$\sigma_1 = R_1/4L_1(1+K),\quad \sigma_2 = R_1/4L_1(1-K) \quad (5)$$

and a parameter making allowance for the load with the beam and having the dimensionality $\sec^{-1}$,

$$\chi = I_0/U_0\sqrt{C_1C_2}. \quad (6)$$

The secondary voltage of the Tesla transformer or, in other words, the accelerating voltage, will then be of the form

$$U_2 = \begin{cases} -\frac{U_0}{2}\sqrt{\frac{C_1}{C_2}}\left(e^{-\sigma_1 t}\cos\Omega_1 t - e^{-\sigma_2 t}\cos\Omega_2 t\right),\ t<t_1\\ -\frac{U_0}{2}\sqrt{\frac{C_1}{C_2}}\left[Ae^{-\sigma_1 t}\cos(\Omega_1 t-\varphi_1) - Be^{-\sigma_2 t}\cos(\Omega_2 t-\varphi_2)\right],\ t_1\leqslant t\leqslant t_2, \end{cases} \quad (7)$$

where

Physics Department, University of Sophia, Bulgaria. Translated from Atomnaya Énergiya, Vol. 46, No. 3, pp. 179-180, March, 1979. Original article submitted May 4, 1977.

 0038-531X/79/4603-0208 $07.50

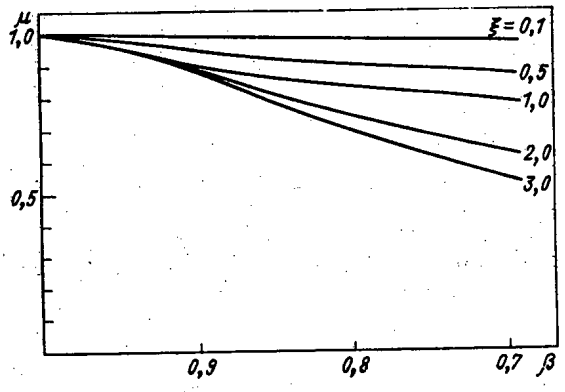

Fig. 1. Dependence of the relative decrease in the amplitude of the accelerating voltage on the moment of injection for different values of the current loads.

$$A^2 = A_1^2 + A_2^2;$$
$$A_1 = \frac{\chi \exp(\sigma_1 t_1)\cos\Omega_1 t_1}{\Omega_1};$$
$$A_2 = 1 - \frac{\chi \exp(\sigma_1 t_1)\sin\Omega_1 t_1}{\Omega_1};$$
$$\operatorname{tg}\varphi_1 = A_1/A_2;$$
$$B^2 = B_1^2 + B_2^2;$$
$$B_1 = -\frac{\chi \exp(\sigma_2 t_1)\cos\Omega_2 t_1}{\Omega_2};$$
$$B_2 = 1 + \frac{\chi \exp(\sigma_2 t_1)\sin\Omega_2 t_1}{\Omega_2};$$
$$\operatorname{tg}\varphi_2 = B_1 = B_2. \qquad (8)$$

The solution of Eq. (7) was found with the assumption that the damping is low, i.e., that $\sigma_1 \ll \Omega_1$ and $\sigma_2 \ll \Omega_2$.

The Tesla transformers employed in direct-voltage accelerators usually have a coupling coefficient K = 0.6. Equation (7) shows that the secondary voltage of the loaded transformer reaches a maximum in the time t_{max}, somewhat shorter than the time for the unloaded transformer, $t^0_{max} = \pi\sqrt{1.6 L_1 C_1}$. It can be shown that with K = 0.6 we have

$$(t_{max} - t^0_{max})/t^0_{max} = \varphi_1/\pi. \qquad (9)$$

The maximum value of the secondary voltage U_{max} depends on the load. For a very low damping and K = 0.6 (which is what is used most often) this dependence can be expressed in terms of only two dimensionless parameters: $\beta = t_1/t^0_{max}$ and $\xi = \chi t^0_{max}$. For this case we have

$$A_1 = \frac{\xi}{\pi}\cos\beta\pi;$$
$$A_2 = 1 - \frac{\xi}{\pi}\sin\beta\pi;$$
$$B_1 = -\frac{\xi}{2\pi}\cos 2\beta\pi;$$
$$B_2 = 1 + \frac{\xi}{2\pi}\sin 2\beta\pi \qquad (10)$$

and therefore,

$$\mu = \frac{U_{2max}}{U^0_{2max}} = \frac{A + B\cos(\Omega_2 t^0_{max} - \psi_2)}{2}. \qquad (11)$$

This dependence is plotted in Fig. 1 for several characteristic values of β and ξ.

LITERATURE CITED

1. E. A. Abramyan and S. B. Vasserman, At. Energ., 23, No. 1, 44 (1967).
2. G. A. Mesyats, A. S. Nasibov, and V. V. Kremnev, Shaping of Nanosecond High-Voltage Pulses [in Russian], Énergiya, Moscow (1970).

RADIATION ALTERATION OF THE PROPERTIES OF GRAPHITE OVER A WIDE RANGE OF IRRADIATION TEMPERATURE AND NEUTRON FLUX

Yu. S. Virgil'ev, I. P. Kalyagina, and V. G. Makarchenko

UDC 621.039.532.21

Investigations have been conducted in recent years of radiation alternation of the physical properties of contruction graphite, including GMZ-brand graphite [1-7], which in combination with the experimental data obtained has permitted establishment of dosage relations for alternations of the following properties: the crystal lattice parameter c, the diameter and height of the crystallites, the electrical resistivity, the dynamic modulus of elasticity, the bending and compressive strength limits, and the geometrical dimensions for the neutron flux range 10^{18}– $2.5 \cdot 10^{22}$ neutrons/cm^2 and an irradiation temperature of 70-90°C.

Since the relative change of the parameter c of graphite depends weakly on the absolute value of this parameter in the case of irradiation [8], data for other brands of graphite [9] were used in establishing the dosage relations. An increase of the parameter c starts to be detected upon irradiation by a flux above $(2\text{-}3) \cdot 10^{19}$ neutrons/cm^2, and stabilization of the relative change ($\Delta c/c$) begins for 70-100°C at a flux above $(3\text{-}4) \cdot 10^{20}$ neutrons/cm^2 (Fig. 1). As the irradiation temperature is increased, the onset of stabilization shifts into the region of higher flux, and $\Delta c/c$ decreases according to the exponential law [8]. In the case of irradiation at a temperature of 950°C, $\Delta c/c \approx 0$.

The diameter and height of crystallites (regions of coherent scattering – RCS), determinable from the width of the diffraction lines, start to decrease after irradiation at 70-100°C by a flux exceeding $(2\text{-}3) \cdot 10^{18}$ neutrons/cm^2. Upon an increase of the irradiation temperature the rate of this decrease is reduced. The dimensions of the crystallites of samples irradiated at 800-950°C by a flux of up to $(1\text{-}1.5) \cdot 10^{22}$ neutrons/cm^2 decreased by approximately a factor of two.

The variation of the parameter c is accompanied by a change in the geometrical dimensions of the samples (Fig. 2). In the case of low-temperature irradiation (70-170°C) by a flux above $3 \cdot 10^{21}$ neutrons/cm^2 a slowing down of the radiation growth of samples cut out parallel to the extrusion axis is traced (see Fig. 2a). However, stabilization is not attained at $8 \cdot 10^{21}$ neutrons/cm^2. The largest relative elongation was 3%.

At a temperature above 250-300°C radiation-thermal shrinkage of the samples occurs, whose greatest rate is observed at 400-500°C. After irradiation by a flux $\sim 2 \cdot 10^{22}$ neutrons/cm^2 the shrinkage reached 4% and was not stabilized. An increase of the temperature to 700-800°C reduced the shrinkage rate; at a flux above $2 \cdot 10^{22}$ neutrons/cm^2 a slowing down of the process was noticed. It is possible to assume that the maximum shrinkage does not exceed 1.5% in this case.

For samples cut out perpendicularly to the extrusion axis the change in the length stabilized at a level of ~4% (see Fig. 2b) after irradiation by a flux greater than $5 \cdot 10^{20}$ neutrons/cm^2 at 70-100°C. As the irradiation temperature increases to 130-170°C the onset of stabilization is shifted into the region of higher flux, and the "saturation" level is lowered.

At a temperature above 250-300°C shrinkage of the samples occurs at a lower rate than for the parallel-oriented samples, and it ceases upon reaching a flux of $\sim 1 \cdot 10^{22}$ neutrons/cm^2, after which it is replaced by "secondary" swelling. The maximum shrinkage does not exceed 1%; the secondary swelling, 0.5%. At a higher irradiation temperature (950°C) the maximum shrinkage decreases to 0.2%, and the secondary swelling starts at a flux above $0.8 \cdot 10^{22}$ neutrons/cm^2, and after irradiation by a flux of $1.4 \cdot 10^{22}$ neutrons/cm^2 it reaches 0.9%. The anisotropy of the change in shape of the GMZ-brand graphite is exhibited in a greater swelling of the perpendicularly oriented samples for low-temperature irradiation, less shrinkage of them above 300°C, and the appearance of secondary swelling at a lower irradiation level.

Translated from Atomnaya Énergiya, Vol. 46, No. 3, pp. 180-182, March, 1979. Original article submitted March 22, 1978.

0038-531X/79/4603-0210$07.50

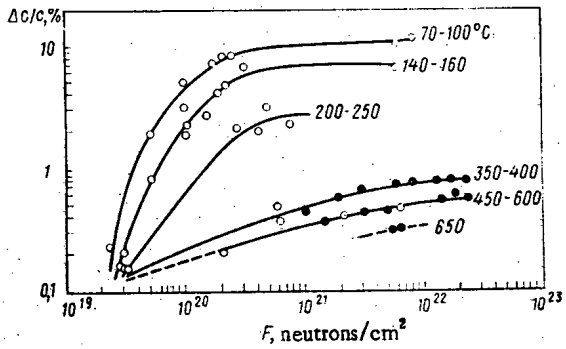

Fig. 1. Dependence of the relative change of the crystal latter parameter c on neutron flux at different irradiation temperatures: O) GMZ-brand graphite; ●) other brands of graphite [9].

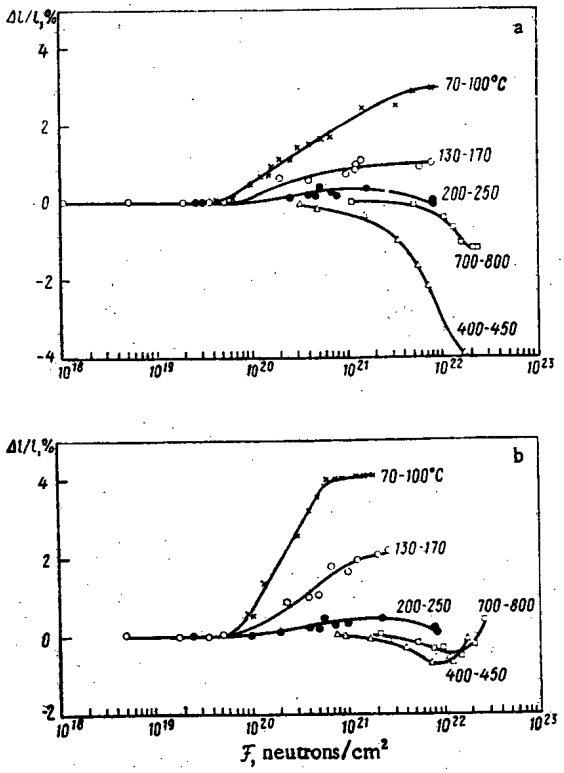

Fig. 2. Dependence of the relative variation of the dimensions of GMZ-brand graphite samples cut out (a) parallel and (b) perpendicular to the extrusion axis on the neutron flux for different irradiation temperatures.

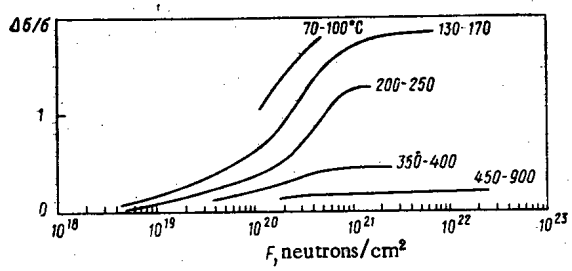

Fig. 3. Dependence of the relative variation of the compressive strength limit of GMZ-brand graphite on the neutron flux at different irradiation temperatures.

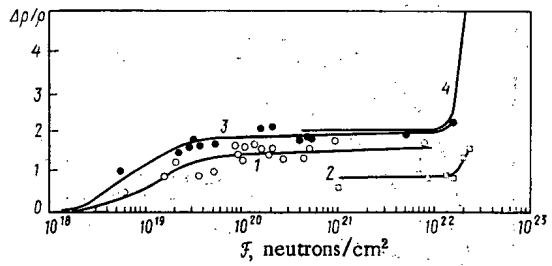

Fig. 4. Dependence of the relative variation of the electrical resistivity of samples of (1, 2) GMZ, (3) VPG, and (4) CSF graphite on the neutron flux at an irradiation temperature of 130-950°C (the samples are cut out parallel to the extrusion axis).

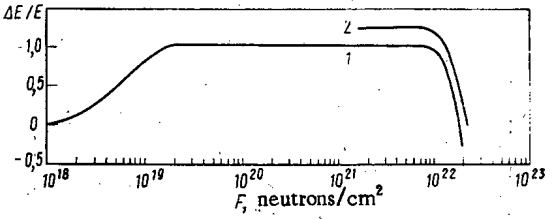

Fig. 5. Dependence of the relative variation of the dynamic modulus of elasticity of GMZ-brand graphite on the neutron flux in the temperature range of 130-950°C for samples cut out (1) parallel and (2) perpendicular to the extrusion axis.

The radiation increase in the strength of the GMZ-brand graphite in the case of compression (σ_c) is practically the same in both directions and is detected at a flux above $4 \cdot 10^{18}$ neutrons/cm^2 (Fig. 3). At 70-100°C the strengthening ($\Delta\sigma/\sigma_c$) is evidently stabilized and amounts to ~200% at 10^{21} neutrons/cm^2.

An increase in the irradiation temperature to 950°C reduces the radiation effect to approximately 20%. The losses in strength observed at a large flux [10] for GMZ graphite does not occur until $2 \cdot 10^{22}$ neutrons/cm^2. The variation of the bending strength limit (σ_b) of the GMZ-brand graphite samples upon irradiation in the 450-950°C temperature range is similar to the variation in the compressive strength limit. There exist definite relationships among the values of the compressive, bending, and tensile strength limits of GMZ-brand graphite which do not vary upon irradiation [2]: $\sigma_c/\sigma_t = 4.27 \pm 0.30$, $\sigma_b/\sigma_t = 2.51 \pm 0.18$, and $\sigma_c/\sigma_b = 1.72 \pm 0.05$, which facilitates their estimation in the flux range $(5-7) \cdot 10^{21}$ to $2 \cdot 10^{22}$ neutrons/cm^2.

The electrical resistivity ρ starts to vary at a flux exceeding $3 \cdot 10^{18}$ neutrons/cm^2, just as do the dimensions of the RCS, and it is stabilized at $(3-5) \cdot 10^{19}$ neutrons/cm^2 (Fig. 4). In the range 70-950°C $\Delta\rho/\rho$ is practically independent of the irradiation temperature. At the same time differences in the density and especially in the degree of completeness of the crystal structure of the samples [11] made out of various batches of graphite have a significant effect both on the absolute value of the electrical resistance and on its variation. The "disjointedness" of curves 1 and 2 for GMZ-brand graphite (see Fig. 4) is explained by this.

VPG-brand graphite, which is more uniform, dense, and possessed of perfect crystal structure, is distinguished by a higher $\Delta\rho/\rho$. The dependence of the electrical resistance of this graphite on the flux is in satisfactory agreement with that obtained for CSF-brand graphite, which is also graphitized at 2800°C (see Fig. 4); $\Delta\rho/\rho$ for CSF graphite does not depend on the irradiation temperature in the range 300-1000°C [10]. The relative variation of the electrical resistivity of perpendicularly oriented samples varies similarly to what has been discussed; however, its absolute value is higher. Samples irradiated at a temperature above 450°C exhibit a new "secondary" increase in the electrical resistance at a flux above $(1-1.5) \cdot 10^{22}$ neutrons/cm^2. A decrease in the dynamic modulus of elasticity corresponds to this result, which becomes less at a flux exceeding $2 \cdot 10^{22}$ neutrons/cm^2 than for unirradiated graphite (Fig. 5).

The variations in the electrical resistivity and the modulus of elasticity due to development of a process of secondary swelling are associated with irreversible changes of the subcrystalline structure of graphite, which are preserved right up to the graphitization temperature (2300°C) [12].

LITERATURE CITED

1. I. P. Kalyagina et al., At. Energ., 36, No. 3, 212 (1974).
2. Yu. S. Virgil'ev, V. G. Makarchenko, and Yu. S. Churilov, Probl. Prochn., No. 1, 95 (1977).
3. Yu. S. Virgil'ev, At. Energ., 36, No. 6, 479 (1974).
4. Yu. S. Virgil'ev et al., At. Energ., 38, No. 5, 304 (1975).
5. L. M. Nikishina, Yu. S. Virgil'ev, and V. G. Makarchenko, in: Construction Materials Based on Carbon [in Russian], No. 13, Metallurgiya, Moscow (1978), p. 57.
6. Yu. S. Virgil'ev, I. P. Kalyagina, and T. N. Shurshakova, in: Construction Materials Based on Graphite [in Russian], No. 5, Metallurgiya, Moscow (1970), p. 37.
7. V. I. Klimenkov et al., in: Radiation Physics of a Solid Body and Reactor Materials Study [in Russian], Atomizdat, Moscow (1970), p. 240.
8. Yu. S. Virgil'ev, At. Energ., 30, No. 3, 312 (1971).
9. T. N. Shurshakova, Yu. S. Virgil'ev, and I. P. Kalyagina, At. Energ., 40, No. 5, 399 (1976).
10. J. Cox and J. Helm, Carbon, 7, No. 2, 319 (1969).
11. Yu. S. Virgil'ev, Izv. Akad. Nauk SSSR, Ser. Neorg. Mater., 9, No. 9, 1546 (1973).
12. Yu. S. Virgil'ev, E. I. Kurolenkin, and T. N. Shurshakova, Izv. Akad. Nauk SSSR, Ser. Neorg. Mater., 13, No. 4, 752 (1977).

THE FORMATION OF TRANSURANIUM NUCLIDES IN CONNECTION WITH THE COMBINED USE OF VVÉR AND RBMK POWER REACTORS

T. S. Zaritskaya, A. K. Kruglov, and A. P. Rudik

UDC 621.039.516.22

The effect of the enrichment of nuclear fuel on the formation of transuranium nuclides in power reactors was discussed earlier [1]. In this article we dwell on the question of the combined use of fuel for VVÉR (water-modulated–water-cooled) and RBMK (high-power water-cooled channel) reactors. As is well known [2], in the standard mode RBMK reactors operate on uranium fuel enriched up to 1.8% in ^{235}U. At the same time VVÉR reactors use uranium fuel enriched up to 3-4% in ^{235}U; an appreciable amount of ^{235}U (~1.0-1.5%) remains in the depleted fuel of VVÉR reactors, and 5-10 kg/ton of a mixture of plutonium isotopes accumulates. Therefore, after purification of fission products VVÉR fuel possesses sufficient reactivity to be loaded into RBMK.

The main purpose of this article is to estimate from the physical point of view the realities of such a possibility for reactors similar in their characteristics to VVÉR and RBMK. Therefore, we will restrict ourselves to approximate values of the initial data, basing our deliberations on [2-4]. Two alternatives have been considered: alternative I) plutonium is extracted from depleted VVÉR fuel and mixed with depleted uranium; the new fuel is loaded into RBMK reactors; alternative II) VVÉR fuel purified of fission products is loaded directly into RBMK reactors. It was assumed in alternative I that there are 4 kg of ^{235}U and 20 kg of plutonium of isotopic composition 60% ^{239}Pu, 24% ^{240}Pu, 11% ^{241}Pu, and 4% ^{242}Pu in each ton of fuel loaded into RBMK reactors. In alternative II the plutonium was not separated from the uranium in the course of regeneration, and fuel containing 15 kg of ^{235}U, 4.76 kg of ^{236}U, and 7 kg of plutonium of the indicated isotopic composition per ton was loaded into RBMK reactors.

The multiplication factors $K_{eff}(0)$ characterizing fresh fuel were calculated with neutron absorption taken into account only in the uranium and plutonium, without taking into account the escape of neutrons from the reactor core, multiplication by fast neutrons, and absorption in construction materials, the moderator, and the coolant:

Translated from Atomnaya Énergiya, Vol. 46, No. 3, pp. 183-185, March, 1979. Original article submitted April 3, 1978.

0038-531X/79/4603-0213$07.50

$$\widetilde{K}_{eff}(0)=\frac{\sum_i \nu_i \hat{\sigma}_i f_i \rho_i(0)}{\sum \hat{\sigma}_k \rho_k(0)}\varphi_s; \quad (1)$$

$$\hat{\sigma}=\sigma_t+\gamma I_b. \quad (2)$$

where σ_t is the effective thermal cross section, I_b is the blocked resonance integral, γ is the rigidity of the spectrum [3], and $\rho_i(0)$ is the concentration of nuclides; the remaining symbols are those generally adopted.

TABLE 1. Effective Resonance Integral of ^{240}Pu

ρ^{240}	I_b^{240}	ρ^{240}	I_b^{240}	ρ^{240}	I_b^{240}	ρ^{240}	I_b^{240}
0	8430	0,007	1694	0,004	2242	0,011	1353
0,001	4577	0,008	1582	0,005	2006	0,012	1295
0,002	3203	0,009	1493	0,006	1829		
0,003	2613	0,010	1420				

TABLE 2. Effective Resonance Integral of ^{242}Pu

ρ^{242}	I_b^{242}	ρ^{242}	I_b^{242}	ρ^{242}	I_b^{242}	ρ^{242}	I_b^{242}
0	1220	0,0024	770	0,0012	936	0,0036	637
0,0004	1110	0,0028	723	0,0016	869	0,0040	611
0,0008	1018	0,0032	677	0,0020	812		

TABLE 3. Effective Multiplication Factors

Mode	$\widetilde{K}_{eff}(0)$
Steady-state RBMK	1,473
Alternative I	1,379
Alternative II	1,398

TABLE 4. Transuranium Nuclides in the Standard Mode of an RBMK, kg/ton

Characteristic of the mode	E, 10^3 MW · days/ton					
	0	4	8	12	16	20
Time, years	0	0,376	0,752	1,128	1,504	1,880
Rigidity of the spectrum γ	0,1650	0,1639	0,1497	0,1308	0,1110	0,0934
^{235}U*	17,8	13,3	9,63	6,70	4,37	2,63
^{236}U	0	0,76	1,34	1,78	2,10	2,30
^{237}Np	0	0,01	0,04	0,08	0,13	0,18
^{238}Pu	0	$5,2\cdot10^{-4}$	$3,8\cdot10^{-3}$	$1,2\cdot10^{-2}$	$2,5\cdot10^{-2}$	$4,4\cdot10^{-2}$
^{238}U	982,2	979,9	977,4	974,8	971,8	968,5
^{239}Pu	0	1,55	2,18	2,36	2,31	2,17
^{240}Pu	0	0,21	0,61	1,04	1,46	1,83
^{241}Pu	0	0,04	0,18	0,33	0,45	0,52
^{242}Pu	0	$2,4\cdot10^{-3}$	$2,5\cdot10^{-2}$	$8,5\cdot10^{-2}$	0,192	0,344
^{243}Am	0	$4,9\cdot10^{-5}$	$1,1\cdot10^{-3}$	$5,6\cdot10^{-3}$	$1,7\cdot10^{-2}$	$3,9\cdot10^{-2}$
^{244}Cm	0	$1,5\cdot10^{-6}$	$7,0\cdot10^{-5}$	$5,0\cdot10^{-4}$	$2,6\cdot10^{-3}$	$7,9\cdot10^{-3}$
Fission products of ^{235}U	0	3,8	6,8	9,2	11,2	12,6
Fission products of Pu	0	0,5	1,8	3,6	6,0	8,9

*Here and in Tables 5 and 6 nuclide concentrations are denoted by the corresponding chemical symbols.

TABLE 5. Transuranium Nuclides upon the Loading of a Mixture of Depleted Uranium with Plutonium (alternative I) into the RBMK, kg/ton

Characteristic of the mode	E, 10^3 MW·days/ton					
	0	4	8	12	16	20
Time, years	0	0,1652	0,3304	0,4956	0,6608	0,8260
Rigidity of the spectrum γ	0,4400	0,3546	0,2808	0,2187	0,1689	0,1316
^{235}U	4,0	3,40	2,80	2,21	1,64	1,13
^{236}U	0	0,11	0,22	0,31	0,40	0,47
^{237}Np	0	$1,8\cdot10^{-3}$	$6,9\cdot10^{-3}$	$1,5\cdot10^{-2}$	$2,4\cdot10^{-2}$	$3,5\cdot10^{-2}$
^{238}Pu	0	$6,5\cdot10^{-5}$	$5,1\cdot10^{-4}$	$1,7\cdot10^{-3}$	$3,9\cdot10^{-3}$	$7,3\cdot10^{-3}$
^{238}U	976,0	974,1	972,1	969,9	967,4	964,6
^{239}Pu	22,0	9,26	6,94	5,11	3,77	2,90
^{240}Pu	4,80	5,31	5,57	5,60	5,41	5,04
^{241}Pu	2,20	2,30	2,29	2,15	1,91	1,62
^{242}Pu	0,80	0,97	1,18	1,44	1,74	2,06
^{243}Am	0	$6,8\cdot10^{-2}$	$13,7\cdot10^{-2}$	$20,8\cdot10^{-2}$	$28,3\cdot10^{-2}$	$36,2\cdot10^{-2}$
^{244}Cm	0	$5,8\cdot10^{-3}$	$2,3\cdot10^{-2}$	$5,3\cdot10^{-2}$	$9,5\cdot10^{-2}$	$15\cdot10^{-2}$
Fission products of ^{235}U	0	0,48	0,97	1,46	1,93	2,36
Fission products of Pu	0	3,79	7,58	11,37	15,17	19,02

TABLE 6. Transuranium Nuclides upon the Loading of Spent Fuel from a VVÉR into an RBMK (alternative II), kg/ton

Characteristic of the mode	E, 10^3 MW·days/ton					
	0	4	8	12	16	20
Time, years	0	0,24	0,48	0,72	0,96	1,20
Rigidity of the spectrum γ	0,2810	0,2429	0,2067	0,1731	0,1428	0,1169
^{225}U	15,10	12,14	9,53	7,17	5,11	3,39
^{236}U	4,76	5,11	5,40	5,63	5,79	5,87
^{237}Np	0	0,15	0,29	0,42	0,54	0,64
^{238}Pu	0	0,008	0,033	0,072	0,123	0,181
^{238}U	973,3	971,3	969,1	966,8	964,2	961,4
^{239}Pu	4,20	3,81	3,43	3,07	2,74	2,44
^{240}Pu	1,68	1,91	2,11	2,27	2,42	2,53
^{241}Pu	0,770	0,876	0,924	0,925	0,890	0,832
^{242}Pu	0,280	0,371	0,484	0,620	0,775	0,950
^{243}Am	0	0,027	0,057	0,092	0,132	0,178
^{244}Cm	0	$2,2\cdot10^{-4}$	$9,2\cdot10^{-3}$	$2,2\cdot10^{-2}$	$4,1\cdot10^{-2}$	$6,8\cdot10^{-2}$
Fission products of ^{235}U	0	2,35	4,51	6,46	8,17	9,60
Fission products of Pu	0	1,95	4,08	6,42	9,00	11,86

The summation in the numerator of Eq. (1) is performed for the fissionable nuclides, while that in the denominator is performed for ^{235}U and ^{236}U, thermal absorption in ^{238}U, and plutonium isotopes. Resonance absorption in ^{238}U is taken into account by the factor φ_8. Blocking of the resonance integrals of ^{240}Pu and ^{242}Pu is significant for RBMK reactors.

The dependence of the resonance integrals on the concentrations of the plutonium isotopes (determined according to [3]) in UO_2 or PuO_2 with a fuel-element diameter of 11.7 mm is presented in Tables 1 and 2. The multiplication factors were calculated from Eq. (1) with $\varphi_8 = 0.89$ (Table 3).

It follows from the data of Table 3 that the reactivity is sufficiently great for alternatives I and II. We will not dwell on this question in greater detail; we emphasize only that in the first place the relative role of poisoning absorptions in construction materials is less for alternatives with a plutonium-containing fuel (I and II) than for the basic (uranium) version of the RBMK, and in the second place if one requires the identical average $\tilde{K}_{eff}$ during the time the fuel is in the reactor, then the depletion depth turns out to be $\sim 20\cdot10^3$ MW·days/ton of U for all three versions (see Table 3).

Calculation of the kinetics of the formation of different nuclides was performed according to the procedure outlined in [3]; blocking of the resonance integrals was taken into account only for ^{240}Pu and ^{242}Pu, as this blocking is insignificant for the remaining nuclides. Values of physical constants adopted from [1, Table 1] were used.

The results of the calculation of the formation of nuclides under different operating conditions of the RBMK are given in Tables 4-6. Here are given the concentrations of the fission products of ^{235}U and the fissionable isotopes of plutonium; the time has been calculated with a neutron flux density of $3.5 \cdot 10^{13}$ neutrons/($cm^2 \cdot sec$); irradiation is performed at a constant power removed from 1 ton of fuel.

The qualitative regularities which are revealed upon analysis of the data of Tables 4-6 are completely natural. In the nuclide formation chain starting in ^{235}U, the yields of ^{237}Np and ^{238}Pu are appreciably reduced in alternative I in comparison with the standard mode of an RBMK, since the ^{235}U charge is reduced, and the ^{237}Np and ^{238}Pu yields in alternative II grew sharply due to the initial charge of ^{236}U, although the ^{235}U charge remained practically the same. In the nuclide formation chain which normally starts with ^{238}U, the yields of ^{243}Am and ^{244}Cm grew in alternatives I and II in comparison with the standard mode of an RBMK, which is caused by the use of plutonium isotopes as the fuel. The quantitative results presented in Tables 4-6 may be useful in connection with discussion of the problem of the advisability of using different kinds of fuel with the addition of plutonium in RBMK reactors.

The authors express deep gratitude to A. K. Kalugin and E. P. Kunegin for useful discussions of the problems considered in this paper.

LITERATURE CITED

1. T. S. Zaritskaya, A. K. Kruglov, and A. P. Rudik, At. Energ., 41, No. 5, 321 (1976).
2. Twenty Years of Atomic Energy [in Russian], Atomizdat, Moscow (1974).
3. A. K. Kruglov and A. P. Rudik, Artificial Isotopes and a Procedure for Calculation of their Formation in Nuclear Reactors [in Russian], Atomizdat, Moscow (1977).
4. Atomic Science and Technology in the USSR [in Russian], Atomizdat, Moscow (1977).

YIELDS OF ^{28}Mg UPON THE IRRADIATION OF MAGNESIUM AND ALUMINUM BY ALPHA PARTICLES

P. P. Dmitriev and G. A. Molin

UDC 539.172.12

The only radionuclide of magnesium which has a half-life convenient for application is ^{28}Mg ($T_{1/2} = 20.93$ h), which is widely used in various investigations.

An isobaric chain is formed upon the decay of ^{28}Mg:

$$^{28}_{12}Mg \xrightarrow[20.93\,h]{\beta-} {}^{28}_{13}Al \xrightarrow[2.24\,min]{\beta-} {}^{28}_{14}Si,$$

i.e., ^{28}Mg is the generator of ^{28}Al. The most intense γ lines accompanying the decay of ^{28}Mg in equilibrium with ^{28}Al are given in Table 1 (the data are taken from [1]).

The excitation functions of the reactions ^{28}Mg (α2p) ^{28}Mg and ^{27}Al (α3p) ^{28}Mg were measured in [2-5], and the excitation functions of the reactions ^{26}Mg (tp) ^{28}Mg and ^{27}Al (t2p) ^{28}Mg were also measured in [4]. Upon the irradiation of aluminum, ^{28}Mg is obtained "without carrier," which is very important for the use of ^{28}Mg in medical investigations. The integration was performed over the range of the indicated excitation functions, and ^{28}Mg-yield curves are obtained as a function of the energy of the bombarding particles (see Fig. 1). The values of the ^{28}Mg yields for the maximum particle energy and the smaller energy values common to these papers are given in Table 2.

The curves of the ^{28}Mg yield upon irradiation of thick targets of magnesium and aluminum by α particles are measured in this paper. Thick samples of metallic magnesium and stacks of aluminum foil (foil thickness of 18.5 mg/cm^2) were irradiated in a deflected beam of the 1.5-m cyclotron of the FÉI. The irradiation pro-

Translated from Atomnaya Énergiya, Vol. 46, No. 3, pp. 185-187, March, 1979. Original article submitted April 24, 1978.

 0038-531X/79/4603-0216$07.50

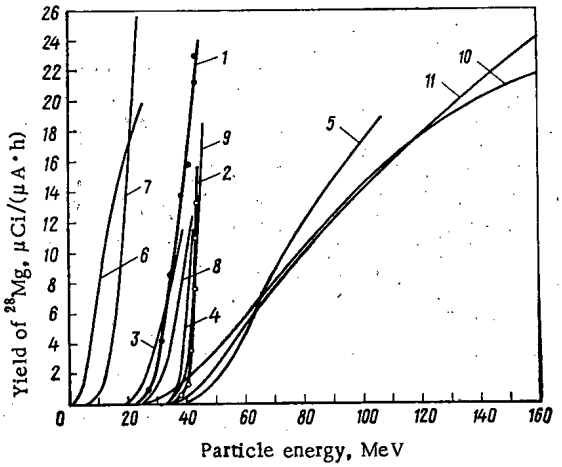

Fig. 1. Dependence of the ^{28}Mg yield on the energy of the α particles and tritons for thick targets made out of magnesium and aluminum: 1) Mg+ α (× 10) [this paper]; 2) Al+ α (× 50) [this paper]; 3) Mg+ α (× 10) [2]; 4) Al+ α (× 50) [2]; 5) Al+ α [3]; 6) Mg+ t (:10) [4]; 7) Al+ p (:5) [4]; 8) Mg+ α (× 10) [4]; 9) Al+ α (× 50) [4]; 10) Mg+ α [5]; 11) Al+ α [5]; ● and ○ denote experiment for 1 and 2.

TABLE 1. γ-Ray Quanta of ^{28}Mg +^{28}Al

Energy of γ quanta, keV	Quanta/ decay, %	Energy of γ quanta, keV	Quanta/ decay, %
1778,8 *	100	400,6	35,9
1342,2	54	30,6	95
941,7	35,8		

*It is emitted by daughter ^{23}Al.

TABLE 2. Comparison of ^{28}Mg Yields

Reaction to obtain ^{28}Mg	Particle energy, MeV	Yield, μCi/(μA·h)	Reference
^{26}Mg (α 2 p)	160	21,7	[5]
	44	2,3	*
		2,4	[5]
		1,4	[4]
		1,5	[2]
	36	0,97	*
		0,99	[5]
		0,51	[4]
		0,89	[2]
^{27}Al (α 3 p)	160	24,0	[5]
	104	15,1	[5]
		18,3	[3]
	44	0,30	*
		1,08	[5]
		0,38	[3]
		0,23	[4]
		0,27	[2]
	40	0,024	*
		0,5	[5]
		0,12	[3]
		0,062	[4]
		0,11	[2]
^{26}Mg (tp)	24	190	[4]
^{27}Al (t 2 p)	24	128	[4]

*This paper.

TABLE 3. ^{28}Mg Yields

Mg + α		Al + α	
E_α, MeV	yield, μCi/(μA·h)	E_α, MeV	yield, μCi/(μA·h)
43,5±0,6	2,30±0,31	43,5±0,6	0,26±0,03
43,5±0,6	2,12±0,29	43,1±0,6	0,22±0,03
41,0±0,7	1,58±0,22	42,5±0,6	0,15±0,02
38,9±0,7	1,38±0,19	41,5±0,7	0,072±0,010
34,8±0,8	0,85±0,13	40,5±0,7	0,025±0,004
31,5±0,9	0,41±0,06	38,0±0,7	0,013±0,002
26,7±1,0	0,093±0,014	—	—

cedure is similar to that described in [6]. The energy of the α particles for irradiation of magnesium was varied by aluminum retarding foil.

The integrated current was measured from the activity of ^{65}Zn in copper monitoring foil. A cross section for the reaction ^{63}Cu (α, pn+ 2n) ^{65}Zn equal to 300 mb at E_α=45 MeV was used for calculation of the integrated current. This value is obtained in the following way: the relative behavior of the cross section of the indicated reaction in the 40-45 MeV range was measured by the foil-stacking method and normalized to the cross section of 521 mb at E_α=40.1 MeV, measured in [7]. The error in the measurement of the integrated current is ~8%.

A significant admixture of ^{24}Na and other radionuclides is formed upon the irradiation of magnesium and aluminum by α particles, which complicates measurement of the ^{28}Mg activity. In order to decrease the distortions the photopeak of γ quanta with an energy of 30.6 keV was measured with the help of a type DGR5-3 Ge(Li) detector with a thickness of 4.8 mm and a beryllium window (for the 122.06 keV γ line of ^{57}Co the half-width is ~2.5 keV). The photoefficiency for the K_α and K_β components of the x-ray radiation of ^{139}Ce was measured, and the photoefficiency for E_γ=30.6 keV is obtained by means of linear extrapolation. A ^{139}Ce reference standard from the OSGI set (error of 3% at the 0.95 confidence level) was used, and the quantum yield of the K_α (62.4%) and K_β (14.0%) components is determined from the data of [1]. A correction was introduced for self-absorption of E_γ=30.6 keV in the irradiated samples. The error in the measurements of the ^{28}Mg activity was 10-12%, and the measurement error of the ^{28}Mg yield was 13-15%. The measured values of the ^{28}Mg yield are given in Table 3 and in Fig. 1.

A comparison of the data on the ^{28}Mg yields given in Fig. 1 and in Table 2 shows their poor agreement. The causes of this are evidently systematic errors in the measurement of the ^{28}Mg activity (background of ^{24}Na) and a strong dependence of the reaction cross section on the energy of the α particles, due to which small errors in the determination of the α particle energy alter appreciably the behavior of the excitation function (and the yield curve). The most effective method of obtaining ^{28}Mg is irradiation by tritons; however, the high cost and toxicity of tritium hinder this approach.

The authors thank Z. P. Dmitriev for help in the research.

LITERATURE CITED

1. N. G. Gusev and P. P. Dmitriev, Quantum Radiation of Radioactive Nuclides [in Russian], Atomizdat, Moscow (1977).
2. R. Lindsay and R. Carr, Phys. Rev., 118, 1293 (1960).
3. U. Martens and G. Schweimer, Z. Phys., 233, 170 (1970).
4. T. Nozaki et al., J. Appl. Rad. Isotopes, 26, 17 (1975).
5. H. Probst et al., J. Appl. Rad. Isotopes, 27, 431 (1976).
6. P. P. Dmitriev et al., At. Energ., 42, No. 2, 148 (1977); 41, No. 1, 48 (1976).
7. N. Porile and D. Morrison, Phys. Rev., 116, 1193 (1959).

SOME PROPERTIES OF FLUCTUATIONS OF THE NEUTRON FIELD IN A NUCLEAR REACTOR

E. A. Gomin and S. S. Gorodkov

UDC 621.039.512.45

Experiment shows that the deviations $\mathring{\Phi}(\mathbf{r})$ of the true values of the neutron field $\tilde{\Phi}(\mathbf{r})$, from the calculated $\Phi(\mathbf{r})$ at each point of a reactor can be treated as random. In large reactors these departures are appreciable, which makes their investigation especially important. In addition, some properties of $\mathring{\Phi}(\mathbf{r})$ are also used in connection with the mathematical processing of discrete internal reactor measurements of the neutron field, which permits improving the accuracy of the energy distribution calculation and raising the reactor power. References 1 and 2 are devoted to the investigation of $\mathring{\Phi}(\mathbf{r})$. The first paper is characterized by a numerical experiment and is based to a certain extent on assumed properties of $\mathring{\Phi}(\mathbf{r})$. In the second paper $\mathring{\Phi}(\mathbf{r})$ were investigated in the simplest single-group one-dimensional model. In particular, it followed from that paper that some properties of $\mathring{\Phi}(\mathbf{r})$ assumed in [1] cannot occur and that they strongly depend on the boundary conditions, and possibly on the boundary shape.

We will attempt to apply the approach of [2] to the two-dimensional case as being more realistic and to compare the results obtained with the results of [1] to find out the degree of applicability of the simplest models. Following [2], let us assume that the neutron flux in the reactor is described by the equation

$$\{\Delta_{r,\varphi}+\varkappa^2(r)\}\,\Phi(r,\varphi)=0;$$

$$r\leqslant 1;\ a\left[\frac{\partial\Phi}{\partial r}\right]_{r=1}=b\Phi|_{r=1}. \tag{1}$$

One can simulate random deviations of $\mathring{\Phi}(\mathbf{r})$ from the solution $\Phi(\mathbf{r})$ of Eq. (1), for example, by random uncorrelated deviations of $\varkappa^2(\mathbf{r})$ proportional to $a\,\delta(\mathbf{r}-\mathbf{r}_0)$, with amplitudes α distributed according to the normal law with dispersion σ_α^2, independent of $\mathbf{r}$. In order to calculate the deviation of the neutron field corresponding to a perturbation $\delta\varkappa^2(\mathbf{r})=\alpha\delta(\mathbf{r}-\mathbf{r}_0)$, let us use, following [2], a linear approximation. It consists of replacing the equation

$$\{\Delta_{r,\varphi}+\varkappa^2(r)+\alpha\delta(\mathbf{r}-\mathbf{r}_0)\}\,[\Phi(r)+\mathring{\Phi}(r)]=0$$

by the approximate one:

$$\{\Delta_{r,\varphi}+\varkappa^2(r)\}\,\mathring{\Phi}(\mathbf{r})+\alpha\delta(\mathbf{r}-\mathbf{r}_0)\,\Phi(r_0)=0,$$

The desired perturbation is obtained in the form

$$\mathring{\Phi}(\mathbf{r},\mathbf{r}_0)=\alpha\Phi(r_0)\sum_m\frac{1}{\lambda_m}\psi_m(\mathbf{r})\,\psi_m(\mathbf{r}_0), \tag{2}$$

where ψ_m are the orthonormalized solutions of the equation

$$[\Delta_{r,\varphi}+\varkappa^2(r)]\,\psi_m(\mathbf{r})=\lambda_m\psi_m(\mathbf{r})$$

with the same boundary conditions as in Eq. (1). All the different ψ_m with the exception of

$$\psi_{m_0}(r)=\Phi(r);\ \lambda_{m_0}=0.$$

are terms in the sum.

We obtain from Eq. (2) the correlation function of the fluctuations in the neutron density:

$$K(\mathbf{r},\mathbf{r}')=\int\mathring{\Phi}(\mathbf{r},\mathbf{r}_0)\,\mathring{\Phi}(\mathbf{r}',\mathbf{r}_0)\frac{1}{\sqrt{2\pi}\,\sigma}\times \tag{3}$$

$$\times\exp\left(-\frac{\alpha^2}{2\sigma^2}\right)d\mathbf{r}_0\,d\alpha=\sigma_\alpha^2\sum_{mn}\psi_m(\mathbf{r})\,\psi_m(\mathbf{r}')\times\int\psi_m(\mathbf{r}_0)\,\psi_n(\mathbf{r}_0)\,\Phi_0^2(\mathbf{r}_0)\,d\mathbf{r}_0.$$

Translated from Atomnaya Énergiya, Vol. 46, No. 3, pp. 187-188, March, 1979. Original article submitted May 15, 1978.

0038-531X/79/4603-0219$07.50

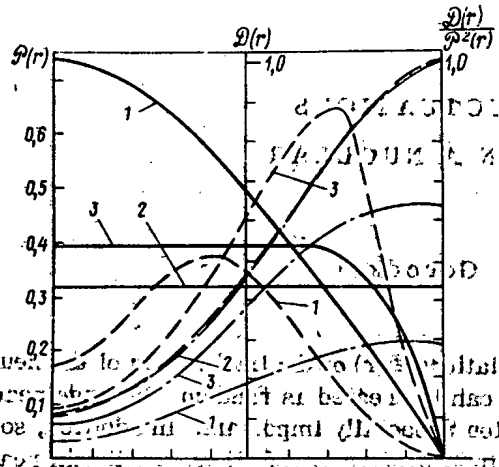

Fig. 1. The functions $\mathcal{D}(r)$ and $\mathcal{D}(r)/\mathcal{P}^2(r)$ for the three kinds of flux distribution $\mathcal{P}(r)$ (1–3).

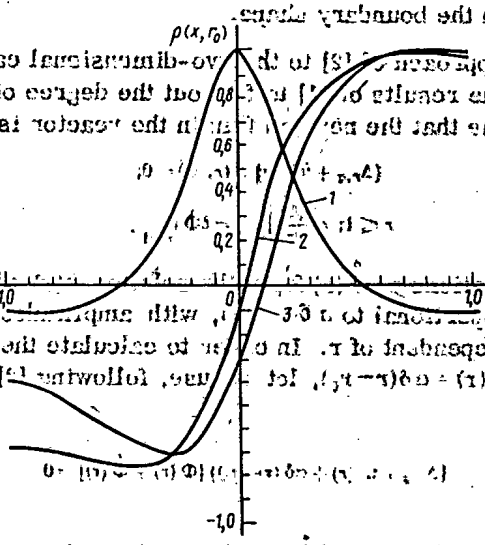

Fig. 2. Normalized correlation functions $\rho(x, r_0)$ at $r_{0y} = 0$ and 1) $r_{0x} = 0$, 2) 0.71; and 3) 1.

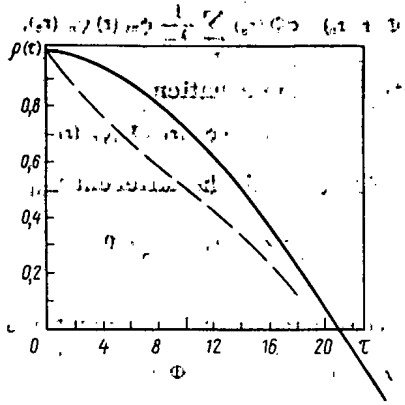

Fig. 3. Average normalized correlation function over the reactor $\rho(\tau)$ (solid curve) and the same function (dashed curve) taken from [1] (τ is the grid spacing unit).

Of greatest interest for reactor calculations are $D(\mathbf{r}) = K(\mathbf{r}, \mathbf{r})$ – the dispersion of the fluctuations in the neutron field at the point r, caused in this case by fluctuations of $\varkappa^2(\mathbf{r})$, and the normalized correlation function $\rho(\mathbf{r}, \mathbf{r}') = K(\mathbf{r}, \mathbf{r}')/\sqrt{D(\mathbf{r})D(\mathbf{r}')}$, which permits assessing the most likely deviation of the neutron flux at the point r for a specified deviation at the point r'.

As a result, we will obtain $D(\mathbf{r})$ and $\rho(\mathbf{r}, \mathbf{r}')$ for three cases:

1. $\left.\frac{\partial\Phi}{\partial r}\right|_{r=1} = 0;\ \varkappa^2(r) = 0.$
2. $\Phi(1) = 0;\ \varkappa^2(\mathbf{r}) = \text{const}$, since $\Phi(\mathbf{r}) \geq 0$.
3. $\Phi(1) = 0;\ \varkappa^2(\mathbf{r}) = 0$ at $\mathbf{r} \leq 0.71$ and $\varkappa^2(\mathbf{r}) = \text{const}$ at $\mathbf{r} > 0.71$, since $\Phi(\mathbf{r}) \geq 0$.

The corresponding value of $\mathcal{P}(r) = \Phi(r) R^2/P$, where Φ is normalized so that $\int \Phi(r)\, dr = P$, is given in Fig. 1. The ratio $\Phi_{max}/\bar{\Phi}$ (nonuniformity coefficient) for these cases takes the values 1, 2.32, and 1.23, respectively. The functions $\mathcal{D}(r) = D(r) R^4/\sigma^2 P^2$ and $\mathcal{D}(r)/\mathcal{P}^2(r)$, are also shown in this figure, indicating a three-dimensional dependence of D(r), although not as strong as in the one-dimensional case [2]. The weak dependence of the shape of the function $D(\mathbf{r})/\Phi^2(\mathbf{r})$ on the form of $\varkappa^2(\mathbf{r})$ is curious.

The functions $\rho(\mathbf{r}, 0)$, $\rho(\mathbf{r}, 0.71)$, and $\rho(\mathbf{r}, 1)$ for case 3 are illustrated in Fig. 2 and show, in agreement with the experimental facts and the results of [1], a strong correlation of the fluctuations of $\Phi(\mathbf{r})$ in which the low spatial harmonics should predominate.

To what extent are results obtained with this simple model comparable with the results of more complicated calculations and experiments? Let us return to the fluctuations of the neutron field caused by fluctuations of the absorption cross sections of individual cells $\delta\Sigma_a = \beta\Sigma_a$. In this case it is necessary to replace σ_α^2 by σ_β^2/M^2 in Eq. (3). Then it is possible to obtain the mean square of the relative deviation $(1/\sigma_\beta^2)\ (D/\Phi^2) = R^2\gamma/M^2$, where $\gamma = 0.0216$, 0.0073, and 0.0159. For an RBMK (high-power water-cooled channel) reactor this will give a mean square deviation of the energy distribution of 6.4, 3.7, and 5.5% for 1% fluctuations of the cell absorption cross sections, which is in good agreement with the experimental value of 5–6% cited in [1].

The average of the relative correlation function over the reactor, which was compared with the experimental–computational value [1], was calculated for case 3 as being the most realistic. The closeness of these curves (Fig. 3), together with the data on the mean square relative deviation of the neutron field, indicates that the results obtained from the simple model calculations may be applicable in more complicated situations.

LITERATURE CITED

1. V. A. Karpov, V. G. Nazaryan, and V. V. Postnikov, At. Énerg., 40, No. 6, 456 (1976).
2. V. K. Goryunov, At. Énerg., 44, No. 4, 357 (1978).

RECIPROCITY PROPERTY OF SYSTEMS FOR SUPPRESSION OF XENON OSCILLATIONS

B. Z. Torlin

UDC 621.039.515: 621.039.516.232

As shown in [1], in first-order perturbation theory the natural frequencies ω of xenon oscillations, as in the theory of Randall [2], are found from the equation

$$\omega^2+b\omega+c=0, \tag{1}$$

where

$$b=a_0+\lambda_{Xe}+\lambda_I-\frac{a_0}{1+\lambda_{Xe}/a_0}\frac{a_{Xe}}{\mu}; \tag{2a}$$

$$c=\lambda_I\left[a_0+\lambda_{Xe}\left(1+\frac{1}{1+\lambda_{Xe}/a_0}\frac{a_{Xe}}{\mu}\right)\right]; \tag{2b}$$

$$a_0=\sigma_{Xe}\bar{\Phi}_0; \tag{2c}$$

here, λ_{Xe} and λ_I are the decay constants of ^{135}Xe and ^{135}I, σ_{Xe} is the neutron-capture cross section of ^{135}Xe, a_{Xe} is the xenon coefficient of reactivity, $\bar{\Phi}$ is the averaged value of the neutron flux in the reactor, and μ is the eigenvalues of the boundary–value problem [3]. We have

$$M_0^2(\Delta\varphi+B_0^2\varphi)+\Phi_0\left(\alpha_T\varphi+\sum_{j=1}^{N}F_j\rho_j\right)+\mu\varphi=0 \tag{3a}$$

with uniform conditions on the outer boundary of the reactor and with the relations

$$\nu_j\rho_j=\int_V K_i\varphi dV,\quad j=1, 2, \ldots, N, \tag{3b}$$

describing the algorithms of the operation of N fast-acting controllers; M_0^2, B_0^2, and Φ_0 are the steady-state values of, respectively, the neutron migration length, the material parameter, and the neutron flux distribution in the reactor, ρ_j and F_j are, respectively, the reactivity introduced by the j-th controllers and its spatial localization, K_j is the weighting function of the shaping of the signal from sensing elements for the j-th control signal, ν_j is equal to unity and zero for a static (proportional) or astatic controller, respectively, and α_T is the power coefficient of reactivity.*

Without allowance for the controllers, system (3) is self-conjugate and its eigenvalues are real. In this case Re $\omega<0$, given satisfaction of the condition $b>0$, which is known as the Randall–John criterion [2]. When the controllers are taken into account, system (3) is nonconjugate and its eigenvalues can be complex, i.e., $\mu=\alpha\pm i\beta$. Then the coefficients in Eq. (1) will also be complex $b=\gamma\pm i\delta$ and $c=\eta\pm i\varepsilon$. In this case the stability criterion is of the form

$$\gamma>\frac{\delta\varepsilon}{2\eta}(1+\sqrt{1+4\eta/\delta^2}), \tag{4a}$$

or, in expanded and somewhat rearranged form,

$$|\mu|^2>\frac{\alpha X}{1+\frac{\lambda_{Xe}+\lambda_I}{a_0}}\left\{1+\frac{\beta}{\alpha}d\right\}, \tag{4b}$$

where

* Here we take account of only the local (fuel) coefficient of reactivity; the reciprocity property does not hold for systems with an appreciable integrated (coolant) coefficient of reactivity [4].

Translated from Atomnaya Énergiya, Vol. 46, No. 3, pp. 189-190, March, 1979. Original article submitted May 15, 1978.

0038-531X/79/4603-0222$07.50

$$d=\frac{\lambda_{Xe}}{a_0}\frac{\frac{\beta}{|\mu|^2}X+\sqrt{\frac{\beta^2}{|\mu|^2}X^2+4\frac{\lambda_I}{a_0}Y}}{2Y};$$

$$X=\frac{a_{Xe}}{1+\lambda_{Xe}/a_0};\quad Y=1+\frac{\lambda_{Xe}}{a_0}\left(1+\frac{\alpha}{|\mu^2|}X\right).$$

It follows from Eq. (4b) that in this case, as for systems with a real eigenvalue spectrum, the stability improves as the neutron flux Φ_0 decreases and $|\mu|$ grows. Since $|\mu|$ is inversely proportional to the squared characteristic dimension, the stability of the system deteriorates.* With fixed dimensions and properties of the medium in the reactor core μ can be altered by the insertion of control rods, different arrangements of the rods, or changes in the operating algorithm.

Within the approximation under consideration the system of spatial control possesses an interesting feature, the reciprocity property.

Let us consider a system, conjugate to system (3), in the form

$$M_0^2(\Delta\varphi^+ + B_0^2\varphi^+)+\Phi_0\alpha_T\varphi^+ + \sum_{j=1}^{N} K_j\rho_j^+ + \mu^+\varphi^+ = 0; \tag{5a}$$

$$\nu_j\rho_j^+ = \int_V \Phi_0 F_j\varphi^+\,dV,\quad j=1,\ 2,\ \ldots,\ N \tag{5b}$$

with the same uniform boundary conditions for φ^+.

It is readily seen that for the eigenvalues φ_n and φ_m^+ of systems (3) and (5) we have the relation

$$(\mu_n-\bar{\mu}_m^+)(\varphi_n,\ \varphi_m^+)=0, \tag{6}$$

where a bar denotes the complex conjugate.

By virtue of the biorthonormality of the eigenfunctions of systems (3) and (5) $(\varphi_n, \varphi_m^+)=\delta_{nm}$, we have

$$\mu_n=\bar{\mu}_n^+. \tag{7}$$

System (3) and its conjugate, system (5), are of the same type. The only difference is that the sensing elements and actuators changed places in them: in system (5) the weighting function for shaping the signal from the sensing elements now is of the form $\Phi_0 F_j$ and the spatial localization of the introduced reactivity is K_j/Φ_0. This assertion can be illustrated most graphically with the example of a system with local sensing elements at the points $\mathbf{r}_{gj}$ and control rods whose ends are at the points $\mathbf{r}_{pj}$. The conjugate system describes such a situation in the same reactor when, conversely, the sensing elements are located at the points $\mathbf{r}_{pj}$ and the rod ends at the points $\mathbf{r}_{gj}$.

Nevertheless, the stability of the neutron field is the same in both cases since it is characterized by the same set of eigenvalues. In this case, the form of the functions φ_n and φ_n^+, which also means the spatial form of the oscillations of the neutron field of systems (3) and (5), can be entirely different owing to the asymmetry of the operators. The reciprocity property formulated above should be taken into account when synthesizing systems of spatial control and in arranging the sensing elements and rods.

The author is indebted to A. D. Galanin, B. P. Kochurov, A.M. Afanas'ev, and V. M. Malofeev for their useful discussion and valuable advice.

LITERATURE CITED

1. A. M. Afanas'ev and B. Z. Torlin, in: Problems of Atomic Science and Engineering, "Nuclear Power Plant Dynamics" Series [in Russian], No. 1, TsNIIatominform, Moscow (1971), p. 15.
2. D. Randall and D. John, Nucleonics, 16, 82 (1958).
3. A. M. Afanas'ev and B. Z. Torlin, At. Énerg., 43, No. 4, 243 (1977).
4. A. M. Afanas'ev and B. Z. Torlin, Preprint ITÉF-2, Institute of Theoretical and Experimental Physics, Moscow (1978).

*With real parameters Eq. (4b) resembles the Randall criterion, since the second term in braces is a small correction to some degree or another.

INTERPRETATION OF DATA ON THE TOTAL SCATTERING CROSS SECTION OF COLD NEUTRONS IN CONDENSED HYDROGEN-CONTAINING MEDIA

V. E. Zhitarev and S. B. Stepanov

UDC 539.171.02+162.2

The total scattering cross section (σ_s) of neutrons at low energy should, at least in a crystalline solid body, depend linearly on the wavelength λ of incoming neutrons [1]. Thus the following conditions must be met: the energy of the neutrons must be small in comparison with the average transmission of energy upon scattering and not too high temperature of the material. Then in the case of inelastic interaction the process of a neutron acquiring energy becomes predominant, and the probability of this process is determined by the possibility of the transmission of energy of different kinds of low-energy motions in the material. The slope a_1 of the straight line characterizing the dependence $\sigma_s(\lambda) = a_0 + a_1\lambda$ is determined by the dynamics of atoms, molecules, and intramolecular groups of atoms [2].

General conclusions of the theory are confirmed experimentally, and it has been established that the dependence $\sigma_s(\lambda)$ is close to linear in the region of cold neutrons ($\lambda \gtrsim 4$-10 Å) not only for solid but for liquid and many gaseous scatterers over a wide temperature range. The simple form of this dependence makes its use attractive in connection with the investigation of the dynamics of a scattering system. Similar attempts were undertaken in the first place for hydrogen-containing compounds whose study is of practical interest. Thus for materials containing the ammonia group NH_4 [3] and the methyl group CH_3 [4] empirical calibration curves are proposed which relate the slope measured at room temperature to the energy barrier of frozen rotation of the corresponding ion. A relationship is presented in [5] which relates the energy barrier for the NH_4 group to the slope of the curve which characterizes the temperature dependence of the scattering cross section $(\Delta\sigma_s/\Delta T)$, obtained in connection with an investigation in ammonia salts for neutrons with $\lambda = 8.5$ Å. The barrier values used in the cited papers were determined earlier by NMR and radiospectroscopy methods.

The authors of this paper propose a new phenomenological form of interpreting the data which is based on an analysis of the temperature dependence of $a_1(T)$.

The interaction cross sections were measured at various temperatures in water [6] and benzene in the liquid state, in solid and liquid diphenyl, and in zirconium hydride at three hydrogen concentrations. The total scattering cross section per hydrogen atom was determined in the calculation by subtracting the absorption cross sections of all the atoms of the molecule from the total interaction cross section and dividing the remainder by the number of hydrogen atoms. The slope of the curve $a_1 = \Delta\sigma^H/\Delta\lambda$ is found by the method of least squares. It turned out that in all cases the results can be represented within the limits of experimental errors in the form

$$a_1(T) = a_{10} \exp(-\varepsilon/kT),$$

where a_{10} and ε are parameters which are independent of the temperature in the first approximation. The experimental data for diphenyl approximated by this formula are given in Fig. 1.

It follows from general concepts that when the proposed relationship is valid, ε is related to a spectrum of possible energy transitions in the material.

The values of ε found by the method of least squares from the relationship given are presented in Table 1 with an indication of the wavelength range in which the linear approximation $\sigma_s^H(\lambda)$ is used and the range of the investigated temperature of the material. Values of the $\hbar(\omega)$-singularity in the low-energy part of the spectra of the materials under discussion are indicated which have been investigated by optical and neutron methods. It is evident that ε corresponds to the region of $\hbar\omega$ in all cases; in some cases it is close to the values of the characteristic energy of definite kinds of vibrational motion in the material.

Translated from Atomnaya Énergiya, Vol. 46, No. 3, pp. 190-192, March, 1979. Original article submitted May 15, 1978.

0038-531X/79/4603-0224$07.50

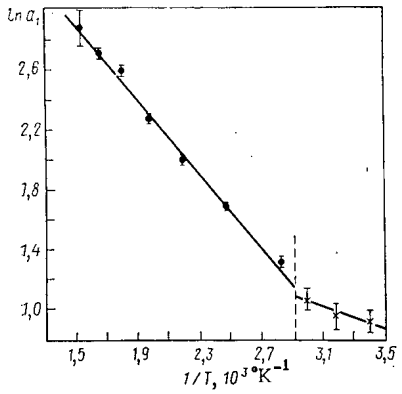

Fig. 1. Slope of the curve characterizing the scattering cross section per hydrogen atom in diphenyl.

TABLE 1. Results of Processing the Slope of Curves Characterizing the Scattering Cross Sections, and Data of Spectral Investigations of Different Materials

Material	Phase	λ, Å	T, °K	ε, eV	ħω, eV
Water	Liquid	8—19	293—523	0,077±0,003	0,005; ~0,021; 0,008; ~0,059 [9];
		6—11	277, 296	0,072 [7]	~0,025; ~0;07 [10]
	Solid	7—11	186, 269	0,028 [7]	0,007; ~0,026; ~0,076 [9]
		11—20	77—273	0,023 [8]	
	Liquid	8—19	293—543	0,059±0,003	0,009; 0,057; 0,098 [11]; 0,012; 0,046;
Benzene	Solid	1,5; 10;2	173—273	~0,008 [9]	0,068 [12]; 0,0043; 0,0078; 0,0086; 0,013 [11]
Diphenyl	Liquid	8—19	353—653	0,103±0,004	~0,013; ~0,03; ~0,05; ~0,12 [11] (290—362 K)
	Solid	8—19	293—333	0,033±0,009	0,006; 0,011; 0,02; 0,04; 0,051; 0,067; 0,097 [12]
ZrH_x	$x=1,01$	8—19	293—543	0,02±0,01	~0,14; 0,015—0,030 [8]
	$x=1,55$	8—19	293—543	0,034±0,004	
	$x=1,80$	8—19	293—543	0,064±0,004	

TABLE 2. Results of an Investigation of the Dynamics of Some Hydrogen-Containing Compounds

Material	ε, eV	$\hbar\omega_r$, eV	$\hbar\omega_t$, eV	V_0, kJ/mole	
				from neutron data	by other methods
MH_4I phase I	0,016±0,003	~0,03 (?) [5]	0,017 (?) [5]	3,2±0,6	~2 [3], neutron
phase II	0,035±0,003 [5]	0,035 [13]	0,012 [5], 0,017 [13]	12,5±1,6	12,3 [13]; 7,1 [15], NMR
$(NH_4)_2S_2O_8$	0,018±0,004 [13]	0,020 [13]	0,019 [13]	3,8±1,4	<2,9 [15], NMR; 4—8 [13], neutron
$(NH_4)_2SiF_6$	0,012±0,003 [13]	0,0208 [13]	0,0115 [13]	2,1±0,4	4—8 [13], neutron
NH_4ClO_4	0,016 [14]	—	~0,012 [2]	~3	<4,2 [15], NMR; <2,1 [13], neutron
NH_4PF_6	0,015 [14]	~0,019 [2]	—	~3	~0,8 [14], ~8 [5], [13], neutron
$K_4Fe(CN)_6 \cdot 3H_2O$	0,025±0,003 [7]	0,053 [7]	0,020 (?) [7]	8,4±1,4	~37 [7], neutron
		0,025 [7] (NMR)	0,014 (?) [7]		8,4±1,7 [7], NMR

Little data is presented in the literature on the temperature dependence of the scattering cross section of cold neutrons. Besides that used in Table 1, it is possible to mention only data for ammonia compounds and some crystalline hydrates. These materials are interesting, in particular, in that their low-frequency spectrum reflects mainly the dynamics of the corresponding groups of atoms (NH_4 and H_2O) and is relatively simple in structure. Table 2 lists, in addition to results of the processing, the characteristic energy of torsional ($\hbar\omega_r$) and translational ($\hbar\omega_t$) vibrations obtained in the spectra of inelastically scattered neutrons and by other methods; the values of the barrier of frozen rotation (V_0) corresponding to atomic groups determined by the NMR method and from neutron data (mainly from the slopes of the $\Delta\sigma_s^H/\Delta\lambda$ and $\Delta\sigma_s^H/\Delta T$ curves) are indicated. One

should note that the assignment of the energy transitions observed in the spectra to kinds of motion is nonunique in some cases, and the presence of torsional vibrations and the barrier values are not quite clear, especially for a material with a low barrier ($V_0 \lesssim 4$ kJ/mole). In the doubtful cases the data in Table 2 are labelled by a question mark.

For comparison, the barriers are given in Table 2 which are obtained from the relationships presented in [5, 7] on the assumption of the presence of torsional vibrations with frequency $\varepsilon/\hbar$. Good agreement with the NMR data is obtained for materials with a relatively high barrier. The results of the investigation of materials with a low barrier are closer to the NMR data and indicate a similarity of the dynamics of the ammonia ion in these materials ($V_0(\varepsilon) \sim 3$ kJ/mole).

Thus the proposed form of interpretation of the temperature dependence of the slope of the curve $\sigma_s^H(\lambda)$ permits determining the energy parameter of a scattering system which characterizes its frequency spectrum. In some cases it is possible to identify this parameter with the energy of specific energy transitions in the material.

LITERATURE CITED

1. G. Placzek and L. Van Hove, Phys. Rev., 93, No. 6, 1207 (1954).
2. E. Yanik and A. Koval'skaya, in: Scattering of Thermal Neutrons [in Russian], P. Égel'staff, editor, Atomizdat, Moscow (1970). p. 422.
3. J. Rush et al., J. Chem. Phys., 37, No. 2, 234 (1962).
4. S. Herdade et al., in: Neutr. Inel. Scatt., IAEA, Vienna (1968), Vol. 2, p. 197.
5. P. Leung et al., J. Chem. Phys., 48, No. 11, 4912 (1968).
6. S. B. Stepanov and V. E. Zhitarev, At. Énerg., 41, No. 2, 130 (1976).
7. J. Rush et al., J. Chem. Phys., 45, No. 4, 1312 (1966).
8. V. Raikhard, in: Spectra of Slow Neutrons [in Russian], Atomizdat, Moscow (1971), p. 255.
9. K. Heinloth, Z. Phys., 163, No. 2, 218 (1961).
10. V. Glezer, in: Spectra of Slow Neutrons [in Russian], Atomizdat, Moscow (1971), p. 5.
11. M. G. Zemlyanov, in: Inelast. Scatt. Neutr. Solids and Liquids, IAEA, Vienna (1965), Vol. 2, p. 221.
12. W. Gläser, Nukleonik, 7, No. 2, 64 (1965).
13. P. Leung et al., J. Chem. Phys., 57, No. 1, 175 (1972).
14. J. Rush et al., Nucl. Sci. Eng., 14, No. 4, 339 (1962).
15. R. Richards and T. Schaefer, Trans. Faraday Soc., 57, Pt. 2, 210 (1961).

AN ANALYTIC SOLUTION OF THE KINETIC EQUATIONS OF A POINT MODEL OF A REACTOR

A. A. Shepelenko

UDC 621.039.512:621.039.514

It is useful in analyzing the starting mode of a reactor for a qualitative understanding of the process and selection of the direction of a numerical calculation to use analytic solutions of the kinetic equations for an arbitrary temporal variation of the reactivity over a rather broad range with several groups of delayed neutrons taken into account.

Among the solutions known in the literature (for example, [1]), that of Hurwitz for slowly varying reactivity possesses the simplest structure. The original solution of Hurwitz [2] does not take account of neutrons from an external source, spontaneous fission, etc. One can show that taking this circumstance into account while preserving the assumptions of Hurwitz with respect to the solution does not lead to a satisfactory description of the behavior of the reactor in the subcritical region. A new solution of the kinetic equations is constructed in this article for slowly varying reactivity which is devoid of this inadequacy.

Let us consider the kinetic equations in the point approximation:

$$\frac{dn}{dt}=\frac{r-1}{\varepsilon}n+\sum_i \lambda_i c_i+\frac{Q}{\varepsilon};$$
$$\frac{dc_i}{dt}=\frac{b_i}{\varepsilon}n-\lambda_i c_i,\quad \varepsilon=\frac{\Lambda}{\beta},\quad \sum_i b_i=1, \tag{1}$$

where t is the time, n is the neutron density, c_i and λ_i are the density and decay constant of the predecessor nuclei of the i-th group of delayed neutrons, b_i is the relative yield of delayed neutrons of the i-th group, Λ is the generation time of the neutrons, β is the total fraction of delayed neutrons, r is the reactivity in units of β, and $Q\varepsilon^{-1}$ is the arrival rate of neutrons from the external source.

Using the substitution of Hurwitz

$$c_i=\frac{b_i}{\varepsilon\lambda_i}\left(\frac{\lambda_i}{p+\lambda_i}+x_i\right)n;$$
$$n=f(t)\,E(t,\ t_0);\ E(t,\ \tau)=\exp\int_\tau^t p(y)\,dy, \tag{2}$$

where p is the largest root of the reactor in our equation

$$r=p\left(\varepsilon+\sum_i\frac{b_i}{p+\lambda_i}\right),$$

we obtain:

$$\varepsilon\frac{df}{dt}=f\sum_i b_i x_i+QE^{-1}(t,\ t_0); \tag{3}$$

$$\frac{d}{dt}\frac{f}{p+\lambda_i}+\frac{x_i f}{\lambda_i}\left(\lambda_i+p+f^{-1}\frac{df}{dt}+x_i^{-1}\frac{dx_i}{dt}\right)=0. \tag{4}$$

Hurwitz assumed that

$$\left|f^{-1}\frac{df}{dt}+x_i^{-1}\frac{dx_i}{dt}\right|\ll p+\lambda_i \tag{5}$$

in Eq. (4).

Translated from Atomnaya Énergiya, Vol. 46, No. 3, pp. 192-193, March, 1978. Original article submitted June 20, 1978.

0038-531X/79/4603-0227$07.50

Substituting the value of x_i in this approximation from (4) into (3), we easily obtain a soluble differential equation for f and finally the following expression for the neutron density:

$$\left(\frac{dr}{dp}\right)^{1/2} n_H = n_0 \left(\frac{dr}{dp}\right)_0 E(t, t_0) + \int_{t_0}^{t} \left[\frac{dr}{dp}(\tau)\right]^{-1/2} Q(\tau) E(t, \tau)\, d\tau, \tag{6}$$

$$\frac{dr}{dp} = \varepsilon + \sum_i \frac{b_i \lambda_i}{(p+\lambda_i)^2}.$$

In the subcritical region ($p < 0$) with constant source and reactivity it follows from Eq. (6) after the passage of a sufficient time interval (in the limit $t_0 \to -\infty$) that

$$rn_H \approx -Q \frac{r}{p} \left(\frac{dr}{dp}\right)^{-1} \tag{7}$$

instead of the exact result $rn = -Q$; at the same time the factor

$$\frac{r}{p} \left(\frac{dr}{dp}\right)^{-1} \to 0 \text{ as } r \to -\infty.$$

This circumstance is related to the fact that Eq. (5) is not satisfied in the subcritical region, where the neutron density is "almost" in equilibrium with the source in the case of slow variation of the reactivity, and the rate $dn/dt = n[p + f^{-1}(df/dt)]$ is small. Consequently, a more plausible assumption in the subcritical region is

$$\left| p + f^{-1} \frac{df}{dt} + x_i^{-1} \frac{dx_i}{dt} \right| \ll \lambda_i, \tag{8}$$

which leads to a simple expression for the neutron density:

$$\frac{r}{p} n_S = n_0 \left(\frac{r}{p}\right)_0 E(t, t_0) + \int_{t_0}^{t} Q(\tau) E(t, \tau)\, d\tau. \tag{9}$$

For constant negative reactivity Eq. (9) gives the exact solution $rn_S \approx -Q$.

Comparison of the approximate solution (9) with the exact one for a monotonic increase of reactivity at a constant rate from a deep subcritical state shows that the solution (9) overestimates the value of n (by a factor of 1.3 for a rate of $0.005\beta/c$ at the critical point, and by a factor of 2 for a rate of $0.030\beta/c$). In the supercritical region the solution (9) gives a qualitatively correct description of the reactor behavior, differing insignificantly from the solution of Hurwitz almost up to the point of criticality by prompt neutrons. If one sets up (6) and (9) with the same power at the critical point and with $Q \equiv 0$, then $n_S/n_H = 1.3$ at $r = 0.5$, and only at $r = 0.9$ does $n_S/n_H = 2$. Thus the solution (9) may be useful in the discussion of the entire starting process.

It is known that the solution of Hurwitz overestimates the neutron density at least in problems with a linear variation of the reactivity [2]. Therefore, it is desirable to obtain a solution of the kinetic equations which agrees with Eq. (9) in the subcritical and with Eq. (6) in the supercritical regions. Using

$$\left| \frac{p - |p|}{2} + f^{-1} \frac{df}{dt} + x_i^{-1} \frac{dx_i}{dt} \right| \ll \lambda_i + \frac{p + |p|}{2} \tag{10}$$

– the simplest expressions which unify in a continuous way the assumptions (5) and (8) – we obtain

$$wn = n_0 \exp\left\{ \int_{t_0}^{t} \left[p + \frac{1}{2w} \frac{dm}{dt} \right] dy \right\} + \int_{t_0}^{t} d\tau Q(\tau) \exp\left\{ \int_{\tau}^{t} \left[p + \frac{1}{2w} \frac{dm}{dt} \right] dy \right\}, \tag{11}$$

where $w = \varepsilon + \sum_i \frac{b_i \lambda_i}{p + \lambda_i} \left(\lambda_i + \frac{p + |p|}{2}\right)^{-1}$ is continuously differentiable and $m = \varepsilon + \sum_i b_i \lambda_i \left(\lambda_i + \frac{p + |p|}{2}\right)^{-2}$ is a continuous function of the reactivity.

LITERATURE CITED

1. D. Hetrick, The Dynamics of Nuclear Reactors [Russian translation], Atomizdat, Moscow (1975).
2. H. Hurwitz, Nucleonics, 5, No. 1, 61 (1949).

SPECIAL ANNIVERSARIES

ACADEMICIAN LEV ANDREEVICH ARTSIMOVICH

B. B. Kadomtsev

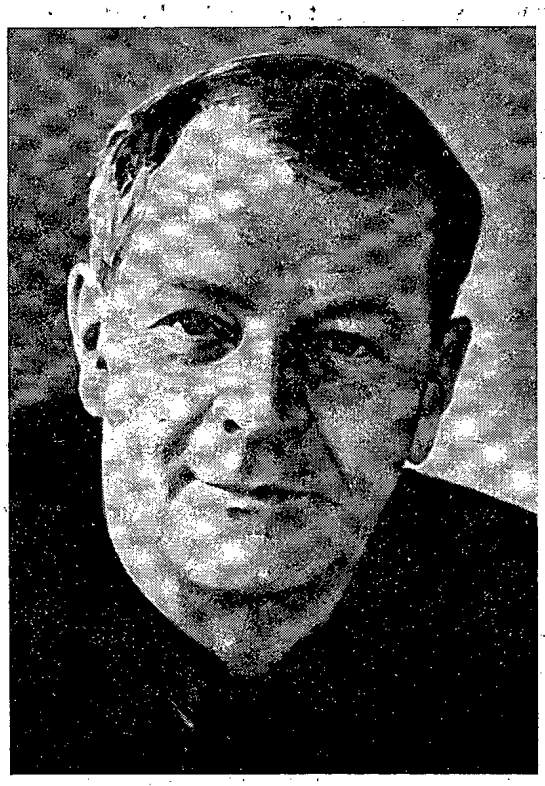

February 25, 1979, would have been the 70th birthday of the eminent Soviet scientist, Academician Lev Andreevich Artsimovich, who has left a brilliant mark in modern physics.

L. A. Artsimovich was born in Moscow into the family of a professor of statistics. In 1928 he completed the Physicomathematical division of the Belorussian State University in Minsk. His scientific activity started in the Leningrad Physicotechnical Institute, which has played an exceptionally large role in the development of Soviet physics.

The first papers of L. A. Artsimovich were concerned with the optics of x-ray emission, but soon his interests were switched to a new field – nuclear physics. In 1936, L. A. Artsimovich jointly with A. I. Alikhanov and A. I. Alikhan'yan showed experimentally the validity of the laws of conservation of energy and momentum during the annihilation of positrons, which at that time – the time of establishment of the science of the microworld – appeared to be far from obvious. In 1935-1940, L. A. Artsimovich conducted a cycle of experiments on the interaction of fast electrons with a substance. The detailed and extremely accurate data obtained by him concerning the dependence of the intensity of the bremsstrahlung and the total energy losses of fast electrons were found to be in total agreement with the predictions of the quantum theory, and thereby verified the principles of this theory.

During World War II L. A. Artsimovich was occupied with investigations on electron optics; after the war he headed the important applied specialization of electromagnetic isotope separation. Under his directions and personal participation, a technical facility was developed and built for the separation of isotopes, a facility millions of time more productive than the modest laboratory equipment existing at the time – mass spectrometers. Isotopes, separated by the electromagnetic method, are finding even wider application in science and the national economy.

Translated from Atomnaya Énergiya, Vol. 46, No. 3, pp. 195-196, March, 1979.

0038-531X/79/4603-0229$07.50

At the start of the 1950s, L. A. Artsimovich began a chapter in a new fundamental scientific–technological problem – controlled thermonuclear reactions. The first experiments to study the physics of powerful electric discharges in deuterium led to the detection of neutron emission. This, obviously, was associated with thermonuclear reactions, but a careful analysis of the experimental data conducted by L. A. Artsimovich, and additional experiments carried out at his urgent request, resulted in the rejection of the extremely tempting but erroneous conclusion concerning the thermonuclear origin of the neutrons.

The first attempt did not lead to success, but under the direction of L. A. Artsimovich a systematic siege of the fortress of controlled thermonuclear fusion was begun, and a prolonged period of persistent investigation of the unusual and unique physics of a high-temperature plasma was started. In the collective, directed by L. A. Artsimovich, extensive and basic experiments on the physics of a high-temperature plasma were conducted. Here the modification of the electric discharge – plasma focus – was detected and investigated in detail (N. V. Filippov and co-workers); the principle of plasma stabilization by a "magnetic well" was demonstrated experimentally (M. S. Ioffe and co-workers); the tokamak concept was suggested and investigated in detail (N. A. Yavlinskii, V. S. Strelkov, and co-workers); investigations were conducted on the study of the physical properties of a high-temperature plasma.

The work of the 1950s was summed up by L. A. Artsimovich in the monograph "Controlled Thermonuclear Reactions," which played a large role in attracting new young talents into this interesting and dynamically developing field of physics. Even in recent years, L. A. Artsimovich devoted much effort to attracting youth into physics and to the organization of scientific investigations on the physics of a high-temperature plasma. His astonishing erudition in all the subtleties of controlled thermonuclear fusion, his faultfinding and occasional but merciless criticism in assessing the results of the investigations, and his exceptional physical keenness made L. A. Artsimovich an acknowledged authority in this field of physics, both in the Soviet Union and abroad. His active participation at international conferences and his initiative in the establishment of closer scientific relations with foreign laboratories greatly contributed to fruitful international collaboration which even today is yielding results and is continuing to develop at a time when, together with the investigations into the physics of the high-temperature plasma, an ever-increasing role is being played by the engineering–physics and technological aspects of thermonuclear fusion.

In the last years of his life. A. L. Artsimovich paid much attention to tokamaks, in which he divined an extremely promising concept, possibly leading to the creation of a thermonuclear reactor. He carried out a careful analysis of the experimental data of tokamaks, and showed the reliability of these data and their promise. Under the guidance of L. A. Artsimovich, tokamaks were built in all the plasma laboratories of the world, and now this is the largest-scale and most promising trend in work on magnetic plasma containment, for thermonuclear fusion. In 1975, after L. A. Artsimovich's death, the Tokamak-10 facility, conceived by him, was activated, exhibiting the expected plasma parameters and confirming the validity of the trend. Based on the results of this and other tokamaks, a new generation of tokamaks is now being built in a number of the world's laboratories, which should achieve a physical demonstration of the solution of the problem of controlled thermonuclear fusion.

L. A. Artsimovich was a prominent organizer of Soviet science. From 1957 he was the Permanent Academician-Secretary of the Division of General Physics and Astronomy of the Academy of Sciences of the USSR, and in this post he did much for the development of these fields of science, and also for the training of scientific personnel.

The vast scientific and scientific–organizational activity of A. L. Artsimovich – a brilliant physicist, a talented, learned, and prominent scientific organizer – has been preserved forever in the memories of those who continue his work.

NIKOLAI ALEKSANDROVICH PERFILOV

K. A. Petrzhak

December 29, 1978, was the 70th birthday of the prominent Soviet scientist, Doctor of Physicomathematical Sciences, Professor Nikolai Aleksandrovich Perfilov.

The scientific activity of N. A. Perfilov is associated with the V. G. Khlopin Radium Institute, in which he started work in 1932 while a student at Leningrad University. The Physics Division of the Radium Institute has played a large role in the development of the physics of the nucleus and cosmic radiation. Many eminent physicists of the Soviet Union, worked in this division, headed then by Professor L. V. Mysovskii, and prominent scientific discoveries were made there. In 1936, after graduating from Leningrad University, Perfilov was admitted as a postgraduate at the Radium Institute and in the first years, under the direction of Professor Mysovskii, he was occupied with research into the newly conceived field of neutron physics and with the construction of a low-pressure Wilson chamber. Comrade Perfilov was among those scientists who studied the fission of the uranium nucleus for the first time in the Soviet Union, in 1939, soon after the discovery of this phenomenon. In the same year, he accomplished two projects: he recorded the fission of the uranium nucleus in the Wilson Chamber and he measured the effective charge of the fission fragments, using the cyclotron at the Radium Institute. His talent as a physicist–experimenter was apparent even in these first projects. His candidate's dissertation, defended in 1941, was devoted to the investigations of nuclear fission of uranium as was his doctoral dissertation, which he defended in 1948.

Thus, since 1939 one of the principal specializations of Perfilov's scientific activity was fission physics. In 1947, he determined for the first time the probability of fission of the uranium nucleus into three fragments, comparable in mass, by the action of neutrons, and for the first time in 1950 he observed the fission process with the capture of slow negative π-mesons by uranium nuclei. From 1950, when a laboratory was set up in the Radium Institute to study nuclear reactions with high-energy particles, Nikolai Aleksandrovich conducted an extensive cycle of investigations into the characteristics of fission of nuclei during high-energy excitation and large angular momenta over a wide range of particle energies and mass numbers of the nuclei. He suggested the systematics of nuclear fissionability by the action of high-energy particles.

Translated from Atomnaya Énergiya, Vol. 46, No. 3, pp. 197-198, March, 1979.

0038-531X/79/4603- 0231$07.50

The second specialization in Perfilov's scientific activity was his work in the field of the photographic method, in the development of which he made a large contribution. His first achievement was the development in 1942-1944 of a differential method of recording charged particles in nuclear emulsions, based on the idea of chemical action on a latent photographic image. This method has been used successfully in recent years in the identification of the far transuranium elements and recording of the heavy component of cosmic radiation. In 1948 N. A. Perfilov developed an exceptionally fine-grained nuclear emulsion, which found extensive application in physics research, In 1958 a fine-grained emulsion was obtained which was sensitive to relativistic particles. In the next few years, under Perfilov's guidance, new methods of processing nuclear emulsions were developed, the nature of the latent photographic image was investigated, and the problem of replacing gelatin with synthetic polymers was solved. Finally, in recent years, new track detectors have been developed in N. A. Perfilov's laboratory, based on single crystals of silver chloride and bromide.

The third prominent specialization in Perfilov's work encompassed questions related to problems of inelastic nuclear interactions of high-energy particles. N. A. Perfilov and co-workers conducted a large cycle of investigations into the phenomenon of nuclei fragmentation in which for the first time the many mechanisms of this phenomenon were clarified, the nonstatistical nature of the processes of formation of fragments in nuclear spallations was demonstrated, isotopic effects and isospin correlations of the cross sections of the fragments were discovered, new models of the formation processes of the fragments were developed, and the first systematization of the formation cross sections of the fragments was made. In this work, the cluster aspects of nuclear structure were also investigated, as were the collective effects in nuclear-nuclear interactions, and the process of total decay of nuclei under the action of high-energy particles. In recent years, N. A. Perfilov has devoted great attention to relativistic nuclear physics.

The latitude and diversity in formulating research problems are characteristic of N. A. Perfilov. In his laboratory, in addition to the development of a photographic method of semiconductor detectors for investigating the fragmentation products of nuclei, new types of detectors were constructed and the solid-state detector method is being widely used in the study of nuclear fission.

N. A. Perfilov has published more than 170 scientific papers in leading Soviet and foreign journals. He is the coauthor of the monograph "Nuclear Reactions by the Action of High-Energy Particles," which was the first generalization of these problems in the literature. He edited the first collection of papers on "Physics of Nuclear Fission" and the monograph "Nuclear Interactions in the Shielding of Space Vehicles." Perfilov's laboratory is a prominent center for the training of scientific personnel. Among the students of Nikolai Aleksandrov are 4 Doctors of Science and 15 Candidates of physicomathematical science. Over many years he taught a course of nuclear physics at Leningrad Polytechnic Institute. Comrade Perfilov has repeatedly been invited to read review reports on nuclear fission, fragmentation processes and the photographic method at international conferences.

N. A. Perfilov has led great organizational work: for 20 years he has directed the Physics Branch of the Radium Institute; from 1953 to the present, he has been the Deputy Director of the Institute for Scientific Work. Through his initiative, physics laboratories have been set up, and an experimental base of the Institute has been developed. Nikolai Aleksandrovich is characterized by efficiency and persistence, fundamentality, and sensitivity and good will toward people.

For his achievements in scientific and scientific-organizational activities, N. A. Perlifov has been awarded the Order of Lenin, the Order of the Red Banner of Labor, the Order of "Badge of Honor," and many medals.

We wish Comrade Perfilov good health and future creative successes.

THIRTY-FIFTH CONFERENCE OF THE COMECON PERMANENT COMMISSION ATOMÉNERGO

Yu. S. Troshkin

The Conference of the COMECON Permanent Commission on the Peaceful Uses of Nuclear Energy was held in Nov. 1978 in Havana (Republic of Cuba).

At the conference great attention was paid to measures associated with the development and coordination of draft agreements and programs of work on problems of nuclear power generation, included in the long-term purposeful program of collaboration for the assurance of economically based requirements of the COMECON member-countries in the principal forms of energy, fuel and raw material. Specific measures were designated for the future improvement of multilateral economic and scientific-technical collaboration of the COMECON member-countries, and also the organization of the activities of the commission, including measures associated with the transformation of its working elements, refinements of the state of the COMECON Permanent Commission Atoménergo, and improvement of project planning. The priority trends of activity were defined and the plan of work in 1979-1980 was confirmed; the plan of work in the field of standardization in this period and the calendar plan-chart for carrying out meetings of the commission, its working elements and other measures in 1979 were also confirmed.

The preparation by the COMECON Secretariat of information concerning the progress of work on problems included in the Coordinated Plan of the Multilateral Integrated Measures of the COMECON member-countries in 1976-1980 was considered, as was the Program of Scientific-Technical Collaboration for the solution of fuel-power problems in 1976-1980 and its longer-term prospects.

In the course of the conference, the question of the organization of collaboration by a plan of accelerated development of science and technology in the Republic of Cuba was considered, in the section relating to atomic energy. The delegations of the countries refined their participation in the individual assignments of this subprogram. The great work of "Interatominstrument" on the development and intensification of economic and coordination activities was noted. The problems were defined, on the solution of which the Union should advantageously concentrate effort. The question of organization within the framework of the International Economic Organization (MKhO) "Interatoménergo" of a system of control and monitoring with the use of computers for nuclear power stations with VVÉR (water-cooled-water-moderated) reactors was considered. It was deemed advisable that the development of this topic should be conducted within the scope of the Program of Collaboration in the field of scientific-research and planning-construction work on the creation of new types of equipment for nuclear power stations.

The information from the Soviet delegation was discussed. This information concerned the preparation of a draft agreement on the creation, by the combined efforts of interested member-countries of COMECON, of production capacities in the Soviet Union for the manufacture of charged-particle accelerators and the deliveries of accelerators from the Soviet Union associated with them. The measures for the preparation of the draft agreement for signing were noted.

The commission endorsed the "Regulations for Nuclear Safety of Research Reactors" and "Regulations for Nuclear Safety of Critical Test Stands," proposals for the specialization of output of isotope production, and also normative-methodological documents in the field of radiation sterilization of materials and plant for medical purposes.

The Commission also considered problems in the field of nuclear instrument design, radiation-shielding techniques, radiation safety, and also collaboration in carrying out reactor-physics investigations on a critical assembly of the VVÉR type between the Central Institute of Physics Research of the Hungarian Academy of Sciences and the Center for Technical Research of Finland.

The meeting of the commission took place in an atmosphere of mutual understanding, and in an environment of businesslike activity.

Translated from Atomnaya Énergiya, Vol. 46, No. 3, pp. 199-200, March, 1979.

0038-531X/79/4603- 0233$07.50

DIARY OF COLLABORATION

A Conference of Specialists on Radiation-Shielding Technique was held Sept. 7-8, 1978, in Kheviz (Hungary). The plan for a COMECON standard "Products for radiation-shielding techniques. Shields composed of lead shielding blocks. General technical requirements," was agreed upon. These were proposed for the draft of the work plan of the COMECON Permanent Commission Atoménergo in 1979-1980, and for the draft of a development plan of standards in 1980.

The participants of the Conference heard reports about the preparation of materials and proposals for standardization of packaging for radioactive substances (flasks, ampuls, tubs, etc.), the ventilation of chambers, boxes, and fume cabinets, and about the results of the symposium on "New Achievements and the Exploitation of Products of Radiation-Shielding Technology," etc.

The Fourteenth Meeting of the Scientific-Technical Coordinating Council (STCC) on the Reprocessing of Irradiated Fuel took place Sept. 26-29, 1978, in Leningrad. The STCC discussed the account of Czechoslovakian specialists concerning the construction of a semi-industrial plant for the production, purification, and compression of fluorine, with a production capacity of up to 1.5 kg/h and intended for the development of the fluoride regeneration process of the mixed BOR-60 uranium-plutonium fuel, and also for the production of fluorine-containing compounds. The fluorine is produced in two electrolyzers, operating at ~100°C. Purified by freezing at −80°C (HF content 2%) or −120°C (HF content 0.2%), it is compressed to 10 kgf/cm^2 and stored in special bottles with a capacity of 525 liters each. Since 1978, individual sections of the facility have been examined and stockpiled. It will be completely assembled in the Insititute of Nuclear Research in Rzhezh as a part of a test stand for developing the uranium side of the fluoride regeneration method for the spent fuel of fast reactors.

Specialists from the German Democratic Republic spoke about the results of experimental work to determine the parameters of a dry method of transporting spent fuel elements with different variants of the container loading and, consequently, of the total intensity of the residual energy release. In one of the reports, a review was given of data on the corrosion of material in different media and an experimental facility was described for testing samples. In another report, methods of determining the hermeticity of fuel elements were explained, based on the measurement of the ^{41}Ar activity in the gaseous coolant. They permit a cassette with damaged fuel elements to be discovered directly in the container before its shipment from the nuclear power station. Great interest was created by a report devoted to a test rig constructed in the German Democratic Republic for testing the strength of packed fuel assemblies when dropped from a height of 9 m. The report was accompanied by a film.

In a report of specialists from the Czechoslovakian SSR the properties of steel, lead, uranium and their effect on the mass-size characteristics of containers were given and the prospects of the use of other materials were discussed: a low-alloy melt based on depleted uranium, alloys of titanium, copper, aluminum, etc. In two reports, an experiment to transport samples of spent fuel from the A-1 nuclear power station was generalized, and the state of proceedings with the preparation for transportation of the fuel-element assemblies of the KS-150 reactor was described. It was assumed that all transportation equipment will be ready by 1981. In one of the reports, information was given about work started in Czechoslovakia on the technicoeconomic assessment of the fuel-element fuel cycle.

In the report of the Bulgarian specialists, three possible schemes for the shipment of fuel from the "Kozlodui" nuclear power station were considered, using automotive, water, and rail transport.

The draft plan of work for the COMECON Permanent Commission in 1979-1980 was considered at the Conference: the techenical plan included assignments on new tasks, and also a course for carrying out the "Spektr" experiment.

In the resolutions of the STCC, it was noted, in particular, that the concentration of radiochemical problems of the nuclear fuel cycle into one working element is opportune and will promote a unified methodological approach and a combined solution of this problem in the COMECON member-countries.

Translated from Atomnaya Énergiya, Vol. 46, No. 3, pp. 199-200, March, 1979.

0038-531X/79/4603-0234$07.50

A Conference of Responsible Representatives in the Field of Isotope Production (SOP-78) was held Oct. 2-5, 1978, in Gradets-Kralov (Czechoslovakia). Proposals for specialization of the manufacture of isotope-production goods were discussed and recommendations were prepared. Information was considered concerning plans for the development of new isotope-production goods in Bulgaria, in the German Democratic Republic, in Poland, and in Czechoslovakia in 1979-1980 (and over a longer period). The possibility was suggested of eliminating the existing duplication of certain work.

Information was presented concerning the work carried out in 1977-1978 in the fields of isotopes and tagged compounds, including their introduction into use. The following papers were noted: "Development and Construction of Special Cyclotrons for the Production of Isotopes," Comparison of the Basic Controlling Parameters of Sample Sources and Solutions," Development of Normative–Methodological Documentation," etc. The conference discussed problems associated with the planning of laboratory metrology of ionizing radiations an of a radiochemical laboratory in the Republic of Cuba, approved the work on the outlining contents, and exposition of pharmacopoeia articles on radiopharmaceutical preparations, for example, on the outlining of special monographs and the status of the outlining and content of pharmacopoeia papers on radiopharmaceutical preparations.

A Conference of Specialists on the Development and Construction of Special Cyclotrons for the Production of Isotopes was held Oct. 3-4, 1978, in Gradets-Kralov (Czechoslovakia). The specialists discussed the draft plan of a cyclotron with a medium accelerated particle energy, prepared by Soviet specialists. The plan for a radioisotope cyclotron has been completed at the contemporary scientific–technological level and corresponds to the requirements imposed on cyclotrons of this type. Because specialists of certain countries had expressed an interest in the application of the cyclotron simultaneously for other purposes, and also taking account of the desires for operative retuning to an acceleration cycle for different particles, the Conference recommended certain modifications to be provided. The completion of a specific modification without a significant increase in the cost of the work can be ensured by the structural execution of the cyclotron on the modular principle. The necessity for developing additional modules will be determined by the interested side upon conclusion of the contract with the outside manufacturer. The development of target devices in the cyclotron assembly was acknowledged to be advantageous.

The Conference discussed the preliminary technical assignment for a minicyclotron with low accelerated-particle energy. It was acknowledged to be advantageous to develop this cyclotron by taking account of its use for the production of short-lived medical radionuclides, and for activation analysis. The following were noted: preparation of technical specifications for neutron-therapy products on a cyclotron with medium accelerated-particle energy, study of the feasibility of developing and manufacturing a positron chamber for diagnostic purposes, preparation of suggestions for the development of methods of separating the short-lived radionuclides and targets irradiated in the cyclotron, etc.

The Fifth Conference of the Authorized Parties of the Agreement on Multilateral International Specialization and Cooperation for the Manufacture of Isotope-Production Products was held Oct. 6-7, 1978, in Gradets-Kralov (Czechoslovakia). The Conference noted that the parties have fulfilled the commitments, arising from the Agreement, concerning meeting the requirements of countries in isotope production with respect to fixed volumes and technical parameters. Work was being continued on increasing the quality of isotope-production products, and also on shortening their delivery periods. At the same time, the drawbacks were noted in the mutual trade in these products between COMECON member-countries.

The parties considered proposals for expanding the glossary of specialized products (in particular, compounds tagged with tritium, ^{13}C and ^{14}C, ^{32}P and ^{33}P, and ^{35}S); problems associated with the appearance of provisional requirements for isotope production products in 1979-1980, and an even longer period, and with refinement of their technical parameters and characteristics.

INFORMATION

SOVIET – FRENCH COLLABORATION IN THE FIELD OF THE PEACEFUL UTILIZATION OF ATOMIC ENERGY

B. A. Semenov

The first Soviet–French agreement on scientific–technical collaboration in this field was signed in 1960. In 1966, in Moscow, an agreement was concluded between the State Committee for Atomic Energy of the Soviet Union and the French Atomic Energy Commission (CEA France) concerning the conduct of scientific research in the field of high-energy physics on the Serpukhov accelerator. The agreement was a major step in the development of large-scale, long-term joint research. Within its framework, since 1971, joint research has been successfully carried out using the French "Mirabel" liquid-hydrogen bubble chamber. Since the start of the experiments, in which several hundred French specialists and the specialists of several other countries have participated during these years, more than a million photographs have been taken which have yielded interesting scientific information. This information was generalized and presented in tens of joint reports and communications of the Soviet–French author collectives.

In accordance with an addition to the agreement of 1966, signed in January 1978, the operation of "Mirabel" has been achieved fully by Soviet specialists. The collection of the planned number of photographs in the chamber was completed in 1977, the photographs were processed in 1978, and the analysis of the results will be conducted before 1980. By mutual agreement, the experiments will be continued for the purposes of increasing the accuracy of the experimental data, due to the increase of the total number of photographs up to 2 million. The joint study of new promising suggestions is being considered, associated with the construction of a hyperon channel, using pulsed superconducting magnets, and with reequipment of "Mirabel" in a cryogenic system with a track-sensitive target.

Within the framework of the second agreement, signed on May 20, 1967, collaboration was achieved in the following fields: fast reactors with sodium coolant; water-cooled–water-moderated reactors; controlled thermonuclear fusion and plasma physics; salt-water distillation; high-energy physics and superconductivity in high-energy physics. In addition, in accordance with the recommendations of the Twelfth Session of the Combined Soviet–French Commission on scientific–technical and economic collaboration, also included in the program were the regeneration of nuclear fuel and nuclear heat supply stations. Collaboration is being achieved in the form of joint work, bilateral seminars, mutual exchange of experience, participation in experiments of both sides, and exchange of technical documentation.

Characteristics of the present stage of Soviet–French collaboration is the conversion with respect to certain important topics on the conduct of joint work by coordinated plans, encompassing the whole period of work under the topic (from 2 to 5 years). At the present time, the working plans have been agreed upon and signed for collaboration on the following topics:

computational and experimental work on fast reactor physics;
fast-reactor steam generators;
sodium technology and corrosion;
investigations of the radiation creep of fuel-element claddings, samples of hexahedral tubes and the work capacity of fuel elements under conditions of a fast power reactor;
reprocessing of spent fuel from the thermal and fast reactors of nuclear power stations by the water method;
reprocessing of spent fuel from fast reactors by the gaseous-fluoride method;
development and construction of superconducting components of an accelerator-storage assembly;
theoretical and experimental study of boiling sodium in fuel assemblies;
tests of a product facilitating dropwise condensation in salt-water distillation facilities;
study of the heat-transfer problems in salt-water distillation facilities with horizontal tubes.

Translated from Atomnaya Énergiya, Vol. 46, No. 3, pp. 201-203, March, 1979.

 0038-531X/79/4603- 0236$07.50

The thematics of fast reactors occupies a central position in Soviet–French collaboration, and encompasses a wide circle of problems associated with the development and operation of reactors of this type: reactor physics, fuel-element cladding materials and hexahedral tubes, sodium technology, operating reliability of steam generators, etc. The parties have organized visits for the mutual exchange of experience, bilateral seminars and conferences, and technical documentation on fast reactors. The complete exchange of technical documentations of the BN-600 and "Phénix" projects occurred in June 1977, and in July 1978 the parties exchanged documentation on the BN-600 and "Superphénix." Thus, one of the most important measures of collaboration has been completed. The parties are studying the data obtained and in accordance with the agreements in 1979 the bilateral seminar "Analysis and Comparison of Technical Decisions Adopted in Planning the Reactor Facilities Superphénix and BN-600" will be held.

However, the principal form of collaboration is the conduct of coordinated investigations within the framework of long-term joint tasks. Of the 10 listed joint tasks, five relate to investigations in the field of fast reactors. Thus, joint work on the investigation of the properties of tube and fuel-element materials in BOR-60, BN-350 and the French "Rhapsodie" and "Phénix" provide for:

the construction of irradiation facilities in each of the countries with joint discussion of the structural features of these facilities and exchange of drawings;
exchange of the corresponding data, essential for these investigations;
fabrication of irradiation facilities, fuel-element assemblies, and samples;
carrying out irradiation and post-reactor investigations;
exchange of data with the issue of joint reports and papers;

Included in the principal stages of work which have already been achieved are:
exchange of essential data, including the delivery to each country of 150-180 m of tubes for the manufacture of fuel elements. The tubes were supplied from materials used for fabricating the fuel-element claddings of BN-600 and "Phénix."
fabrication in the USSR of two experimental assemblies with fuel elements based on uranium–plutonium fuel, with claddings of French tubing. These fuel-element assemblies will be delivered in the near future for irradiation in BOR-60;
fabrication in France of tubes of materials produced in the USSR, and irradiation facilities for investigating radiation creep in samples of materials also made in the USSR. The irradiation facilities for BN-350 and "Rhapsodie" are in the stage of manufacture.

In the fourth year, a joint program of investigations into the physics of fast reactors will be completed successfully. It consists, in particular, in a mutual verification of the fast reactor calculations. The French specialists will calculate our reactors (critical assemblies) using French methods of calculation and systems of numerical constants, and will compare them with the results of experiments and, conversely, Soviet scientists will calculate the French reactors and the results of the calculations will be compared with the data of the corresponding French experiments.

Interesting experimental data on the physics of fast reactors, including an assessment of the nuclear data essential for the calculation of power-generating reactors, have been obtained on the four French facilities "Mazurka," "Minerva," "Rhapsodie," and "Phénix" and on the five Soviet facilities BFS-26, BFS-30, BOR-60, BR-10, and BN-350. It is planned to conduct further joint investigations to calculate the heat-release fields and the core parameters during burnup, to estimate the transactinide and fission product cross sections, to analyze models of fast reactors with heterogeneous cores, etc. The program of investigations of the most important physical parameters of fast reactors (e.g., breeding factor, efficiency of control and safety organs, etc.), intended for 4 years, obviously will be extended.

Joint work on the subject "Fast-Reactor Steam Generators" is oriented at this stage on the investigation of small steam–water leaks into the sodium and the associated behavioral effects of structural materials. A study of the corrosion stability of steels with sodium and the transfer process of carbon in the steel–sodium system, and the behavior of suspended matter in the sodium circuits was the object of joint investigations on the topic "Sodium Technology and Corrosion." In the course of work on these topics, the parties exchanged detailed information with a description of the investigations carried out, details of the test facilities, procedures and results of the experiments. They have prepared on this basis, in consultations with specialists, a program of future experiments, and have exchanged technical reports on the results of the investigations.

Collaboration has been successfully developed within the framework of joint work on the development and modeling of superconducting dipoles for accelerator-storage assemblies. At the present time, in the Institute

of High-Energy Physics, Saclay, and in the D. V. Efremov Scientific-Research Institute of Electrophysical Equipment, models of a dipole with a length of 1 m are being manufactured. Models of the dipole, made by each Institute, will be shipped to the Institute of High-Energy Physics at the beginning of 1979 for testing.

Support in conducting long-term joint investigations is clearly manifested in the plans for collaboration in the next few years. Thus, within the framework of the 2-yr program in 1978-1979, as already mentioned, 10 long-term joint investigations will be completed and some of them will be continued in the course of 3-5 years. Two of the new joint tasks have been organized in the field of chemical reprocessing of nuclear power-station fuel. Within the framework of the joint work on "Reprocessing of Spent Fuel of Thermal and Fast Nuclear Power-Station Reactors by the Water Method," coordinated investigations will be conducted on the study, comparison and choice of the optimum characteristics of different types of extraction and filtration plant, and technical requirements for extractants and diluents and methods of their regeneration have been developed. Methods and means of monitoring the technological regeneration process will also be compared, and optimum schemes of technological monitoring have been developed jointly. Joint investigations will also be conducted to choose the optimum technology for reprocessing liquid and solid radioactive wastes, obtained during reprocessing of spent fuel, and on the storage of radioactive wastes in geological formations and trapping gaseous fission products. Within the framework of this joint task, the transportation of spent fuel will be considered and also the development of recommendations for its storage before reprocessing. Agreement has been reached on the conduct of joint work on the gaseous-fluoride reprocessing of fast-reactor nuclear fuel. Although this method is being considered by both sides as a reserve method in relation to the main method – water – it was decided to carry out a joint study of the feasibilities and prospects of facilities for the regeneration of spent fast reactor fuel by the gaseous-fluoride technology. Both tasks have been calculated on a 5-yr period (up to 1982).

Within the framework of the other new topic of collaboration – "Nuclear Heat-Supply Stations" – it is proposed to discuss scientific–technical problems of their planning, technicoeconomic basis of utilization at conferences of specialists in France and in the Soviet Union, and also the types and parameters of reactor facilities, schemes and constructional decisions and safety assurances will also be discussed.

Collaboration is being successfully accomplished in the field of controlled thermonuclear fusion and plasma physics. Soviet and French specialists have participated in experiments on the Soviet facilities T-10 and T-11 and on the French TFR, "Vega," and "Petula." In February 1978, a bilateral seminar was held, at which plans for superconducting systems of the T-10M and "Torus-II" facilities were discussed. A program was worked out and preparations are underway for further joint experiments, which include the measurement of the spectrum of low-energy x-ray emission by means of semiconductor detectors, the measurement of plasma emission at double electron-cyclotron frequency on the T-10, and investigations of the transfer coefficients and dynamics of impurities on the TFR-6000. The conduct of joint experiments on the procedure for low-temperature heating of the plasma on TM-4 (electron heating) and the facilities "Petula" (magnetic pumping) and "Vega" (low-hybrid resonance) is being provided for.

Soviet–French collaboration in the field of salt-water distillation is being examined closely, and in the next few years will be accomplished within the framework of two working plans. In one of these, a French dropwise condensation stimulator will be tested on the Soviet salt-water distillation facility, which will improve the heat-transfer characteristics of salt-water distillation equipment. Within the framework of the other joint tasks, both sides will conduct investigations of salt-water distillation facilities with horizontal-tubular film equipment.

The examples described above do not exhaust all the thematics and forms of Soviet–French collaboration.

The minutes of collaboration in 1978-1979 between the State Committee for Atomic Energy of the USSR and the French Atomic Energy Commission (CEA), prepared on the basis of working plans for joint tasks, and also the agreed measures for the mutual exchange of experience, participation in experiments by both sides, exchange of technical documentation, the conduct of bilateral seminars and meetings of specialists, provides for conducting over these 2 years about 60 events in the Soviet Union and France, in which about 300 French and Soviet specialists will participate.

Thus, Soviet–French collaboration in the field of the peaceful use of nuclear energy bears a wide, stable, and long-term nature and is an excellent example of mutually advantageous collaboration between governments with a different social order.

INTERNATIONAL EXHIBITION AND CONFERENCE ON THE NUCLEAR INDUSTRY, "NUCLEX-78"

Yu. M. Cherkashov

The regular exhibition took place in Oct. 1978 in Basel, Switzerland. At the same time, the Conference on Nuclear Power Generation was being held, at which 118 reports were presented, distributed over four sections: fast reactor-breeders and high-temperature gas-cooled reactors; fuel technology and reprocessing of radioactive waste; operating experience with nuclear power stations, and the protection of the environment in conditions of nuclear production.

The reports of the Soviet specialists were received with interest, which can be judged from the number and topics of the problems specified in the course of the concluding discussions. The problems concerned the capital costs of the BN-600 reactor under construction, and the period of its introduction, reprocessing of fast reactor fuel, international collaboration of the Soviet Union on fast reactors, construction periods of the BN-600 reactor, etc.

In the course of the discussions the leader of the Soviet delegation, F. M. Mitenkov, in a separate address spoke at the request of the French specialists, on the problems of the choice of the loop and integral grouping of a BN-type reactor facility. On the question of whether now, based on the operating experience of the BN-350, the British PFR, and the French "Phénix," it is possible to answer to what extent the maintenance-suitability affects the choice of grouping of the reactor facility, it was said that in the Soviet Union there is experience in operation of BN-350 with a loop-grouping and constructional experience of the BN-600 with integral grouping. An analysis, carried out during development of the BN-600 project, showed that on the whole, problems of safety with integral grouping are solved more completely and more simply. At the same time, maintenance-suitability can be provided by both versions of grouping. In the next few years, both types of fast reactors will be operating in the Soviet Union, which will make it possible to verify these solutions.

Replying to a question by the Soviet delegation, the French specialists explained the rejection of the use in the "Superphénix" of modular steam generators, which has functioned reliably in the "Phénix," on purely ecomonic considerations. The maximum thermal loading of the "Superphénix" steam generator is expected to be ~600 kW/m^2 by comparison with 560 kW/m^2 for the "Phénix" steam generator.

From the reports presented at the Conference, the conclusion can be drawn that, as usual, effort is being directed abroad for the construction of nuclear power stations with sodium-cooled fast reactors. Judging by the reports, France had advanced further into this problem than the other Western countries. Completion of installation of the "Superphénix" is designated for 1981, the start of industrial operation, in 1983. Construction of the "zero" cycle has just taken place.

The reports on the results of work carried out on fast-reactor projects with helium cooling were concerned with constructional, technological, and experimental development of fuel elements and fuel cassettes.

More than 20 reports at the conference were devoted to the construction and operation of high-temperature gas-cooled thermal neutron reactors. In the report on the 10-yr operating experience with AVR (Federal German Republic), it was noted that, on the average, the power utilization factor during this period amounted to 0.76, and in individual years it reached more than 0.9. The activity of the coolant was significantly reduced by comparison with the first years of operation, despite the temperature being increased to 950°C (against 750°C). The annual discharge of radioactive inert gases amounted to 20 and 25 Ci of tritium. Investigations have been carried out and the results published concerning the migration of fission products throughout the circuits. In one of the reports, the operating experience of the Fort St. Vrain (U.S.A.) nuclear power station was discussed, The helium leakages from the circuit, leaks from the steam-generator tubes and troubles with the sealing system of the gas blower, which have occurred, were noted. It was indicated that the reactor operated for 80 days at 70-80% of capacity. The discharge of fission products into the circuit was found to be lower than the calculated level. The reactor projects, presented by France, for a nuclear power station with

Translated from Atomnaya Énergiya, Vol. 46, No. 3, pp. 203-204, March, 1979.

0038-531X/79/4603-0239$07.50

a capacity of 1200 MW(el.) is based on the earlier well-known design of a high-temperature gas-cooled reactor of the firm General Atomics (USA), with a capacity of 1160 MW. It differed in a more average gas temperature at the reactor outlet (650°C) and in increased helium pressure (70 kgf/cm^2). The principal thermal circuit of the nuclear power station also has undergone changes – gas steam superheating has been excluded. These measures are being proved with the desire to simplify the system of licensing in the construction of nuclear power stations. The HHT-600 (Federal Republic of Germany) was discussed in detail – this is an experimental–commercial nuclear power station with a single-circuit gas-turbine installation (N_{el} = 675 MW and η_{el} = 41%; T_{helium} = 850°C). The basis of the developed design are the results of the operation of a 50 MW(el.) experimental facility in Oberhausen (pyrogeneous helium heating, analogic cycle). Several further reports were devoted to a single-circuit nuclear power station with a capacity of 1240 MW(el.), including the development of structural materials, graphite, air-cooling towers, helium–helium and water–helium heat exchangers.

The results of the preliminary development of a high-temperature helium loop heat exchanger (1000°C) were presented by Japanese specialists at the conference. In addition, data concerning an investigation of the compatibility of structural materials in a pure helium environment were contained in several reports; the determination of the coefficients of friction for different materials, of insulation thermal conductivity, of water penetrability through the heat-exchanger walls, and of the principal problems of constructing reactor vessels of prestressed ferroconcrete for power–technological and single-circuit installations with a gas turbine were discussed.

Of the data on channel-type reactors, a report on the operating experience and fuel characteristics of CANDU reactors was of definite interest. A mockup of this reactor was shown at the exhibition, with individual structural components, and the operating characteristics of nuclear power stations with this type of reactor were presented. The high reliability of the plant was noted, and the advantage of a channel-type reactor in the capability of on-stream fuel recharging. The successful development of machine recharging has permitted a utilization factor of installed capacity in four reactors of the Pickering (Canada) nuclear power station of up to 90%.

In both the reports and the exhibits, the construction of equipment for measuring the energy release, dosimetric instruments and the construction of information-measurement and controlling systems for nuclear power stations was extensively highlighted. The progress in achieving excellent equipment quality was noted; this was due to the use of computer techniques (especially of microprocessors). Opinions were expressed about the necessity for further development work in the direction of increasing the reliability of instruments and control systems, of increasing sensitivity, dynamic range and life of detectors. High-temperature fission chambers, boron-containing neutron counters, thermocouples and acoustic noise sensors are proposed as detectors for data about the reactor core parameters.

It was noted in the reports on information-measurement and controlling systems that the use of controlling computer systems (CCS) in BWR (boiling-water reactors) is being developed and will be developed, as the use of CCS will allow the operator to successfully control the nuclear power station and reduce the cost of the control system. The principal functions fulfilled in real time by CCS include: calculating of the core; monitoring and control of the reactor core; mapping, signalization and recording of events; monitoring the efficiency of other systems. The core calculation consists in obtaining a three-dimensional power distribution in the core (taking into account Doppler effects and xenon poisoning), based on a three-dimensional model of the core.

The following basic concepts are used in the construction of CCS:
a hierarchial-decentralized structure of the system, ensuring a high flexibility and reliability;
a high-level system (principal computer system), possessing a high reproducibility;
the use of light displays for simple and efficient "operator–process" link;
construction of an input–output system based on microprocessors;
maximum use of standard components;
a developed mathematical base with a large collection of working programs.

The mathematical base for monitoring and controlling the reactor core essentially must include the following programs: control with rods and mapping their position on a display; determination of the state of the reactor; calculations of the correction factors for intrazone energy release detectors.

Reports were heard about the separation of uranium isotopes, forecasts of the development of nuclear power generation, requirements in uranium and the possibilities of producing it in Western countries up to 2000 A.D. The reprocessing of spent fuel, conversion with it, its transportation and storage were also considered. The radiological monitoring of personnel and the environment were discussed, discrepancies in the

estimates of personnel dosage loadings, experience accumulated on the collection of low-activity liquids and the consequences resulting from this dose level of population irradiation, and the protection of water systems from the discharge of cooling water. The initial data and the results of a numerical estimate were presented, of discharges during normal operation and during hypothetical accidents of pressurized water and boiling water reactors for nuclear power stations of this type.

The International Exhibition and Conference "Nuclex-78" reflected the present level of development of nuclear power generation and its problems. A study of the data will bring benefit in the practical activities of specialists in this field.

THIRD AMERICAN – SOVIET SEMINAR ON STEAM GENERATORS FOR FAST REACTORS

V. F. Titov

A Seminar on the Reliability and Safe Operation of Steam Generators for Sodium-Cooled Fast-Reactor Breeders was held in Oct. 1978 in Tampa, Florida. Eleven reports by Soviet specialists and 12 reports by American specialists were presented. In addition, each side gave information about the completion of joint programs. The reports and communications were divided according to thematics into four sessions: structural analysis, effect of operating conditions on material behavior, heat exchange and thermohydraulics, and leaks and their detection.

In the reports by Soviet specialists at the first session, the results of investigations carried out on the basis of a steam-generator project for nuclear power stations with BN-600 reactors were considered, as were general assessments of the prospects for double-walled steam generators. In the reports of the American specialists, the state of work carried out by the firm of Atomics International on the steam generator for the Clinch River nuclear power station (CRBR) was analyzed, including the presentation of the results of a test-rig break-in of an experimental 30-MW module. Calculations of the simultaneous effects of seismic shocks and rupture of the heat-exchange tubes showed that it will be necessary to increase significantly the thickness of the load-carrying components of the CRBR steam-generator housing, in comparison with the first versions of the project. A great deal of work has been carried out on the technology of welding, local heat treatment, and monitoring of the welding quality of the tubes to the tube panels. For reactors following after CRBR, three concepts are being considered: a modernized version of the "hockey stick" by Atomics International, a double-walled straight-through tubular steam generator by Westinghouse at Tampa, and a coil helicoidal steam generator by Babcock and Wilcox (see Table 1). There are no decisions concerning which of the structures is optimum, and therefore, they are being developed in parallel. The principal problem of the double-walled design continues to be the indication of the site of a leak and its repair. The most sound design is the "hockey stick" steam-generator design (PLBR), but for this an extensive research program has also been designated. All prospective versions have high-capacity modules and multiple circulation in the evaporator. Together with the cycle of the use of high-pressure superheated steam (t_{super} ~460°C, p~16 MPa), a low-temperature cycle of saturated steam with a pressure of 7.2 MPa is being considered. The material of the designs being developed is pearlite unstabilized steel 2.25% Cr–1% Mo.

At the second session, the reports of Soviet specialists were considered, which concerned the results of metallographic and corrosion investigations of a straight-through steam generator with S-shaped coils, dismantled after 30,000 h of operation in BOR-60, lifetime tests of single and multitube models of the evaporator and steam superheater of the BN-600 steam generator, and also concerning an investigation of the constants of decarbonization of pearlite steel 2.25% Cr–1% Mo and carbonization of 08Kh18N9 steel.

A report of the American specialists was devoted to the investigations of the decarbonization constants of steel 2.25% Cr–1% Mo, in which the effect of heat treatment and purity of the metal on the rate of decarbonization is described, as is the effect on its reduction with time. The American specialists have established that the rate of corrosion of this steel for the CRBR steam generators is approximately identical for all heat-exchanging zones, including in the critical region, and amounts to ~20 μm/yr. In this case, the sodium content in the

Translated from Atomnaya Énergiya, Vol. 46, No. 3, pp. 205-206, March, 1979.

0038-531X/79/4603-0241$07.50

TABLE 1. Steam Generator Characteristics of Future Reactors

Index	"Hockey stick"			With double-walled tubes		With helicoidal tubes	
	prototype module (MSG)	CRBR	PLBR	version with high-capacity superheat cycle	low-temperature cycle	version with high-capacity superheat cycle	low-temperature cycle
Thermal capacity of module, MW	30	120 – evaporator 80 – superheater	288	292	482	435	322
Diameter of housing, m	0,46	1,37	1,83	2,34	2,29	4,29	4,22
Multiplicity of circulation	1	2	6	—	6	—	4
Sodium temp. at inlet, °C	446	502	482	482	435	482	435
Pressure of generated steam, MPa	17,6	10,68	15,69	15,69	7,2	15,69	7,2
Temp. of generated steam, °C	384	485	457	457	t_s (287,8)	457	t_s (287,8)

water was increased to 12-30 μg/liter (norm 3 μg/liter). During investigations of fretting, wear, and adherence of the tubes in remote-control lattices, the contact loadings, friction path length, sodium temperature, and the holding period in the absence of a relative displacement of the contacting components were varied. The large set of investigations of fretting and wear allowed the American specialists to select the tube lattice of 2.25% Cr–1% Mo–Nikonel-718 steel.

In the American reports at the third session, heat exchange in a "hockey stick" steam generator was considered, as well as for a helicoidal tubular bundle and double-walled tube, with an analysis of the numerical heat-exchange equations and their correlations according to the results of experimental work on models, in particular, in the supercritical region. The refined equations will provide for carrying out the heat calculations with an error of ±5%. Nevertheless, margins of the heat-exchange surface are assumed in CRBR of 42% for the evaporator and 30% for the steam superheater. This is explained by the premeditated conservative approach to the construction of the first-generation steam generators.

In the reports of the Soviet specialists, concentratometric and acoustic methods of detecting leaks were considered, operating experience of a leak indication system in the BN-350, and numerical estimates of hazards in the case of large leaks. A design of an "inverted" steam generator, based on an experiment with a small leak, was analyzed. The American reports were devoted to investigations of small leaks and the process of their spontaneous development and to the development of leak-detection systems. The American program of investigating large leaks, consisting of two stages, was reported: the first stage consists of an investigation for the CRBR steam generator, and the second stage is a study of large leaks for future design projects. The program includes conducting experiments on large-scale models. The excellent convergence of the Soviet and American results of investigations of hydrodynamic and temperature effects in the case of large leaks was noted. In the experiments with small leaks, data have been obtained which differ in the spontaneous development time of the leak.

The Soviet specialists visited the Westinghouse engineering works at Tampa, which produces steam generators and volume compensators for LWR nuclear power stations and they familiarized themselves with the manufacture of these components at this plant.

The specialsts attending the Seminar noted that it was of a constructional nature. The discussion of technical information was of mutual interest from the point of view of improvement of steam generators.

MEETING OF THE INTERNATIONAL WORKING GROUP OF IAEA ON HIGH-TEMPERATURE REACTORS

V. N. Grebennik

The conference was held in Sept. 1978 in Vienna. Specialists from 13 countries and representatives of OECD/NEA organizations participated. The conference program consisted of three sections: reports on the development programs of high-temperature reactors (HTR) in the world; discussion of technical reports on HTR, their use and role in nuclear power generation; resolution of organizational problems, concerning the preparation and distribution of proceedings and reports, and the planning of conferences in 1979-1980.

In the reports and communications of the specialists, information was given about HTR nuclear power stations that are operating, under construction, and planned. The high-temperature reactor AVR (Federal German Republic) has been operating for four years at a helium coolant temperature of 950°C. The reliable operation of the pellet fuel elements of different structural and technological versions was noted, and also included those intended for the first charge of the THTR prototype reactor. The planned volume of experimental work on AVR is planned for completion in 1983. THTR, with a capacity of 300 MW (el.), construction of which is being completed at Schmehausen, is planned to be started up in 1981. At present, assembly of the main plant has been completed, the assembly of the pellet fuel elements for the first charge is ready, and the protective housing of the nuclear power station is being constructed. Another prototype high-temperature reactor of the Fort St. Vrain nuclear power station (U.S.A.), with a capacity of 330 MW (el.) and with lumped-type fuel elements, is operating at 70% capacity. New detectors for recording the neutron fluxes, temperatures, and pressures have been installed in it. The reasons for the origination of helium temperature and pressure fluctuations in different zones of the reactor, which occur when operating at a capacity of 50-55%, are being investigated. In 1978, the causes of increased moisture in the circuit were investigated and eliminated. Different systems and equipment for attaining the design capacity were tested and prepared.

Work on HTR in certain economically developed countries has been directed in recent years at concentration of efforts in the field of more efficient commercial introduction of this type of reactor. The United States as before, is devoting priority consideration to the use of HTR for electric power purposes. In relation to their future introduction, the firm of General Atomics has the support of the Association for Gas-Cooled Reactors (GCRA) and of the government. At the present time, negotiations are underway with power-generating firms concerning orders for a series of HTR nuclear power stations with a capacity of 900 and 1350 MW (el.), which it is proposed to introduce in 1989-2000 A.D. In contrast to the Fort St. Vrain nuclear power station, an electric drive for the main gas blowers will be used in these designs. The fuel cycle of the reactors has not been finally chosen, but investigations are being conducted in the following main directions: 93% ^{235}U/Th (HEU), 20% ^{235}U/Th (MEU), and a low-enrichment uranium cycle (LEU). Completion of acceptance and introduction of the closed fuel cycle, including chemical reprocessing and refabrication of the fuel elements, is proposed in the U.S.A. in 1995.

Some countries (Soviet Union, Poland, France, and Japan) have paid considerable attention to the power-technological utilization of HTR for the chemical, petroleum, metellurgical, and other branches of industry. The Japanese program is directed at the use of high-potential thermal energy in the steel-casting and chemical industries. The immediate aim of Japan for gas-cooled reactors is the construction of a superhigh-temperature experimental reactor (VHTR) with a capacity of 50 MW (th.) and with a helium outlet temperature of 1000°C. Planning operations have been completed, and construction is proposed to take place in 1979-1985. At the present time, work is proceeding on a safety foundation, seismic investigations are being conducted, and reactor tests are being made of lumped fuel elements and structural materials. In the Soviet Union, possibilities are being studied of using HTR thermal energy for power-technological processes, associated with the production of different energy carriers and chemical raw materials. Processes such as thermoelectric production of hydrogen in a closed sulfuric acid cycle of water decomposition and the production of ammonia based on the steam catalytic conversion of methane are being considered. Work is being carried out on an experimental

Translated from Atomnaya Énergiya, Vol. 46, No. 3, pp. 206-207, March, 1979.

0038-531X/79/4603-0243$07.50

power–technological facility with a BGR-50 high-temperature reactor with helium coolant. In this reactor, with a capacity of 50 MW (el.), it is proposed to use pellet fuel elements. Plans are under way for prototype thermal and fast reactors with a capacity of 300-400 MW (el.). In Poland, the power–technological use of HTR is being investigated, and the main interest is being directed toward the gasification of coal. The main interest in France at present appears to be toward HTR in connection with the requirement for high-temperature energy in the production of hydrogen from methane and its use for the gasification of coal, and the production of thermal energy and steam for the petroleum industry.

In the Federal Republic of Germany it is proposed to use HTR for both electric power and also for power–technological processes. Work has been concentrated on designs of demonstration stations, based on high-temperature reactors with pellet fuel elements: HHT-600 for electric power with a helium turbine capacity of 600 MW (el.) and air cooling. The helium temperature at the reactor outlet is 850°C and the station efficiency is <41%; PNP-500, for the production of technological heat with a capacity of 500 MW (el.) and a helium temperature of 950°C. This reactor has two cooling circuits, equal in capacity, one of which is intended for the hydrogasification of brown coal, and the second for the combined steam and hydrogasification of bituminous coal. The total productivity of the nuclear power station with respect to synthetic gas is $\sim 70 \cdot 10^3$ m^3/h. Construction of both nuclear power stations is planned for the end of the 1980's. In the 1990's, the introduction of several large-scale commercial stations is proposed: HHT-1200, with a capacity of 1200 MW (el.) and PNP with a capacity of 3000 MW (th.).

In order to substantiate the trend of HTR, a large volume of experimental investigations are being carried out at the present time in many countries:

reactor tests of fuel and structural materials are being conducted, and facilities are being constructed for the chemical reprocessing of fuel elements;

different plant components are being developed: reactor vessel of prestressed ferroconcrete, heat-exchange plant, accessories, etc.;

helium turbines, hot-gas conduits and thermoinsulators are being tested on large-scale test rigs;

steam and hydrogasification processes of coal are being studied on experimental facilities;

the safety of HTR and of the facilities intended for power–technological purposes is being studied.

The important role of fast breeder reactors in the development of nuclear power generation was noted at the Conference. Some countries are working on two concepts of these reactors: with sodium (LMFBR) and with helium coolant (GCFR). Work on GCFR is being conducted in European countries constituting the OECD/NEA, and also in the Soviet Union and United States.

The conditions of preparing proceedings and reports and their distribution among the countries participating in the activities on HTR were defined at the Conference. Conferences of specialists on the most urgent aspects of HTR were also discussed and recommended, to be conducted within the framework of the IAEA in 1979-1980. These include conferences on the safety of fast reactors with helium coolant, on graphite, on the utilization of HTR for power-technological purposes, etc. Participation in these conferences will allow specialists of different countries to exchange opinions and to discuss specific technical problems.

During recent years, in connection with the considerable volume of research on HTR, some countries (Federal Republic of Germany, the United States, Switzerland, Japan, France, etc.) have concluded bi- and tripartite agreements for the joint solution of various problems. This will allow experience to be exchanged, and thereby will curtail expenditure on research and carry it out over shorter periods. International collaboration on HTR within the framework of the IAEA also is an important condition for the successful development of this specialization, opening up possibilities for the widespread industrial use of atomic energy.

INTERNATIONAL CONFERENCE ON NEUTRON PHYSICS AND NUCLEAR DATA FOR REACTORS AND OTHER APPLIED PURPOSES

G. B. Yan'kov

The Conference was held in Sept. 1978 at Harwell, Great Britain, and was the second conducted in accordance with the recommendations of the IAEA International Committee on Nuclear Data, in which was indicated the advisability of replacing one of the larger IAEA conferences on this subject (with a convening period of 4-5 years) by annual conferences on a 3-yr cycle. This replacement will make it possible to accelerate the exchange of new ideas and data, and to discuss them more thoroughly and extensively with smaller expenditures of effort and means. There were 200 pariticpants at the conference representing 31 countries; reports (a total of 13) were presented at the plenary and two parallel sectional sessions.

The directive of the Conference was: neutron energy (requirements, measurements, estimates, integral experiments, calculations by well-known models) for reactors, and, to a lesser degree, for thermonuclear reactors, systems of assurance, biomedicine and other applied purposes.

Nuclear data for reactors encompasses not only the conventional fields (calculation of the reactor itself, its operation and safety), but also all other elements of the fuel cycle – the buildup of the transactinides and fission fragments, cooling, storage and reprocessing of irradiated fuel, and burial of waste. In the course of the conference, the fundamental principle set forth as the basis for establishing the accuracy of the values of the principal reactor parameters was mentioned repeatedly: elimination of high-cost reserves at different levels of reactor technology, which it is necessary to introduce when predicting the values of these parameters with a lower error. Starting from this principle, the British specialists have, for example, formulated the following requirements on the error of the values of certain parameters: K_{eff}, 0.5% for fresh fuel and 0.5-1% for irradiated fuel; KV, 2%; Doppler effect, 10-15%; sodium void effect, 10-15%; etc. Hence follow the required results for the accuracy of nuclear characteristics, e.g., for the resonance and fast neutron energy regions: ν, 0.3% for fissile isotopes and 1% for raw material isotopes (^{238}U, ^{232}Th); σ_f, 1% for all isotopes; σ_c or α, 4% for fissile and 3% for raw material isotopes; etc. Less stringent requirements are imposed for these characteristics on $^{240,241}Pu$.

Reports were presented at the conference on the further refinement of the fission cross sections of $^{235,238}U$ and ^{239}Pu over a wide range of neutron energies, the capture cross section for a large number of nuclei by a study of the Doppler effect, determination of neutron-resonance parameters and the preparation of averaged characteristics – force functions and the average distances between levels. Part of the reports were devoted to the uses of fast-neutron eleastic-scattering cross sections and reactions with a yield of different products, γ-emission, and neutron-multiplication cross sections, in particular, for (n, 3n) and (n, 4d) reactions in $^{235,238}U$.

Together with the future intensive buildup and refinement of data for the main fissile, raw-material and structural materials, investigations of the transactinides and individual nuclei – fission products – have been intensified signficiantly. For example, taking account of the new data presented at the conference, it can be stated that the fission cross section of ^{241}Am is known now with an error of ~5% for neutron energies of 0.001-15 MeV, except for a narrow region of 2-20 keV, where discrepancies amount to 30-40%. Recent experimental data confirm the Soviet data of Shpak et al., obtained in 1969. The American data, obtained by underground nuclear explosion, are sharply different from the whole set of current experimental data.

For fission fragments, besides the conventional work on the yields and half-lives, work on the neutron capture cross sections of individual nuclei was discussed. Experimental values and the results of theoretical calculations, which had been undertaken mainly by French specialists, were presented.

Translated from Atomnaya Énergiya, Vol. 46, No. 3, pp. 207-208, March, 1979.

0038-531X/79/4603-0245$07.50

Considerable attention was devoted to integral experiments for fast and thermal reactors. A special project, carried out at Los Alamos (U.S.A.) on a homogeneous cylindrical reactor containing 200 kg of ^{235}U, was devoted to a resolution of the contradictions for describing the reactivity of central samples, which occurs in the Argonne assemblies. The ratio of close to unity obtained between the calculated (by means of ENDF/B IV data) and the measured reactivity of central samples, gives the basis for confirmation that neglected heterogeneous effects are to blame for the discrepancies. Essentially, in the reports on integral experiments, the experimental data were compared with the estimated values of the ENDF/B library.

Of the reports concerned with nuclear data for thermonuclear reactors, a Swedish report on the refinement of characteristics, assumed as the standard of the reaction $^{6}Li(n, \alpha)T$ for neutron energies 1-4 MeV, should be noted with interest. A dependence of the angular distribution of the reaction products on the neutron energy has been discovered, which is found to be in agreement with calculations by R-matrix theory. In parallel with measurements of the direct reaction, the cross section of the reverse reaction T (α, ^{6}Li)n has been studied over the corresponding energy range, in which ^{6}Li nuclei were detected at an angle of 0° to the system of magnetic analyzer and surface-barrier detector.

In the field of neutron-radiation therapy, the most essential data for understanding interaction processes of fast neutrons in the human body are the number and energy spectrum of charged particles generated during the bombardment of carbon and oxygen with neutrons of energies 10-60 MeV.

In the section on the development of new methods, facilities, and instruments, attention was devoted to the American report on the electronuclear production of fuel. The basic idealogy of this is: to construct a target of thorium fuel elements, in which ^{233}U would be accumulated by irradiation with a high-powered accelerator, and these fuel elements would be put into thermal reactors without reprocessing and after a specified burnup (again without reprocessing), they would go into a waste storage vault. The danger of this scheme was mentioned, from the point of view of the possible theft of fissile materials. It was confirmed that, according to calculations, the cost of electric power in such a scheme is only 30% greater than in normal light-water reactors.

The participants in the conference visited some of the Harwell laboratories and familiarized themselves with the accelerator parameters and with the research being conducted on them according to the theme of the conference. They were shown a linear 136-MeV electron accelerator under construction; a pulsed neutron source (up to 5 nsec), intended mainly for measurements of nuclear data on resonance and fast neutrons and for the study of the structure and dynamics of a substance by means of slow neutrons; a 160-MeV synchrotron, which has a base length of 100 m for neutron investigations, and is to be used also for the production of medicinal radionuclides, and also a 450-kV Cockcroft–Walton accelerator, with a 14-MeV neutron source, used for the investigation of (n, α) reactions on structural materials. The specialists were shown a family of electrostatic accelerators of 3 MV and 6 MV and a tandem accelerator with a proton energy of 13 MeV, and also an isochronous cyclotron; a 3-MV accelerator which is pulsed (0.5 nsec) by a neutron source and is used also for the analysis of materials by means of the proton beam in a spot with a diameter up to 4 μm. Various reactions for thermonuclear applications are investigated on the tandem accelerator; on the 6-MV accelerator and cyclotron, radiation damage is investigated by means of charged particles, for example, niobium, in the cyclotron.

It should be mentioned that the work of the conference proceeded smoothly and was well-organized. Its proceedings will be published.

SYMPOSIUM, "INTERNATIONAL GUARANTEES-78"

N. S. Babaev

An international symposium was held Oct. 2-6, 1978 in Vienna, Austria in accordance with an arrangement under the guarantee of nuclear materials. More than 400 participants from 32 countries and 5 international organizations took part in the plenary sessions; more than 120 reports were presented for discussion (8 of which were reports of the Soviet specialists).

The reports were considered along these lines:

planning criteria of arrangements for facilitating the uses of international guarantees;

electronic processing of data for the guarantees;

the use of guarantees on facilities for the manufacture of fuel elements and power reactors;

storage and supervision of nuclear materials;

destructive and nondestructive measurement methods;

assessment of data for guarantees;

advanced concepts and systems for monitoring nuclear materials;

uranium–thorium fuel cycles;

reprocessing of spent fuel.

During the discussion of the reports, the reasons for such a high level of interest in the symposium became obvious, which reduced to the following.

The progressive introduction of nuclear technology into the different specializations of science and technology (in the first place, for the production of electric power and in technological processes) causes an increase of the total quantity of nuclear materials in the countries of the world. This attracts for itself an increased interest toward the strategy of application of guarantee procedures and leads to a marked increase of inspections at facilities where nuclear materials are located. Thus, in 1971 more than 234 inspections were carried out; in 1974, 474; in 1977, 706 inspections in 45 countries.

At the symposium in 1970 in Karlsruhe, reports were considered on the application of guarantee procedures mainly only for reactors, and in 1975 facilities were added to them, associated with low-enrichment uranium technology. At the symposium of 1978, questions on the application of guarantee procedures to the whole section of the nuclear fuel cycle were discussed.

Taking into consideration that nuclear materials possess such special features as high and constantly increasing cost, danger in handling and the possibility of using them for terrorist purposes, the majority of countries recognized the necessity of introducing centralized systems of accounting and monitoring for their use on government scales. National systems of accounting and monitoring have been developed on the basis of accumulated experience, in the first place that of international organizations. In its most concentrated form, the experience in accounting and monitoring of nuclear materials has been generalized in an IAEA system of guarantees, the principles of which are acknowledged to be more efficient than those of certain national systems of accounting. At the present time, with the creation of national systems, such IAEA exploitations are used as accounting procedures for nuclear materials; presentation of accounting information; transmission and processing of information; analysis of the nuclear material balance, and also procedures and methods of verification of the information presented.

Characteristic moments, appearing during discussion of the use of guarantee procedures at nuclear fuel-cycle establishments, were the point of view regarding the necessity of using constructive solutions and devices

---

Translated from Atomnaya Énergiya, Vol. 46, No. 3, pp. 209-210, March, 1979.

0038-531X/79/4603-0247$07.50

during the design of facilities, which would ensure the efficient application of guarantees, and also a desire to include in the information on processed fuel, not only data about the content of uranium and plutonium isotopes, but also about the transplutonium elements.

The reports concerning the use of guarantees at different uranium enrichment plants were of undoubted interest: for the planning of a factory in the Federal Republic of Germany, using the jet method (production 200 tons separate work units/yr), "Eurodif" gaseous-diffusion factory in France (production $10.8 \cdot 10^6$ separative work units/yr), and the centrifugal facility at Ninge-Tore in Japan (nominal production 50 tons spearative work units/yr). The scheme for the use of guarantees, proposed by the Japanese specialists, provides for a "closed" zone for technological plant and two zones of nuclear material balance (the first, the stockpile of uranium hexafluoride and the second, the area of the technological plant) with various key measurement points. The most important of these must be to accurately monitor the feed flows, of light and heavy fractions, and the concentration of uranium isotopes. In the opinion of the French specialists, it is necessary to pay special attention to monitoring receipt and shipment of nuclear materials from the factory and monitoring, which ensures that all movements of nuclear materials take place through the monitoring zone, that there are no changes in the operating cascade, and that no auxiliary facility should originate in the factory zone.

The Japanese specialists, on the basis of an analysis of the operation of a facility using the pyrex process, with a production of 0.7 metric ton/day of uranium and the possible introduction of the process with both zirconium and steel claddings, proposed three zones of material balance for accounting and monitoring at spent-fuel reprocessing factories. In the first zone, where discrepancies in the data of shipment and receipt are recorded, are included stocks of spent fuel, mechanical handling chambers, dissolver, cleaning spaces and the inlet measuring flask; in the second, rooms for chemical processes, treatment of waste, and analytical and technological laboratories; in the third, stock rooms for storage of plutonium and uranium. The key measurement points, in accordance with the material-balance approach, are located according to two basic criteria: determination of the nuclear-material flows (9 points) and physical stock-taking (7 points).

Part of the reports were devoted to the development of accurate methods of determining the amounts of nuclear materials and their concentration in accountable reservoirs. By using a combination of different methods (isotopic dilution and isotopic correlations), the determination error amounted to less than 1%. Great attention was devoted to the use for monitoring of the method of isotopic correlations, the establishment of the analytical relations between the fuel burnup, the concentration of uranium and plutonium isotopes, and their ratios. Further improvement of the method and increase of its accuracy will probably be possible on the basis of the ESARDA data bank, which should collect the experimental data in this field.

A serious problem for the development of a procedure of guarantees associated with a high concentration of fissile isotopes in samples from heat-releasing assemblies, are fast critical assemblies and reactors. In the reports on this subject, different alternatives were considered for ensuring monitoring and inspection at critical assemblies with highly enriched fuel, thus allowing rapid reliable determination of any unauthorized withdrawal of significant quantities of nuclear materials. Great attention was paid to the necessity for setting up a comprehensive system of control and monitoring during the movement of fissile materials, using neutron and gamma-detectors with standard methods of supervision, and preservation of accounting used at present by IAEA inspectors.

A review report by V. M. Gryazev (Soviet Union) elicited great interest for the participants at the symposium. Results were discussed of an investigation of the application of new physical methods and procedures for monitoring nuclear materials by the example of the "Spektr" critical assembly and the BOR-60 reactor.

In summing up the symposium, it can be said that tendencies for the development of guarantee procedures for the accounting and monitoring of fissile nuclear materials of the whole fuel cycle, from extraction of the uranium to the storage of radioactive wastes, were revealed most clearly.

SOVIET-AMERICAN CONFERENCE ON "HIGH-FREQUENCY PLASMA HEATING IN TOROIDAL SYSTEMS"

V. V. Alikaev

At the present time, high-frequency methods of heating plasma in closed systems are developing mainly in the range of cyclotron frequencies, low-hybrid and ion-cyclotron resonances, and also MHD-resonances. These trends are being developed in both the Soviet Union and in the United States. A comparison of the prospects of these methods of plasma heating was one of the main topics discussed at the conference, which was held in June 1978 in Sukhumi. According to general opinion, at present no preference can be given to any trend, and all four methods should be investigated.

In the review report of J. Willis, a comprehensive program of the American investigations of hf-plasma heating in tokamaks was given. In almost every tokamak, existing or planned, hf methods of heating are employed. As yet, preference is being given in the American thermonuclear program to plasma heating by the injection of fast atoms. At present, experiments have started on ion-cyclotron heating in the PLT facility. Encouraging results having been obtained on TFTR, construction of an assembly with this heating is proposed, with a total power of ~50 MW. The provisional cost of the project is ~30-50 million dollars. Now, a project is being considered for the use of ion-cyclotron heating in the ALCATOR facility with the following parameters: frequency f=200 MHz and power P=2-4 MW. Preparation of these experiments has started on the "Macrotor," "Caltex," and "Tokapol" facilities.

Electron-cyclotron plasma heating in tokamaks has been used only in the Soviet Union. This is because the high-powered generators in the millimeter wave range (gyrotrons) are operating in the Soviet Union. The problems associated with the construction of these generators for electron-cyclotron heating were discussed in the report presented by coworkers of the Institute of Applied Physics of the Academy of Sciences of the USSR and the I. V. Kurchatov Institute of Atomic Energy. In 1978, the firm of Varian (U.S.A.) developed a pulsed gyrotron with a frequency 28 GHz and a power 200 kW. Preparations for experiments with these generators were carried out on the "Elmo Bampi," "Torus," ISX, and "Microtor" facilities, An assembly with a total power of 2 MW has been constructed on the EVT facility, which will operate in the continuous mode.

A review of the experiments on plasma heating in the low-hybrid resonance frequency range on the American ATC, ALCATOR, and DOUBLET IIA facilities was given by S. Bernaby. In the experiments, a small group of ions with a relatively small lifetime are heated to a high energy. On the TM-3 (USSR) and DOUBLET IIA facilities, an effective heating up of the electron component is observed by using an excitation system of strongly decelerated waves. In the experiments on the FT-1 facility (USSR), heating up of both ions and electrons of the main component of the plasma is observed, in a regime when low-hybrid resonance conditions were achieved in the central regions of the plasma core. Experiments are planned on this method of plasma heating on the PLT ($p \simeq 1$ MW), ALCATOR-C (f=4000 MHz, P=4 MW) and DOUBLET III ($P \simeq$ 5-10-MW devices). The cost of the experiment on the DOUBLET III facility is provisionally estimated at 10-20 million dollars.

In the report presented by J. Tataronis, excitation and damping of Alfvén waves in a heterogeneous plasma was considered. In the United States, experiments in this range of frequencies ($f < f_{i.cycl}$) were carried out on the "Proto-Cleo" facility. With an input power of 100 kW and a plasma density of $2\ 10^{12}$ cm^{-3}, heating up to both ions and electrons was observed. A more intense heating up of ions was obtained on the Soviet facility R-02. The ion temperature, averaged over the cross section, reached 200 eV with a plasma density of $5 \cdot 10^{13}$ cm^{-3}. The heating efficiency amounted to 70%. Such experiments are being planned in the United States, to be conducted on the facility at the California Institute of Technology in 1979.

In the concluding session, the participants in the conference came to the unanimous opinion that, in the next 2 to 3 years, significant progress should be expected in investigations on uhf- and hf-plasma heating in closed systems.

Translated from Atomnaya Énergiya, Vol. 46, No. 3, p. 210, March, 1979.

0038-531X/79/4603-0249$07.50

NINETEENTH INTERNATIONAL CONFERENCE ON HIGH-ENERGY PHYSICS

V. I. Zakharov

Conferences of this kind (they are frequently also called "Rochesters") assemble once every 2 years and by tradition are the most representative forums for discussing elementary-particle physics. Tradition was not changed this time: about 950 physicists were present, representing the most prominent laboratories in the world. Important experiments were completed just prior to convening the conference (August, 1978). An innovation in the organizational aspect was the location for holding the Conference: previously they had taken place alternately in the USSR, the U.S.A., and Western Europe, but now it was being held in Japan.

The development which has occurred in recent years in elementary-particle physics was summarized in sectional (the first three working days) and plenary (second three days) sessions. Because of the large volume of material presented at the conference, particular attention was paid to review papers. Only part of the time at the sectional sessions was assigned for original reports concerning the most prominent projects.

The last few years have been important in the development of elementary-particle physics. Perhaps it may be said first of all, that we know the Lagrangian of interaction, responsible for a whole wealth of phenomena, observed with the energy of particle accelerators available at present for experiment (a few tens of GeV in a center of inertia system). This does not mean, of course, that every phenomena can be described in detail, as in the majority of cases there is no strict computational scheme which will permit conversion of knowledge of elementary interactions into predictions for the observed quantities. But cases yielding to calculation also are not rare, and together with certain qualitative consequences they give confidence and validity to the overall pattern. The current table of elementary particles appears as follows:

Leptons: $(e, \nu_e), (\mu, \nu_\mu), (\tau, \nu_\tau)$
Vector bosons: γ(photon) $W^{\pm}$, Z^0 (intermediate bosons)
Scalar bosons: H (Higgs particles)
Quarks: u, d, s, c, b, t (?)
Gluons: G_β^α (eight vector particles)
Graviton: g

The majority of the particles here, obviously familiar to the reader, we shall discuss in a later "supplement".

At the time of the conference in Tokyo, data were received which completely substantiated the existence of a new pair of leptons: a charged τ and the corresponding ν_τ neutrino. The mass of the charged lepton is

$$m(\tau) = (1782 \pm 3) \text{ MeV},$$

and the mass of the neutral lepton (neutrino) is

$$m(\nu_\tau) < 250 \text{ MeV}.$$

It is expected that $m(\nu_\tau) = 0$.

The first data about the τ-lepton were obtained in the U.S.A. (SLAK) and its properties were investigated in greatest detail in the Federal Republic of Germany (DESY). At the present time, not only the mass and spin (1/2) of the new lepton are known, but the relative probability of its different modes of decay as well. Without going into detail, we note that in every appearance, the pair (τ, ν_τ) is the simple repetition of the pair (e, ν_e) and (μ, ν_μ): The new charged lepton appears with its neutrino, and has decayed as a result of V−A interaction. The only known difference in the properties of the leptons reduces to their mass.

If leptons are observed directly experimentally, then the same cannot be said about the intermediate vector bosons $W^{\pm}$, Z^0 and the Higgs scalar particles. Their mass, obviously, is so large that they could be observed

---

Translated from Atomnaya Énergiya, Vol. 46, No. 3, pp. 211-212, March, 1979.

 0038-531X/79/4603-0250$07.50

on the existing facilities, and now several accelerator projects aimed at the discovery of these particles are being considered in earnest.

Although W, Z, and H have not been observed experimentally, their discovery may be assumed in the future (this refers especially to $W^{\pm}$ and Z^0). This confidence is due to the successes of the Weinberg–Salam theory, which is based on their existence and has received conclusive verification in experiments of recent years. It is well known that this theory unites electromagnetic and weak interactions. The union should be understood in the same sense that the coupling constant in the Lagrangian is identical for weak and electromagnetic interactions. The difference in the reaction velocities, caused by weak and electromagnetic interactions and observed experimentally at low energies, is because the particles responsible for the weak interaction – intermediate bosons – are massive, and because the photon is massless. As the coupling constant of electromagnetic and weak interactions is small, then there is no difficulty, knowing the bare Lagrangian, in calculating the cross sections of the processes with participation of photons.

The Weinberg–Salam model contains one parameter, the so-called Weinberg angle, which should be determined from experiment. Processes of the type

$$\nu_\mu N \to \nu_\mu N,\ \nu_\mu N \to \nu_\mu X,\ \nu_\mu e \to \nu_\mu e$$

are critical for the verification of the theory, i.e., processes caused by weak neutral currents (here X denotes an arbitrary constant, and ν_μ is the muon neutrino). It follows from the conference data that all these processes are actually described by one parameter and the value of the Weinberg angle is found to be equal to

$$\sin^2\theta_W = 0.22 \pm 0.02.$$

The corresponding predictions for the mass of the intermediate bosons thus appear:

$$m(W^{\pm}) \simeq 75\ \text{GeV},\ m(Z^0) \simeq 90\ \text{GeV}.$$

The only (but serious) problem for the Weinberg–Salam theory was, until recently, the negative results of experiments to find the effects of parity violation in eN-interactions, which are predicted by theory. Parity violation should lead to specific phenomena in atomic physics; however, in the first experiments (Oxford, Great Britain; Seattle, U.S.A.) they were not detected. However, just a few months before the conference in Tokyo, co-workers of the Institute of Nuclear Physics of the Siberian Division of the Academy of Sciences of the SSSR, L.M. Barkov and M. S. Zolotarev, detected the phenomenon of rotation of the plane of polarized light of a laser during the passage of lead vapor, and the value of the observed effect agreed with theory. Indirect confirmation of this result was the measurement of the scattering cross section of polarized electrons by hydrogen and deuterium. An experiment, conducted on the SLAK accelerator, confirmed the applicability (effected in another energy region than the atomic physics experiments) of the theory to eN-interactions. Therefore, at the present time there is no doubt in the validity of the Weinberg–Salam model. Certain details, however, may change, but for the final explanation of the structure of weak interactions, it would be important of course to detect the intermediate bosons and Higgs particles in an experiment. Until the properties of the vector bosons can be predicted sufficiently well, then the properties of the Higgs particles will remain, to a considerable degree, indeterminate.

Let us consider now the quark part of the table of elementary particles. The most important innovation here is the observation of the new narrow mesons Υ and Υ':

$$m(\Upsilon) = 9.46\ \text{GeV},\ \Gamma(\Upsilon \to e^+e^-) \simeq (1.4 \pm 0.3)\ \text{keV},$$

$$\Gamma_{\text{tot}}(\Upsilon) < 50\ \text{keV},\ m(\Upsilon') = 10.01\ \text{GeV},$$

$$\Gamma(\Upsilon' \to e^+e^-)/\Gamma(\Upsilon \to e^+e^-) \simeq 1/3.$$

These mesons were observed in $pN \to \Upsilon(\Upsilon')X$ and $e^+e^- \to \Upsilon(\Upsilon')$ processes. The honor of the discovery of the phenomenon (Lederman group, U.S.A.) belongs to experiments of the first type, and the conclusive and detailed investigation of the properties of the new items (DESY) belongs to the second type of experiments. The unique interpretation of the new mesons is the hypothesis that they represent bound states of new heavy quarks of charge $-1/3$:

$$\Upsilon,\ \Upsilon' \sim (\bar{b}b)$$

(b is the initial letter in the word "beautiful"). For the reader who is familiar with the history of the discovery of the J/Ψ-particle with mass 3.1 GeV, this interpretation is not surprising. History is being repeated in the well-known sense. It is to be expected, of course, that following the discovery of Υ, Υ' the observation will follow also of particles with a new quantum number of the type (bu), (ub), (bd), (db) .... We note, incidentally,

that similar expectations in the case of the c-quark (charmed particles) were corroborated. At the present time, detailed data have been obtained about the spectroscopy of the charmed mesons and their properties. Without listing the results, we can say that they are all found to be in accordance with theoretical expectations.

Finally, in the table, one of the quarks – the (t)-quark – is labeled with a question mark ("t" from "top"). As yet, there are no direct indications of its existence. This is the expected partner of the b-quark in the doublet in the Weinberg–Salam model. For the time being, it is difficult to say what is the mass of the particles containing t-quarks, but there is no doubt that searches for them will be intensive in the high-energy colliding e^+e^--beam accelerators which are coming into operation.

Both the quarks and the gluons have not been observed directly. These are the so-called "colored" particles, which appear only at small distances, and when attempting to isolate them they become (most likely – infinitely) heavy. Therefore, the confidence in their reality is based principally only on the success of theoretical calculations. The corresponding theory of strong interactions – quantum chromodynamics – is found to be at the center of attention of many theoreticians and experimentalists. Much attention was paid to quantum chromodynamics at the conference. Not everything is yet understood. One of the central problems is unsolved: why colored particles are not observed in the free state. But these unresolved questions, in our view, do not detract from the confidence and reality of their existence.

We have dealt mainly on the successes of theory and experiments, which obviously answers the objective state of affairs. The reader might note, however, certain "venomous" questions, with which we have not concerned ourselves. In particular, theory is unable to calculate the spectrum of leptons and quarks. Thus, the number of elementary particles is as yet taken by theory as a datum, but is not predicted by it, so that this number is found to be quite large. It is probable that there exists a fusion not only of weak and electromagnetic interactions, but also of strong interactions. At a higher energy, or at even smaller distances, it is possible that a gravitational interaction is joined to them. A theory of such fusion is as yet unknown, although attempts to discover its structure are being made. These and other questions future experiments, theories, and conferences will have to answer.

ALL-UNION SEMINAR "ELECTRONIC (AUTOMATIC) METHODS OF CONCENTRATION OF MINERALS"

B. V. Nevskii, M. L. Skrinichenko,
and A. P. Tatarnikov

At the seminar, held in Oct. 1978 in Moscow, were heard and discussed for the first time the reports (a total of 41) of different institutes, establishments and departments concerning the state and prospects for developing automatic methods of sorting ores of nonferrous, ferrous, and rare metals, coal, and other solid minerals. An exchange of scientific–technical and production experience was also conducted.

Automatic methods of sorting are based on the use of differences in the physical properties of the individual lumps or portions of ore. They are sorted in special separators – ore-sorting robots. For this characteristic by which the lumps are separated, there can be natural or artificial radioactivity, color and luminescence of the minerals and rocks, their electrical and thermal conductivity, magnetic susceptibility, etc. Accordingly, different methods have been developed (radiometric, activation, absorption, photometric, luminescent, conducto- and magnetometric, radiowave, etc.).

Automatic methods have opened up broad new possibilities in solving the complex and varied problems of mineral-reprocessing technology. They can be applied with great effect to classes of coarseness from 300 (100) mm to 25 (5) mm. Their use allows even in the initial stages of technological schemes withdrawal of a considerable quantity of tailings (up to 20–35% of the original ore) to the dumping ground, and in certain cases separation of even rich concentrates, without recourse to expensive crushing of the ores and without the expenditure of reagents.

Translated from Atomnaya Énergiya, Vol. 46, No. 3, pp. 212–213, March, 1979.

 0038-531X/79/4603-0252$07.50

The use of these methods ensures a higher efficiency and profit in the extraction and reprocessing of mineral raw materials. Great attention at the Seminar was paid to the state and development of nuclear-physical methods of sorting ores, based on the application of different sources of ionizing radiations (isotopes, x-ray facilities, reactors and accelerators), and also to the radiometric method of sorting radioactive ores. These problems were reflected in 32 reports.

The radiometric method is widely employed in industry in the Soviet Union and abroad. Part of the methods have been developed on the basis of the use of isotopic sources. A photoneutron method of sorting beryllium ores, based on the use of ^{124}Sb, has been introduced into industry. A gamma-absorption method of sorting iron and chromium ores is close to introduction or is being adopted, as well as neutron-absorption method of sorting boron ores. The development of an x-ray radiometric method of sorting ores of nonferrous and other metals is underway, as well as a method of sorting rubble and other structural materials by scattered radiation. Based on the use of x rays, x-ray luminescence sorting of diamond-containing ores has been effected under industrial conditions. This method is being developed for application to ores of nonferrous and rare metals. Successes have been achieved in the development of activation methods of sorting minerals. An experimental neutron-activation concentration facility SO-2 has been built and is operating. The ores before sorting are irradiated in a neutron multiplier, operating in the subcritical mode. The facility is intended for the development of a technology of irradiation and sorting of nonradioactive ores, in particular containing such elements as fluorine, manganese, vanadium, gold, copper, aluminum, etc.

The possibility was noted at the seminar of the widespread use of high-powered large-scale electron accelerators for sorting minerals.

Practice has confirmed the high economic efficiency of the new methods of mineral concentration. With a sorting cost of 0.5 to 1 ruble per 1 ton of original ore, the annual economic effect to individual establishments, depending on the specific conditions and scales of application of automatic sorting, usually amounts to hundreds of thousands to millions of rubles.

The participants in the seminar worked out recommendations for the future development of automatic methods of mineral sorting, in particular, defined the most promising directions for future work, and acknowledged as advantageous the creation of a special scientific-production amalgamation for the development and manufacture of ore-sorting plant and instruments.

NINTH RADIOCHEMICAL CONFERENCE IN CZECHOSLOVAKIA

A. S. Solovkin

In the work of the conference, held in Sept. 1978 in Pishtani, more than 140 specialists participated, and about 90 reports were submitted on sections of extraction, analytical chemistry in the nuclear fuel reprocessing cycle, extraction chromatography, physicochemical problems of the nuclear fuel reprocessing cycle, ion exchange and sorption, and radiation chemistry.

Three review reports of the Czechoslovakian specialists were devoted to problems originating during the operation of nuclear power stations: radiation safety, plant decontamination, regeneration, utilization and burial of waste (liquid, solid and gaseous), protection of the environment, regeneration of spent fuel with a burnup of up to 30,000 MW · day/ton, analysis of radioactive effluents, etc.

Part of the reports was concerned with the chemistry of technetium and palladium. In the review report of A. F. Kuzina (USSR), data on technetium were presented, which can be used for solving certain analytical problems of its concentration and determination, and the composition and properties of a large number of complex compounds were described. These properties can be used for qualitative and quantitative analysis, identification of compounds and oxidation state, and also the separation and removal of metals present in solutions by chromatographic and extraction methods. In some reports of the Czechoslovakian specialists (F. Matsashek et al.), the extraction of technetium and palladium from nitrate media by solutions of tri-n-octylamine (TOA) and TBP in different dilutions was considered in detail. Technetium and palladium can be separated quantitatively

Translated from Atomnaya Énergiya, Vol. 46, No. 3, pp. 213-214, March, 1979.

0038-531X/79/4603-0253$07.50

from fission products by extraction from 0.5-1 M HNO_3, and their reextraction is carried out with an aqueous ammonia solution. It was established that the presence of palladium in a system of 30% TBP–dodecane–nitric acid (0.5-3M) and an increase of the temperature of the system in its presence, has a significant effect on the radiolytic degradation of the extractant. Another fission product – molybdenum – does not show any effect in this case (Z. Novak, Poland). Extractant degradation and the effect of degradation products on the behavior of certain metals in the chemistry of the fuel element regeneration process was investigated in detail. In part of the papers, the use of salts of different metals with organic compounds as extractants is described. As shown in the reports of the Czechoslovakian specialists (I. Rais, M. Kirsh, et al.), cobalt dicarbolide $H^+C_4B_{18}\cdot H_{15}Cl_7Co^-$ dissolved in nitrobenzene is a selective extractant for the Cs^+ ion, which allows this cation to be efficiently separated from a mixture of fission products. The reagent is very stable to γ-radiolysis and the action of nitric acid.

Reports were interesting, in which the use of tertiary benzyldialkylamines and quaternary salts of benzyltrialkylammonia was considered for solving the technologically important problem of the extraction of the rare-earth elements and americium from nitric acid media (simulators of the water-tailing solutions from fuel element regeneration). It was shown that these extractants allow the rare-earth elements and americium to be efficiently separated from cesium, strontium, zirconium, iron and other fission and corrosion products. The extractants studied are stable to γ-radiolysis (V. Edinakova et al.). The extraction method of discriminating and separating the rare-earth elements by means of the new extractant tetraphenylimidodiphosphonate was described by specialists from the German Democratic Republic (E. Hermann et al.).

In the section on analytical chemistry in the nuclear fuel reprocessing cycle, interesting reports were submitted on the different methods of the quantitative determination of uranium, plutonium, neptunium, etc.

In one of the reports of the Czechoslovakian specialists, the results of work were given on the investigation of the spent fuel of the A-1 nuclear power station by radiochemical, mass-spectrometric and γ-spectrometric methods. In this case, the first two methods were used for the calibration of the nondestructive γ-spectrometric method, which in future will be used as a control.

In Czechoslovakia, the method of isotopic dilution with mass-spectrometric completion of analysis has been used successfully. In a joint Czechoslovakian–Yugoslavian report, high characteristics of the quantitative (not worse than 0.15%) determination of uranium, plutonium and neodymium were given for the analysis of the A-1 nuclear power station spent fuel, using the Varian TN-5 mass spectrometer. The NBS (USA) standards were used and 2-5 μg of uranium and ~0.1 μg of plutonium or neodymium were taken for the analysis. These same authors have carried out work on the γ-spectrometric determination of ^{106}Ru, $^{134,137}Cs$ and ^{144}Ce, using semiconductor Ge(Li)-detectors (range 400-1300 keV).

I. Feist (Czechoslovakia) reported the results of the use of submersible domestic silicon detectors for determining integrated α-activity and α-spectrometric measurements. A method of preparation of targets for α-spectrometric measurements is interesting (M. Beran, Czechoslovakia). A layer of zirconium phosphate (~10 μ) is applied to a backing of stainless steel; the α-emitter (^{239}Pu, ^{241}Am, etc.) is adsorbed onto it and then the spectrometric measurements are carried out. Thus, emitters with different sorption properties can be separated [for example, Pu(IV) and Am(III)].

A precision coulometer has been developed and is being tested (A. Shvets, Czechoslovakia). Its operating principle is as follows: An electric current is applied to the working detector with a specified frequency and electrolysis takes place. In the author's opinion, the instrument will allow coulometric analysis to be conducted with an error of hundredths of one-percent.

Interest was created in a report concerning the determination of microquantities of neptunium by differential polarography. The neptunium is converted electrochemically to the tetravalent state and is determined polarographically by a dropping mercury electrode. It can be measured reliably down to a concentration of $5\cdot10^{-7}$ M, the limit of detection is $2\cdot10^{-7}$ M, and the error is about 2% for 10^{-5} M and 10% for 10^{-6} M. The method is used for both aqueous and organic solutions (TBP+dodecane). Neptunium is determined without preliminary separation from plutonium and uranium with a ratio of M:Np = 10^3 and $5\cdot10^4$, but in the presence of fission products a preliminary separation is necessary

In the section on physicochemical problems of the nuclear fuel reprocessing cycle, reports were presented which were of interest from the point of view of intensifying concepts concerning the nature of the processes taking place in solutions of many elements (both actinides and fission products), with which radiochemistry is concerned: the state of radioiodine in the liquid and gas phase during dissolution of fuel elements (P. Putrik et al., Czechoslovakia), the state of trace concentrations of ^{144}Ce in aqueous solutions of inorganic acids (P.

Benesh et al., Czechoslovakia), physicochemical principles of the separation of individual fission products (in particular, promethium) for the manufacture of radioactive sources (N. E. Brezhneva et al., USSR), formation and properties of mono- and di-n-butylphosphates of certain metals which are important in radiochemistry (A. S. Solovkin, USSR), radiation-chemical reduction of Pu(VI) in nitric acid solutions (M. V. Vladimirova et al., USSR) and the effect of complex formation on the rate of reduction of plutonium compounds (A. V. Stepanov et al., USSR), stability of Pu(IV) and Pu(VI) in nitric acid solutions in conditions of intense α-radiolysis (A. G. Rykov et al., USSR), and also the electrolytic reduction of Pu (IV) in extraction processes for separating uranium and plutonium (A. Pochinailo et al., Poland). In a recent paper, data were given about the conditions of electrochemical separation of uranium and plutonium in a counter-current extraction (with TBP) process in mixer-settlers. The authors have investigated different structural materials for the anode and cathode. The anode is platinum, and for the cathode material gold, tantalum, zirconium, graphite, and pyrographite can be used. The acidity of the aqueous phase is 2M HNO_3 and the current is 200 mA/cm^2. In counter-current conditions, satisfactory results have been obtained for the separation of uranium and plutonium.

The reports presented at the conference will be published.

ATOMIC-HYDROGEN POWER GENERATION AND TECHNOLOGY*

Reviewed by Yu. I. Koryakin

In recent years, considerable attention has been devoted to hydrogen, due mainly to the hope and desire, by means of its extensive utilization, of overcoming certain difficulties in satisfying rapidly growing power requirements. The use of hydrogen as a secondary energy resource precedes its production. In solving the problem associated with the considerable costs of primary power, an important if not decisive role is assigned to atomic energy, more precisely, to high-temperature nuclear reactors.

The book being reviewed, of which the essence of the contents is well reflected in its title, is perhaps the first attempt to introduce the reader to the essence of the main questions of the atomic-hydrogen problem. This attitude and aim of the editorial staff, which is headed by V. A. Legasov, is logically and categorically justified. An attempt to completely and comprehensively answer the numerous questions of atomic-hydrogen technique and technology would "dissolve" the principal key scientific–technical problems, not to mention that the volume of the book would increase sharply.

The realization of such attitude is not always simple, and especially in this case, when the book is not a monograph, but represents a collection of papers of a quite large assembly of authors. In this case, one is frequently involved with the difficulty of coordination or balancing of the sometimes subjective attitudes of individual authors in relation to the position and importance of "his" problem and questions on the general aspects of the problem as a whole. It is precisely this problem that is solved quite well. The introductory paper by the President of the Academy of Sciences of the USSR, A. P. Aleksandrov, concerning the prospects of the use of atomic energy for power generation and the foreward by the editor-in-chief of the book, contribute in no small measure to the fundamental attitude. Strictly, they also state its principal directive, and define the problems and the boundaries of the atomic hydrogen problem in all their diversity.

In accordance with this, in 11 of the papers which constitute the main content of the book, the following principal topics are highlighted: methods and special features of hydrogen production, assessment of a nuclear reactor as a technical means for achieving this from the position of the necessary transformation or obtaining temperature, nuclear-physics, and material-study characteristics, and the possible spheres of introduction of nuclear reactors into power technology.

The editorial staff of the collection well know that perhaps paramount in the whole problem is the conformity of the possibilities of high-temperature reactor techniques with the power–technological requirements, mainly temperature. Therefore, the account of the principal considerations concerning the feasibility of this confirmity and the engineering feasibilities is assigned an important place. Hopes of its achievement, obviously are encouraging and the authors show this, by describing not only the existing experience but also by assessing the different paths for solving the main problem.

The use of a large list of Soviet and foreign literature references (about 300 entries) relates to the positive aspects of the data given.

On the whole, it is impossible not to agree with the preface to the book, in which the hope is expressed that the collection will extend the participants in the solution of the exceptionally important and promising atomic-hydrogen problem.

*Issue 1, Atomizdat, Moscow (1978), 246 pp., 2 figures, price – 80 kopecks.

Translated from Atomnaya Énergiya, Vol. 46, No. 3, pp. 215-216, March, 1979.

 0038-531X/79/4603-0256$07.50

V. V. Goncharov, N. S. Burdakov,
Yu. S. Virgil'ev, V. I. Karpukhin,
and P. A. Platonov

ACTION OF IRRADIATION ON THE GRAPHITE IN NUCLEAR REACTORS*

Reviewed by A. P. Sirotkin

Graphite, as a result of its exceptional properties, finds extensive application in reactor technology. The book being reviewed is the second monograph in the Russian language, and is being issued 10 years after the first monograph "Nuclear Graphite," by S. E. Vyatkin et al. During this time, many papers have been published, devoted to the investigation of the characteristics of reactor graphite. Work is continuing on the creation of new grades. As its properties depend on the raw materials used and the special features of technology, then the physicomechanical properties of Soviet reactor graphites under irradiation, given in the book, are of special interest.

The book describes the technologies of producing graphite with a density of 1.65 to 1.9 g/cm^3, and the crystal structure and physical properties are considered, including the dependence of the rate of oxidation on the processing temperature, creep, and nonuniformity of properties. The main attention is devoted to the change of physical properties during neutron irradiation. The principal factors affecting the material during irradiation are considered, as are methods of determining the neutron fluence damaging the graphite. It is noted that graphite is one of the most sensitive materials to a change not only of the fluence, but also to the flux density and the neutron spectrum. Radiation defects and the degree of change of its properties are determined by the number of displaced atoms, which is the result of the combined action of both irradiation and annealing. Unfortunately, the authors do not make recommendations, beyond that energy to calculate the neutron fluence when estimating the effect of irradiation of graphite: above 0.18 MeV, 50 keV or with respect to the equivalent fission neutron flux.

Great attention is paid to the dimensional deformation of graphite during irradiation the description of oxidation, consideration of the design and operating conditions of nuclear reactor stacks, their shielding and efficiency with the inclusion of experimental data. In this book, which includes a large list of literature references, the specific stage of the investigations is summarized. It will be of undoubted interest for designers, operators and scientific workers occupied with graphite reactors.

* Atomizdat, Moscow (1978), 272 pp., 3 figures.

Translated from Atomnaya Énergiya, Vol. 46, No. 3, pp. 215-216, March, 1979.

0038-531X/79/4603-0257$07.50

A. B. Mikhailovskii

PLASMA INSTABILITIES IN MAGNETIC TRAPS*

Reviewed by A.M. Fridman

Recent achievements in the heating and containment of a thermonuclear plasma in tokamaks have involved special attention to the processes taking place in the plasma. The complex geometry of magnetic surfaces in traps, formed by a system of external and internal currents, determines the diverse and at times nontrivial physical mechanics of instabilities, the most active of which are interpreted by collective processes. The initial stage of the majority of collective processes, as a rule, is associated with the development of some or other instability (or several at once). Therefore, the importance of constructing a theory of plasma instabilities, taking into account the actual geometry of operating facilities, or facilities under construction, is obvious. The book being reviewed is devoted to an account of the central divisions of this theory, which have been formulated in recent years.

The book describes the theory of the principal plasma instabilities in both open (adiabatic) and closed (toroidal) traps. The stability of the tokamak plasma is discussed in the greatest detail. The author draws the attention of the readers to the following circumstances. When investigating the stability of the tokamak plasma in the approximation of a circular plasma cylinder or by the model of a plane plasma layer in a gravity field, disregarding the existing effects, the following can be found: shear, magnetic well, bottle effects, effects of finite orbits, and magnetic particle drift. These effects in some way or other are associated with the curvature of the magnetic surfaces of the tokamak, and are investigated in detail in the book by A. B. Mikhailovskii. The author has noted and studied the role of Alfvén waves in the plasma dynamics of the tokamak.

Great attention in the book is devoted to the description of the effect of various stabilizing factors: ellipticity and triangularity of cross section, and the effects of a finite β. The investigation of the stabilizing influence of the latter at present is acquiring special interest because of the analysis of the energy balance carried out at the I. V. Kurchatov Institute of Atomic Energy. Analysis showed the necessity of having a plasma in reactor-tokamaks with the maximum possible β. As mentioned, despite the fact that instabilities represent the greatest danger in a low-pressure plasma, and are stabilized in a finite-pressure plasma, the stabilizing role of such factors as the temperature gradient, collisions between particles, the longitudinal current gradient (shear), groups of fast particles, and certain other factors, as a rule increases with increase in β. Hence, it would be hasty to draw a conclusion about the stabilizing effect of a finite β. Following the logic of the author, we conclude that increases in plasma stability can be achieved by optimization of the destabilizing factors and not by a reduction of β.

One of the conclusions of the author is given here, which is important for the physicist–experimenter. In our opinion, other no less useful conclusions can also be cited.

The urgency of the publication of the monograph is clear. For specialists it will become a reference book, and it will assist students and graduate students to master new efficient methods of investigating plasma instabilities.

*Atomizdat, Moscow (1978), 295 pp., 2 figures. Price – 50 kopeks.

Translated from Atomnaya Énergiya, Vol. 46, No. 3, p. 216, March, 1979.

0038-531X/79/4603-0258$07.50

Lithuanian Mathematical Journal

A cover-to-cover translation of *Litovskii Matematicheskii Sbornik*

Editor: **P. Katilius**
Academy of Sciences of the Lithuanian SSR

Associate Editor: **V. Statulevičius**
Secretary: **E. Gečiauskas**

An international medium for the rapid publication of the latest developments in mathematics, this new quarterly keeps western scientists abreast of both practical and theoretical configurations. Among the many areas reported on in depth are the generalized Green's function, the Monte Carlo method, the "innovation theorem," and the Martingale problem.

This journal focuses on a number of fundamental problems, including:

- weak convergence of sums of a random number of step processes
- asymptotic expansions of large deviations
- concentration functions of finite and infinite random vectors
- linear incorrect problems in Hilbert space.

Subscription: Volume 18, 1978 (4 issues) $150.00

Random Titles from this Journal

Limiting Poisson Processes in Schemes for Summation of Independent Integer-Valued Processes—R. Banys
Formal Differentiation in Spaces of Geometric Objects—R. V. Vosylius
Scalar Products of Hecek L-Series of Quadratic Fields—É. Gaigalas
Characterization of Stochastic Processes with Conditionally Independent Increments—B. Grigelionis
Limit Theorems for Products of Random Linear Transformations on the Line—A. K. Grincevicius
One Limit Distribution for a Random Walk on the Line—A. K. Grincevicius
Estimate of Remainder Term in Local Limit Theorems for Number of Renewals in the Multidimensional Case—L. Griniumiene
Solvability of a Differential Equation in a Subspace—B. Kvedaras
Modelling of a Nonlinearity by a Sequence of Markov Chains—V. V. Kleiza
Density Theorems for Sectors and Progressions—F. B. Koval'chik
Mathematical Modelling of the Combustion Process in the Chamber of a Liquid Propellant Rocket Engine—J. Kolesovas and D. Svitra

NEW RUSSIAN JOURNALS

IN ENGLISH TRANSLATION

BIOLOGY BULLETIN

Izvestiya Akademii Nauk SSSR, Seriya Biologicheskaya

The biological proceedings of the Academy of Sciences of the USSR, this prestigious new bimonthly presents the work of the leading academicians on every aspect of the life sciences—from micro- and molecular biology to zoology, physiology, and space medicine.

Volume 5, 1978 (6 issues) $175.00

SOVIET JOURNAL OF MARINE BIOLOGY

Biologiya Morya

Devoted solely to research on marine organisms and their activity, practical considerations for their preservation, and reproduction of the biological resources of the seas and oceans.

Volume 4, 1978 (6 issues) $95.00

WATER RESOURCES

Vodnye Resursy

Evaluates the water resources of specific geographical areas throughout the world and reviews regularities of water resources formation as well as scientific principles of their optimal use.

Volume 5, 1978 (6 issues) $190.00

HUMAN PHYSIOLOGY

Fiziologiya Cheloveka

A new, innovative journal concerned *exclusively* with theoretical and applied aspects of the expanding field of human physiology.

Volume 4, 1978 (6 issues) $175.00

SOVIET JOURNAL OF BIOORGANIC CHEMISTRY

Bioorganicheskaya Khimiya

Features articles on isolation and purification of naturally occurring, biologically active compounds; the establishment of their structure, methods of synthesis, and determination of the relation between structure and biological function.

Volume 4, 1978 (12 issues) $225.00

SOVIET JOURNAL OF COORDINATION CHEMISTRY

Koordinatsionnaya Khimiya

Describes the achievements of modern theoretical and applied coordination chemistry. Topics include the synthesis and properties of new coordination compounds; reactions involving intraspheral substitution and transformation of ligands; complexes with polyfunctional and macromolecular ligands; complexing in solutions; and kinetics and mechanisms of reactions involving the participation of coordination compounds.

Volume 4, 1978 (12 issues) $235.00

THE SOVIET JOURNAL OF GLASS PHYSICS AND CHEMISTRY

Fizika i Khimiya Stekla

Devoted to current theoretical and applied research on three interlinked problems in glass technology; the nature of the chemical bonds in a vitrifying melt and in glass; the structure-statistical principle; and the macroscopic properties of glass.

Volume 4, 1978 (6 issues) $125.00

LITHUANIAN MATHEMATICAL JOURNAL

Litovskii Matematicheskii Sbornik

An international medium for the rapid publication of the latest developments in mathematics, this quarterly keeps western scientists abreast of both practical and theoretical configurations. Among the many areas reported on in depth are the generalized Green's function, the Monte Carlo method, the "innovation theorem," and the Martingale problem.

Volume 18, 1978 (4 issues) $150.00

PROGRAMMING AND COMPUTER SOFTWARE

Programmirovanie

Reports on current progress in programming and the use of computers. Topics covered include logical problems of programming; applied theory of algorithms; control of computational processes; program organization; programming methods connected with the idiosyncracies of input languages, hardware, and problem classes; parallel programming; operating systems; programming systems; programmer aids; software systems; data-control systems; IO systems; and subroutine libraries.

Volume 4, 1978 (6 issues) $95.00

SOVIET MICROELECTRONICS

Mikroelektronika

Reports on the latest advances in solutions of fundamental problems of microelectronics. Discusses new physical principles, materials, and methods for creating components, especially in large systems.

Volume 7, 1978 (6 issues) $135.00

Send for Your Free Examination Copy

PLENUM PUBLISHING CORPORATION, 227 West 17th Street, New York, N.Y. 10011
In United Kingdom: Black Arrow House, 2 Chandos Road, London NW10 6NR, England
Prices slightly higher outside the U.S. Prices subject to change without notice.